

Republic of Iraq
Ministry of Higher Education
and Scientific Research
University of Misan
College of Science
Department of Biology



Biosynthesis of Some Nanoparticles from Pathogenic Bacteria and Evaluation their Antibacterial and Antitumor Activities

A Thesis Submitted to

The college of Science / University of Misan as Partial Fulfillment of the Requirements for the Master's Degree of Science in Biology

By

Hawraa Khalaf Abbood

B.Sc.Biology / Misan University (2019)

Supervisors

Assit.Prof. Dr. Rashid Rahim Hateet

2025 A.D

1446 H.D

بِسْمِ اللَّهِ الرَّحْمَنِ الرَّحِيمِ

قُلْ هَلْ يَسْتَوِي الَّذِينَ يَعْلَمُونَ وَالَّذِينَ لَا يَعْلَمُونَ إِنَّمَا

يَخْتَفِرُ الْأُولَىٰ وَالْآخِرُونَ

سورة الزمر آية (9)

صدق الله العلي العظيم

Dedication

*To The Sun and Moon Which Lighting my Life by Pave the Way
to my Success...*

My Father & My Mother

*To Those who have supported me and are Waiting
for my Success...*

My Brothers & My Close Friends

To who have Given me him Time and Knowledge...

My Supervisor

Acknowledgements

Firstly, I would like to thank Allah very much, for this work, and the prayer and peace of Allah be upon our Master and prophet Muhammad and his divine good family.

*I would like to express my sincere gratitude to my supervisor **Prof. Dr Rashid Rahim Hateet** for highly inspiring guidance, patience, motivation, enthusiasm and immense knowledge, continuous support for completing this thesis. Much appreciation is offered to the head of The Department of Biology, **Assistant Professor Dr. Saleh** for help to complete my work. I can also extend my sincere thanks and appreciation to all those who helped me from the members of the College of Science and also the members of the College of Medicine, especially the honourable **Dr. Hamoud** and the respected **Dr. Muhammad**, in addition to the members of the Children and Maternity Hospital. I would like to thank my close friend, Assistant Professor **Samah Naeem**, and **Dr Hassan Ghali** for their continuous support in completing the research requirements.*

Thanks to everyone who supported me.

Hawraa

Supervisor Certification

I certify that this thesis (**Biosynthesis some Nanoparticles from Pathogenic Bacteria and Assessment Antibacterial and Antitumor Activity**) has been prepared under my supervision as a fulfilment of the requirement for the Master's Degree of science in Biology.

Signature.....

Asst. Prof. Dr. Rashid Rahim Hateet

College of Science

Misan University

Date: / / 2025



Head of biology Department Recommendation

According to the recommendation of the supervisors, this thesis is forwarded to the examination committee for approval.

Signature.....

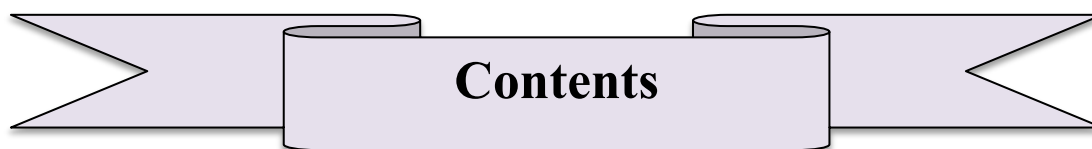
Asst. Prof. Dr. Saleh Hassan Jazea

Head of biology Department

College of Science

Misan University

Date: / / 2025



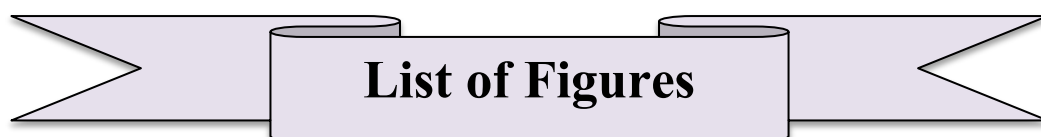
Contents

Subject	Page
Contents	I
List of Figures	IV
List of Tables	VIII
Abbreviations	IX
Summary	XII
Chapter one Introduction and literature review	
1.1. Introduction	1
1.2. The aim of the study	3
2. literature review	4
2.1. Nanotechnology: History and future	4
2.2. Nanoparticles (NPs)	6
2.3. Preparation methods of Nanostructure	7
2.3.1. Top-down and Bottom-up Approaches	7
2.4. Classification of nanomaterials based on origin	9
2.5. Classification of nanomaterials based on the structural configuration-composition	9
2.6. Classification of nanomaterials based on the number of dimensions	10
2.7. Nanoparticle synthesis methods	11
2.7.1. Physical method	11
2.7.2. Chemical method	11
2.7.3. Biological method	12
2.8. Applications of bio-synthesized NPs	13
2.9. Types of NPs	14
2.10. Green synthesis of NPs	16

2.10.1.Nanoparticles biosynthesis by bacteria	16
2.10.2. Nanoparticles biosynthesis by Fungi	18
2.10.3. Nanoparticles biosynthesis by Plants	20
2.11. Bacterial pathogenicity	22
2.12. Virulence factors of bacterial pathogenicity	22
2.13.Medical applications	23
2.13.1.Antimicrobial activity	23
2.13.2. The cancer	24
2.13.3.Liver and colon cancer	24
2.13.4. Anticancer activity	25
2.14 Cancer treatment with nanotechnology	26
2.15.Physical characterization of NPs	27
2.15.1. UV–Visible microscopy	27
2.15.2.Fourier transform infrared spectroscopy (FTIR)	27
2.15.3.Zeta potential analysis	27
2.15.4.X-ray diffraction analysis	27
2.15.5.Field-emission scanning electron microscopy (Fe-SEM) and energy dispersive spectroscopy (EDX)	27
2.15.6.Transmission electron microscopy (TEM)	28
2.15.7.Atomic force microscopy	28
Chapter Two Materials and Methods	
2.1. Materials and Methods	29
2.1.1. Equipment	29
2.1.2 Culture media	30
2.1.3 chemicals and biological materials	31
2.2.Method	32
2.2.1. Sample collection	32
2.2.2.Bacteria isolation	33

2.2.3 Identification of Bacteria	33
2.2.3.1 VITEK-2 system	33
2.2.3.2 Molecular identification of bacteria	34
2.2.3.2.1 Extraction of bacterial genomic DNA	34
2.2.3.2.2 Confirmation of the presence of extracted DNA	34
2.2.3.2.3 Amplification of 16S rDNA gene	34
2.2.3.2.4 Electrophoresis of PCR Products	35
2.2.3.2.5 Sequencing of 16S rDNA gene	35
2.2.4. Preparation of (Haucl ₄ .3H ₂ O, AgNO ₃ , Na ₂ SeO ₃)	35
2.2.5. Biosynthesis of NPs	36
2.2.6. Characterization of NPs	36
2.2.6.1. Physical characterization	36
2.2.6.1.1. UV–Visible microscopy	36
2.2.6.1. 2. Fourier transform infrared spectroscopy (FTIR)	37
2.2.6.1.3. Zeta potential analysis	37
2.2.6.1. 4. X-ray diffraction analysis	37
2.2.6.1.5. Fe-SEM and EDX	37
2.2.6.1. 6. TEM	37
2.2.6.1.7 AFM	38
2.2.6.2. Biological characterization	38
2.2.6.2.1. Antibacterial activity	38
2.2.6.2.2. Anticancer activity	38
Chapter three Results and Discussion	
3.1. Isolation of bacteria	40
3.2 Identification of Bacteria	40
3.3 Biosynthesis of NPs	42
3.4 Characterization of NPs	45
3.4.1. Physical characterization	45

3.4.1.1. UV–Visible microscopy	45
3.4.1.2. Fourier transform infrared spectroscopy (FTIR)	48
3.4.1.3. Zeta potential analysis	51
3.4.1.4. X-ray diffraction analysis	53
3.4.1.5. Fe-SEM	58
3.4.1.6 EDX	63
3.4.1.7. TEM	69
3.4.1.8.AFM	74
3.4.2.Biological characterization	76
3.4.2.1.Antibacterial activity	76
3.4.2.2.Anticancer activity	81
Chapter four Conclusions and Recommendations	
Conclusion	96
Recommendations	97
References	98



List of Figures

Number and Title of Figure	Page
Fig (1.1) Approaches of nanoparticle synthesis	8
Fig (1.2) Classification of Nanomaterials (a) 0D clusters and spheres, (b) 1D nanofibers, rods, and wires, (c) 2D films, networks, and plates,(d) 3D Bulk Nanomaterial	11
Fig (1.3) Numerous methods of Nanoparticle synthesis	12
Fig (1.4) Applications of green synthesized nanoparticles in environmental and biomedical fields.	14

Fig (3.1) gel electrophoresis using primers amplified appeared between (1000-1500pb)	41
Fig (3.2) colour change of supernatant for AuNPs produced by <i>A. baumannii</i>	42
Fig (3.3) colour change of supernatant for AgNPs produced by <i>P.aeruginosa</i>	43
Fig (3.4) colour change of supernatant for Ag ₂ ONPs produced by <i>P.aeruginosa</i>	43
Fig (3.5) colour change of supernatant for SeNPs produced by <i>S. marcescens</i>	44
Fig (3.6) Uv-visible of AuNPs produced by <i>A. baumannii</i>	45
Fig (3.7) Uv-visible of AgNPs produced by <i>P.aeruginosa</i>	46
Fig (3.8) Uv-visible of Ag ₂ ONPs produced by <i>P.aeruginosa</i>	46
Fig (3.9) Uv-visible of SeNPs produced by <i>S. marcescens</i>	47
Fig (3.10) FTIR analysis of AuNPs produced by <i>A. baumannii</i>	48
Fig (3.11) FTIR analysis of AgNPs produced by <i>P.aeruginosa</i>	49
Fig (3.12) FTIR analysis of Ag ₂ ONPs produced by <i>P.aeruginosa</i>	50
Fig (3.13) FTIR analysis of SeNPs produced by <i>S. marcescens</i>	51
Fig (3.14) zeta value of AuNPs produced by <i>A. baumannii</i>	52
Fig (3.15) zeta value of AgNPs produced by <i>P.aeruginosa</i>	52
Fig (3.16) zeta value of Ag ₂ ONP produced by <i>P.aeruginosa</i>	53
Fig (3.17) zeta value of SeNPs produced by <i>S. marcescens</i>	53
Fig (3.18) XRD analysis of AuNPs produced by <i>A. baumannii</i>	54
Fig (3.19) XRD analysis of AgNPs produced by <i>P.aeruginosa</i>	55
Fig (3.20) XRD analysis of Ag ₂ O ₃ NP produced by <i>P.aeruginosa</i>	56
Fig (3.21) XRD analysis of SeNPs produced by <i>S. marcescens</i>	57
Fig (3.22) Fe-SEM image of AuNPs Produced by <i>A. baumannii</i>	58
Fig (3.23) The histogram of the size distribution of AuNPs Produced by <i>A. baumannii</i>	59

Fig (3.24) Fe-SEM image of AgNPs Produced by <i>P.aeruginosa</i>	60
Fig (3.25) The histogram of the size distribution of AgNP Produced by <i>P.aeruginosa</i>	60
Fig (3.26) Fe-SEM image of Ag ₂ ONP Produced by <i>P.aeruginosa</i>	61
Fig (3.27) The histogram of the size distribution of Ag ₂ ONP Produced by <i>P.aeruginosa</i>	61
Fig (3.28) Fe-SEM image of SeNPs Produced by <i>S. marcescens</i>	62
Fig (3.29) The histogram of the size distribution of SeNP Produced by <i>S. marcescens</i>	62
Fig (3.30) EDX analysis of AuNPs produced by <i>A. baumannii</i>	64
Fig (3.31) EDX analysis of AgNPs produced by <i>P.aeruginosa</i>	64
Fig (3.32) EDX analysis of Ag ₂ ONP produced by <i>P.aeruginosa</i>	65
Fig (3.33) EDX analysis of SeNPs produced by <i>S. marcescens</i>	65
Fig (3.34) EDX-Mapping image of AuNPs produced by <i>A. baumannii</i>	67
Fig (3.35) EDX-Mapping image of AgNPs produced by <i>P.aeruginosa</i>	67
Fig (3.36) EDX-Mapping image of Ag ₂ O ₃ NP produced by <i>P.aeruginosa</i>	68
Fig (3.37) EDX-Mapping image of SeNPs produced by <i>S. marcescens</i>	69
Fig (3.38) TEM image of AuNPs Produced by <i>A. baumannii</i>	69
Fig (3.39) The histogram of the size distribution of AuNPs Produced by <i>A. baumannii</i>	70
Fig (3.40) TEM image of AgNP Produced by <i>P.aeruginosa</i>	71
Fig (3.41) The histogram of the size distribution of AgNPs Produced by <i>P.aeruginosa</i>	71

Fig (3.42) TEM image of Ag ₂ O ₃ NP Produced by <i>P.aeruginosa</i>	72
Fig (3.43) The histogram of the size distribution of Ag ₂ O ₃ NP Produced by <i>P.aeruginosa</i>	72
Fig (3.44) TEM image of SeNP Produced by <i>S. marcescens</i>	73
Fig (3.45) The histogram of the size distribution of SeNP Produced by <i>S. marcescens</i>	74
Fig (3.46) AFM image (three-dimensional) of AuNPs produced by <i>P.aeruginosa</i>	75
Fig (3.47) AFM image (three-dimensional) of AgNPs produced by <i>P.aeruginosa</i>	75
Fig (3.48) AFM image (three-dimensional) of Ag ₂ O ₃ NP produced by <i>P.aeruginosa</i>	76
Fig (3.49) AFM image (three-dimensional) of SeNPs produced by <i>S. marcescens</i>	76
Fig (3.50) Result of NPS as antibacterial agents	77
Fig (3.51) Inhibition zone of NPs on <i>E.coli</i> a) AuNPs b) AgNPs	78
Fig (3.52) Inhibition zone of NPs on <i>E.coli</i> a) Ag ₂ O ₃ NPs b) SeNPs	78
Fig (3.53) Inhibition zone of NPs on <i>S. aureus</i> a) AuNPs b) AgNPs	79
Fig (3.54) Inhibition zone of NPs on <i>S. aureus</i> a) Ag ₂ O ₃ NPs b) SeNPs	79
Fig (3.55) Inhibition zone of Gentamycin on a) <i>S. aureus</i> b) <i>E.coli</i>	80
Fig (3.56) HT-29 cell line treated with a concentration of 160 µg/ml of AuNPs produced by <i>A.baumannii</i> with crystal violet dye	82
Fig (3.57) HepG2 cell line treated with a concentration of 160 µg/ml of AuNPs produced by <i>A.baumannii</i> with crystal violet dye	83
Fig (3.58) MEF cell line treated with a concentration of 160 µg/ml of AuNPs produced by <i>A.baumannii</i> with crystal violet dye	83
Fig (3.59) Curves IC ₅₀ of AuNPs for HT-29, HepG2 and MEF cells	84

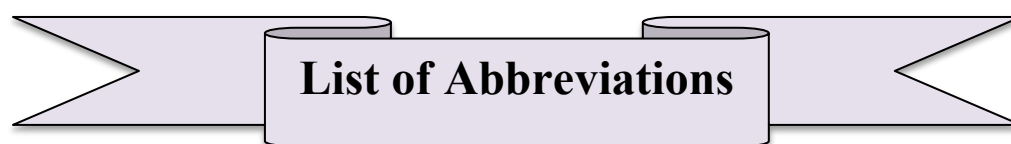
Fig (3.60) HT-29 cell line treated with a concentration of 160 µg/ml of AgNPs produced by <i>P.aeruginosa</i> with crystal violet dye	86
Fig (3.61) HepG2 cell line treated with a concentration of 160 µg/ml of AgNPs produced by <i>P.aeruginosa</i> with crystal violet dye	86
Fig (3.62) MEF cell line treated with a concentration of 160 µg/ml of AgNPs produced by <i>P.aeruginosa</i> with crystal violet dye	87
Fig (3.63) Curves IC ₅₀ of AgNPs for HT-29, HepG2 and MEF cells	87
Fig (3.64) HT-29 cell line treated with a concentration of 160 µg/ml of Ag ₂ ONP produced by <i>P.aeruginosa</i> with crystal violet dye	89
Fig (3.65) HepG2 cell line treated with a concentration of 160 µg/ml of Ag ₂ O ₃ NP produced by <i>P.aeruginosa</i> with crystal violet dye	90
Fig (3.66) MEF cell line treated with a concentration of 160 µg/ml of Ag ₂ ONP produced by <i>P.aeruginosa</i> with crystal violet dye	90
Fig (3.67) Curves IC ₅₀ of Ag ₂ ONP for HT-29, HepG2 and MEF cells	91
Fig (3.68) HT-29 cell line treated with a concentration of 160 µg/ml of SeNPs produced by <i>S. marcescens</i> with crystal violet dye	93
Fig (3.69) HepG2 cell line treated with a concentration of 160 µg/ml of SeNPs produced by <i>S. marcescens</i> with crystal violet dye	93
Fig (3.70) MEF cell line treated with a concentration of 160 µg/ml of SeNPs produced by <i>S. marcescens</i> with crystal violet dye	94
Fig (3.71) Curves IC ₅₀ of SeNP for HT-29, HepG2 and MEF cells	94



List of Tables

Number and Title of Table	Page
Table (1.1) Some types of bacteria produced different NPs	17
Table (1.2) Some types of fungi produced different NPs	19
Table (1.3) Some types of plants produced different NPs	21
Table (2.1) Apparatus used during the study period	29
Table (2.2) Equipment used during the study period	30
Table (2.3) Culture media	30
Table (2.4) Biological and chemical materials	31
Table (2.5) Clinical samples collection	32
Table (2.6) Preparation of PCR reaction compound	34
Table (2.7) PCR Program for implification the 16 srDNA gene	35
Table (3.1) Bacterial colonies properties	40
Table (3.2) Results of the analysis of the sequence of the nitrogenous bases of the DNA of the studied bacterial species and their comparison with the isolates found in GenBank.	41
Table (3.3) NPs with color change ,media and incabation hours	44
Table (3.4) Uv-visible wave length of NPs	47
Table (3.5) The various bands and Functional groups of AuNPs	48
Table (3.6) The various bands and Functional groups of AgNPs	50
Table (3.7) The various bands and Functional groups of SeNPs	51
Table (3.8) Debye-Schwarr equation of AuNPs	54
Table (3.9) Debye-Schwarr equation of AgNPs	55
Table (3.10) Debye-Schwarr equation of Ag ₂ O ₃ NP	57
Table (3.11) Debye-Schwarr equation of SeNPs	58

Table (3.12) Elements ratios of NPs by EDX	66
Table (3.13) Inhibition zone diameter of NPs and Gentamycin on <i>S. aureus</i> , <i>E. coli</i>	77
Table (3.14) results of statistical analysis of AuNPs concentrations on HT-29, HepG2 and MEF cell line	82
Table (3.15) the results of the statistical analysis of AgNPs concentrations on the colon, liver cancer and MEF cell line	85
Table (3.16) the results of statistical analysis of Ag ₂ O ₃ NP concentrations on the colon, liver cancer and MEF cell line	89
Table (3.17) results of statistical analysis of SeNPs concentrations on colon, liver cancer and MEF cell line	92



List of Abbreviations

Abbreviations	Key
AFM	atomic force microscopy
AuNPs	gold nanoparticles
AgNPs	Silver nanoparticles
Ag ₂ ONPs	Silver oxid nanoparticles
AgNO ₃	Silver nitrate
°C	Celsius degree
DMSO	Dimethyl sulfoxide
EDX	Energy Dispersion Analysis of X-ray
FTIR	Fourier Transform Infrared
FESEM	Field Emission Scanning Electron Microscope
HauCl ₄ .3H ₂ O	Tetrahydrochloride
MHA	Müller-Hinton agar
mm	Milli meter
µg/mL	Microgram per milliliter

Na ₂ SeO ₃	Sodium selenate
NA	Nutrient agar
NB	Nutrient broth
NPs	Nano Particles
Nm	Nano meter
PCR	Polymerase chain reaction
ROS	Reaction oxygen species
SPR	Surface plasmon resonance
SeNPs	Selenium nanoparticles
TEM	transmission electron microscopy
UV	Ultraviolet-Visible
XRD	X-Ray Diffraction
0-D	Zero dimensional
1-D	One dimensional
2- D	Two dimensional
3-D	Three dimensional

Summary

The study was conducted in the Biotechnology laboratory at the College of Science / University of Maysan in addition to some health institutions (Al-Sadr Hospital, Al-Zahrawi Hospital, Children and Maternity Hospital) during a period extending from January to April. The current study aimed to synthesize some nanoparticles by some pathogenic bacteria isolated from different sources. Ten types of bacterial isolates were collected (blood, wounds, burns, urine) and the molecular diagnosis was made for four types of them by Polymerase chain reaction (PCR) in addition to their diagnosis by 2-Vitek device. The diagnosis results showed that the bacterial isolate isolated from the blood was *Acinetobacter baumannii*, while the bacterial isolate isolated from the wounds was *Pseudomonas aeruginosa*, and the bacterial isolate isolated from the burns was also *Pseudomonas aeruginosa*, in addition to the bacterial isolate isolated from the urine, which was *Serratia marcescens*, and three of them were registered in the GeneBank. After that, biosynthesis processes were carried out to obtain the NPs under study.

When treating bacterial filtrates with gold tetrachloride salt (HAuCl_4), the results showed a colour change in the filtrate of the isolate *A. baumannii* from transparent yellow to dark red after incubation for 24 hours as an indicator of its ability to synthesize gold nanoparticles (AuNPs), while no colour change occurred in the filtrates of other isolates when treated with the same salt. On the other hand, work was done on the biosynthesis of silver and silver oxide nanoparticles, where bacterial filtrates were treated with silver nitrate salt (AgNO_3), and after incubation for 72 hours, the biosynthesis succeeded in changing the colour of the filtrates of the two isolates *P. aeruginos* and *P.aeruginos* from transparent yellow to dark brown as an indicator of the synthesis of both silver and silver oxide nanoparticles (AgNPs, Ag_2O_3 NPs) respectively, while no colour change appeared in the filtrates of other isolates when treated with the same salt. The bacterial isolates were tested at the same steps for the synthesis of selenium nanoparticles, where the results showed a colour change only for the filtrate of the *S. marcescens* isolate from transparent yellow to light orange when the bacterial filtrates were treated with sodium selenite salt (Na_2SeO_3) for 48 hours as preliminary evidence of the occurrence of biosynthesis of SeNPs, while the filtrates of the other isolates did not show a colour change when treated with the same salt. To confirm the biosynthesis of

the synthesized NPs, some advanced physicochemical tests were performed., where the results showed that the surface plasmon resonance (SPR) of the biosynthesized particles of (*A. baumannii*, *P. aeruginosa*, *P. aeruginosa*, *S. marcescens*) was determined at wavelengths (560, 426, 430, 298 nm) respectively. (FTIR) analysis showed that the NPs are surrounded by functional groups attached to them, while the zeta potential analysis showed the stability of the particles, as SeNPs were more stable at (-19.8mv) compared to other NPs. As for the nature of the crystalline structure of the NPs, they were cubic crystalline particles for AuNPs and AgNPs and hexagonal for SeNPs when examined by X-ray diffraction analysis (XRD). As for the morphology, size and distribution of the particles, they were examined by high-resolution scanning electron microscope (FESEM) and transmission electron microscope (TEM). Some of the particles were spherical and regular in shape, and some were close to spherical, irregular and homogeneously distributed and had sizes within the nanoscale range. The average size of the particles (Au, Ag, Ag₂O₃, Se) was (68, 45, 88, 92 nm) respectively when examined by FESEM and the average particle size (22, 29, 17, 51 nm) respectively when examined by TEM while the presence of elements (Au, Ag, Ag₂O₃, Se,) in the studied bacterial filtrates was confirmed by (EDX) examination.

Some biological applications have been conducted, including testing the antibacterial activity of the synthesized NPs against two pathogenic bacteria, *Staphylococcus.aureus* and *Echerichia.coli* using the disk diffusion method. The results showed that the synthesized NPs have good activity against both types of tested bacterial isolates and the statistical analysis results confirmed the presence of statistically significant differences at the 0.05 level between the values compared with the antibiotic gentamicin. The cytotoxicity of the synthesized NPs was also tested against human colon cancer cells (HT-29) and human liver cancer cells (Hep-G2) compared with normal mouse embryonic stem cells (MEF) using different concentrations (10, 20, 40, 80, 160 µg/mol). The results revealed that the synthesized NPs possessed inhibitory ability against the mentioned cancer cells in a concentration-dependent manner, where the inhibitory concentration for half of the cells IC₅₀ of AuNPs synthesized by *A. baumannii* against cell lines (MEF, HepG2, HT-29) was (1100, 73, 111) µg/mol, respectively. While the IC₅₀ of AgNPs synthesized by *P. aeruginosa* was (489, 62, 102) µg/mol, respectively. While the IC₅₀ of Ag₂O₃NPs synthesized by *P. aeruginosa* was (671, 94, 125) µg/mol, respectively, while

the IC₅₀ of SeNPs synthesized by *S. marcescens* was (683, 59, 75) µg/mol, respectively. The results of statistical analysis using Graph Pad Prism confirmed the presence of significant differences between the inhibitory concentrations of cancer cells at a significance level of 0.05.



Chapter one

Introduction

&

literature review

1.1 Introduction

Recently, the importance of nanotechnology has increased, which is the technology that includes the manufacture and applications of small-sized materials whose dimensions range from 1-to 100 on the nanoscale, and has integrated with other sciences, including medical sciences, where it has gained a wide scope in therapeutic applications, the most important of which is cancer treatment, where nanoparticles are used for diagnosis as well as treatment and as antioxidants (Senapati *et al.*, 2018; Madani *et al.*, 2020; Shi, 2021). Metallic NPs have a wide scope in materials science due to their unique chemical and physical properties that differ from free materials (Ealia & Saravanakumar, 2017). One of the most important characteristics of NPs is the increase in their surface area relative to their volume, which has given them thermal and mechanical properties (Muddapur *et al.* 2022). Scientists have turned, about nanotechnology, to the biological method in the biomanufacturing of nanoparticles for several reasons, including low cost and because they are A safe and environmentally friendly method, and also free of pollutants compared to physical and chemical methods that often use high energy and toxic chemicals and are therefore a source of concern for biological applications (Muddapur *et al.*, 2022; Zadeh *et al.*, 2022). The biological extracts of the organisms that produce the particles contain enzymes that participate in the reduction process of dissolved metal ions and convert them into nanocrystals (Kitching *et al.*, 2015; Ali & Mohammed, 2021; Dewan, 2022). Research has focused largely on using bacteria as a means of synthesizing many metal nanoparticles and their oxides due to the abundance of bacteria and their ability to adapt to harsh conditions.

Many bacteria can reproduce very quickly, allowing for rapid experiments and the observation of multiple generations within a short timeframe, also they can be grown on simple, inexpensive media. Factors like temperature, oxygen levels, and nutrient availability can be easily controlled in a laboratory setting. These advantages make bacteria an ideal choice for studying a wide range of biological processes (Pantidos & Horsfall, 2014). Many studies, including the current study, aim to synthesize multiple nanoparticles and evaluate the microbial effectiveness to eliminate many pathogenic bacteria that are resistant to many antibiotics. Nanoparticles, the most prominent and famous of which are silver nanoparticles, have a high ability to inhibit bacteria (Dewan & Hateet, 2023). Nanoparticles also have anticancer effectiveness, as nanoparticles such as gold, silver and selenium affect cancer cells as well as free radicals at certain concentrations. It is worth

noting that they affect cancer cells only without affecting normal cells, as they work to kill cancer cells through many mechanisms, the most important of which is programmed cell death (Patil *et al.*, 2019).

The term cancer is currently used to refer to a group of diseases characterized by abnormal (these cells have mutations in their DNA) and uncontrolled cell growth (these cells divide and multiply rapidly without the usual signals) (Martínez-Jiménez *et al.*, 2020). Cancer development can be summarized through four different stages: tumour initiation, tumour spread, tumour spread to nearby and distant organs, as well as resistance to chemotherapy (Lytle *et al.*, 2018; Colaprico *et al.*, 2020). Cancer affects various organs of the body such as the brain, lung, breast, colon, and also the liver. Liver cancer is the sixth most common malignant tumour worldwide, and the incidence and mortality rates are still increasing. Although partial resection and liver transplantation have achieved success in treating advanced stages of liver cancer, the therapeutic effects remain unsatisfactory due to the high probability of relapse after the operation (Ji *et al.*, 2023). Colon cancer (CC) and rectal cancer (RC) are considered to be one tumour entity, known as colorectal cancer (CRC), in all areas of clinical practice and research. This is predicated on the idea that the big bowel, which is regarded as a single organ, is where CC and RC grow (Paschke *et al.*, 2018). A cancer's death rate is influenced by its type as well as the patient's sex, race, and other societal characteristics. Men are more likely than women to die from colorectal cancer. (Gogoi *et al.*, 2022). Cancer is treated after diagnosis using chemotherapy. Due to the side effects and damage resulting from its use, the effect of radiation on healthy cells, and increased drug resistance, new methods and approaches have been discovered from natural and harmless sources to apply as anti-cancer alternatives to traditional treatments (Mansoori *et al.*, 2017; Wang *et al.*, 2020). Scientists have been able to invent a modern technique called tissue culture, which facilitates the knowledge of the effect of experimental treatment on different types of cancerous and normal cells outside the body by using cancer cell lines and normal cell lines and knowing the extent of their toxic effect on these cells (Koch *et al.*, 2021).

1.2 The Aims of the study

1-Isolation and molecular identification for some species of pathogenic bacteria from different sources (blood, wounds, burns, urine).

2-Testing the ability of pathogenic bacteria under study to bio-synthesize some types of nanoparticles such as gold (Au NPs), silver (Ag NPs), silver oxide (Ag₂O₃ NPs) and selenium (Se NPs).

3-Characterization of the properties of the above-mentioned bio-synthesize nanoparticles using some physicochemical tests, which are (Uv-visible, FTIR, XRD, Fe-SEM, TEM, AFM, EDX-mapping, Zeta potential).

4-Evaluating the activity of the bio-synthesize nanoparticles in the current study as antibacterial agents against two species of pathogenic bacteria, Gram-positive *Staphylococcus aureus* and Gram-negative *E.coli* .

5- Study of the cytotoxic effect of bio-synthesize nanoparticles on normal cell lines (MEF), human liver cancer cell line (Hep-G2), and human colon cancer cell line (HT-29) .

2. Literature Review

2.1 Nanotechnology: History and Future

The study of NPs is not new; in fact, the 1925 chemistry Nobel Prize winner Richard Zsigmondy was the first to suggest the idea of a "nanometer." He was the first to use a microscope to measure the size of particles like gold colloids and was the first to use the term "nanometer" to describe particle size. The Nobel Prize-winning scientist Richard Feynman is credited with developing contemporary nanotechnology. In his presentation "There's Plenty of Room at the Bottom," delivered at the 1959 American Physical Society meeting at Caltech, he put forth the concept of manipulating matter at the atomic level. Almost 15 years after Feynman's discussion, a Japanese scientist called Norio Taniguchi used the word "nanotechnology" to refer to semiconductor processes that occurred on the order of a nanometer. According to Taniguchi, materials can be processed, separated, consolidated, and deformed by a single atom or molecule as part of nanotechnology. After Kroto, Smalley, and Curl discovered fullerenes in the 1980s, Eric Drexler of the Massachusetts Institute of Technology (MIT) borrowed ideas from Feynman's "There is Plenty of Room at the Bottom" and Taniguchi's phrase "nanotechnology" in his 1986 book "Engines of Creation." The Next Wave of Nano-technology Feynman's theories have now been proven correct, and this novel idea opened up new avenues for thought. Richard Feynman is considered the father of modern nanotechnology because of his visionary 1959 lecture, "There's Plenty of Room at the Bottom," where he proposed the concept of manipulating individual atoms and molecules. This sparked significant interest in the field, leading to the development of nanoscience and nanotechnology in the early 21st century. The US's national science ambitions were heavily influenced by Feynman's fame and his notion of manipulating matter at the atomic level. In a speech at Caltech on January 21, 2000, President Bill Clinton argued for financing research in this new field. The 21st Century Nanotechnology Research and Development Act was signed into law by President George W. Bush three years later (National Nanotechnology Initiative, 2015). Nano-technology has rapidly expanded and developed into the foundation for incredible industrial applications during the past fifty years or so. For example, in the pharmaceutical communities of practice, nanotechnology has had a major impact on medical devices such as drug delivery systems, imaging probes, and diagnostic biosensors. (Nie *et al.*, 2007). Nowadays, the food and cosmetics industries make extensive use of nano-materials to improve bioavailability, shelf life, packaging, and manufacturing. Zinc oxide quantum dot

NPs are used to demonstrate anti-microbial activity against food-borne microorganisms (Jin *et al.*,2009). These days, nano-technology affects people's daily life. The potential advantages are numerous and varied. However, there are many worries about possible health and environmental hazards as a result of the widespread human exposure to NPs. These concerns gave rise to other scientific disciplines such as nanotoxicology and nanomedicine. Nanotoxicology is the study of potential negative health effects of nanoparticles (Oberdörster *et al.*,2005). Tissue engineering, biomaterials, biosensors, and bioimaging are subsectors of nanomedicine, which was created to investigate the advantages (Egusquiaguirre *et al.*,2012; Gu *et al.*,2013) and risks (Chen and Schluesener,2008) of nanomaterials used in medicine and medical devices. Some potential benefits of medical nanomaterials include better surgical tissue repair, reduced inflammation, antimicrobial coatings for medical equipment, enhanced medication delivery, and the detection of circulating cancer cells. However, the absence of reliable toxicity data means that the potential to affect human health is still a major concern (Shah *et al.*,2021).

Nanotechnology is the process of developing and building nanostructured materials for a range of applications. To comprehend and modify the physical and chemical properties of nanomaterials, which have at least one dimension of around 1 to 100 nm, this crucial technology is required. Although "nano" is merely a prefix for "10⁻⁹," the world of materials becomes fascinating as materials reach smaller than 100 nanometers (Shah *et al.*,2021). The field of nanobiotechnology is the subfield of nanotechnology that focuses on the biological realm (Logothetidis,2012). Three types of nanoparticles are used in biology: organic, inorganic and mixed (organic/inorganic). Nanomaterials can transform into functionalized alternatives that are reusable. Common types of nanomaterials include fullerenes, dendrimers, quantum dots (QDs), and nanotubes. (Khalid *et al.*,2020). Due to their unique physical and chemical characteristics that distinguish them from their bulk equivalents, including chemical reactivity, strength and hardness, electrical resistivity, electrical conductivity, diffusivity, and varied and adaptive biological activity. Research interest in nanomaterials has grown exponentially (Holban *et al.*,2016). NPs are composed of three layers since they are not simple molecules: (a) the surface layer, which can be functionalized using a range of small molecules, metal ions, polymers, and surfactants; (b) the shell layer, which is entirely distinct from the core chemically; and c)the core, which is essentially the NP's centre and usually refers to the NP itself (Shin *et al.*, 2016;

Khan *et al.*,2019). For many uses, including analytical chemistry, nanoparticles are especially intriguing (Sajid & Płotka-Wasyłka,2020) and anti-microbial activity (Dewan & Hateet,2023; Alewi & Hateet,2023; Hassan *et al.*,2023; Maktoof & Hateet, 2024) For example, gold (AuNPs), silver (AgNPs), and platinum (PtNPs) have been applied in cosmetics to the pharmaceutical product; some known metallic NPs including selenium (SeNPs) (Shoeibi & Mashreghi,2017) , copper (Hassan *et al.*,2023), iron (Fe) (Fahmy *et al.*,2018), and zinc oxide (Neamah *et al.*,2023) have also been used in anti-microbial applications, medical treatment and cosmetics preparation.

2.2 Nanoparticles (NPs)

A nanoparticle, which is much smaller than the world of common objects, and is characterized by Newton's laws of motion, but larger than an atom or simple molecule, which is susceptible to quantum mechanics, is the most fundamental building component for making a nanostructure. (Horikoshi & Serpone,2013) The nanoparticles exhibit unique physical, chemical, and biological properties at the nanoscale as opposed to their counterparts at greater dimensions. The causes of this phenomenon include increased mechanical strength, a relatively higher surface area to volume, increased reactivity or stability in a chemical process, etc (Ealia & Saravanakumar,2017) Generally speaking, NPs range in size from 1 to 100 nm. Metallic nanoparticles (NPs) differ from bulk metals in their chemical and physical characteristics, such as their greater specific surface areas, lower melting temperatures, tensile strengths, point-specific optical properties, and specific magnetizations. These differences may make metallic NPs appealing for a variety of industrial applications (Horikoshi & Serpone,2013). Size and shape are two of the primary parameters examined in the characterization of NPs. Additionally, we may assess the surface chemistry to some degree and estimate the size distribution, degree of aggregation, surface charge, and surface area (Minelli,2016). Other characteristics and potential uses of the NPs may be impacted by the size, size distribution, and organic ligands on their surface. Additionally, as a preliminary step following nanoparticle manufacturing, the NPs' crystal structure and chemical makeup are carefully examined (Mourdikoudis *et al.*,2018).

There are relationships between NPs toxicity and their Physical and Chemical Properties:

1- The size and surface area of the NP play a major role in determining its unique mechanism of interaction with living systems. The high reaction capacity and catalytic activity of NPs are determined by their extremely large specific surface area.

2- NPs are characterized by their ellipsoids, cylinders, sheets, cubes, rods, spheres, and cylinders. The form of NPs greatly influences their toxicity.

3- Even though NPs' size and shape have a significant impact on their toxicity, other elements like their chemical makeup and crystal structure also have a role (Sukhanova *et al.*,2018).

4- The crystal structure of NPs affects their toxicity as well. A human bronchial epithelial cell line and titanium oxide nanoparticles with various crystal lattice types have been used to investigate the connection between crystal structure and toxicity.

5- Since it essentially dictates how NPs interact with biological systems, their surface charge has a significant impact on their toxicity.

6- NPs must have a shell applied to their surface to alter their optical, magnetic, and electrical characteristics. This shell is used to increase the stability of NPs, decrease their aggregation capacity, and improve their biocompatibility and solubility in water and biological fluids. As a result, the shell makes NPs less harmful and gives them the ability to interact selectively with various cell types and biological substances. Furthermore, the shell has a significant impact on NP pharmacokinetics, altering the patterns of NP accumulation and distribution within the body (Sukhanova *et al.*,2018).

2.3 Preparation Method of Nanostructures

2.3.1 Top-down and Bottom-up Approaches

The synthesis of NPs is categorized into two classes, namely “top-down” and “bottom-up” based on the way of NPs formation Fig (1.1). The top-down method, The destructive approach is applied in this synthesis. After breaking down into smaller molecules, the bigger molecules (bulk material) eventually became nanoparticles. Physical vapour deposition, grinding, milling, and other destructive

techniques are examples of top-down synthesis (Ijaz et al.,2020). Using several characterisation approaches, they found that milling duration had an impact on the total size of the nanoparticles. According to the Soherer equation, it was found that as milling time increased, the crystal-lite size of the nanoparticles shrank. X-rays show that the particle size gets smaller with time. Additionally, the SEM result matched the X-ray pattern. (Ijaz et al.,2020) The synthesis of colloidal carbon spherical particles with sizes ranging from 20 to 50 nm was done using the top-down method.

Since NPs are made from comparatively simpler materials, the bottom-up method—also known as the building-up approach—is used in reverse. Techniques like sedimentation and reduction serve as examples of this. It consists of spinning, biological synthesis, green synthesis, and sol-gel (Khan *et al.*,2019). Precursors or raw materials should be in molecular dispersion, or previously dissolved, to allow the addition of an antisolvent or to create an environment that promotes the formation of nanoparticles. This is a common feature of the methods developed by this approach; the use of surfactants or stabilizers is crucial in these methods (Alcalá et al.,2023). Among the bottom-up methods are electrodeposition, hydrothermal synthesis, colloidal precipitation, sol-gel synthesis, and organometallic chemical routes.

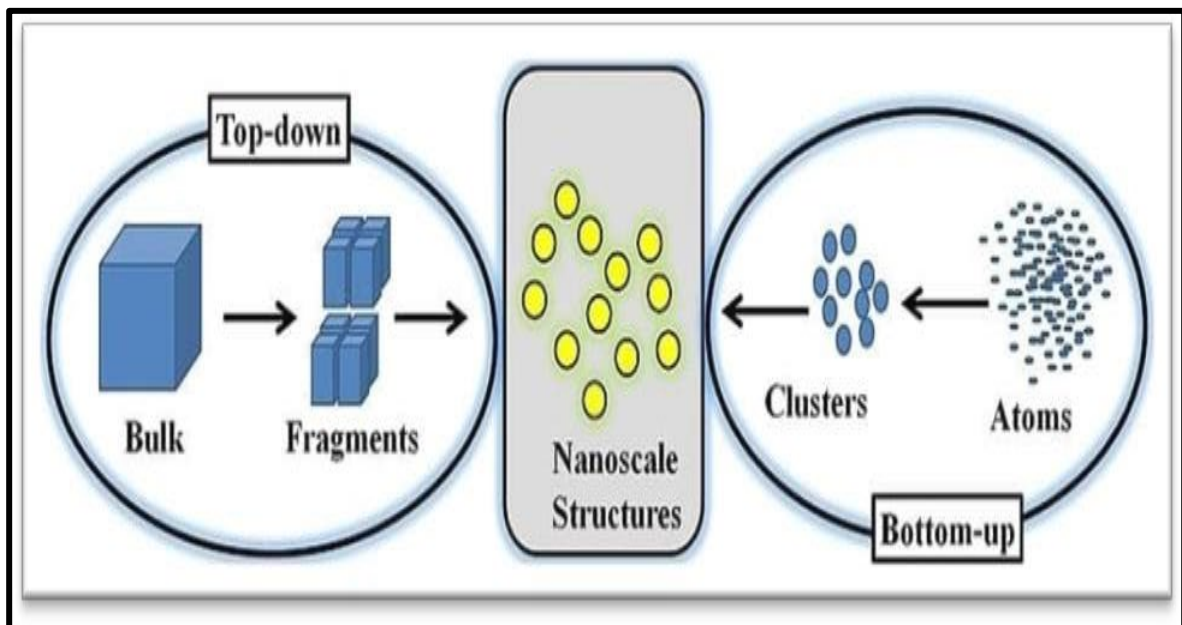


Fig (1.1) Approaches of NPs synthesis (Böhringer& Rutherford,2008)

2.4 Classification of Nanomaterials Based on Origin

2.4.1 Natural Nanomaterials

Examples of the variety of natural nanomaterials found in nature include viruses, protein molecules, minerals like clay, natural colloids like milk and blood (liquid colloids), fog (aerosol type), gelatin (gel type), mineralized natural materials like shells, corals, and bones, ocean spray, lotus leaves, gecko feet, spider silk, insect wings and opals, and volcanic ash (Khan & Hossain,2022).

2.4.2 Artificial Nanomaterials

Examples of artificial nano-materials that are purposefully created utilizing exacting mechanical and manufacturing processes are carbon nano-tubes and semiconductor NPs like quantum dots (QDs). Depending on their structural composition, nanomaterials are classified as metal-based materials, dendrimers, or composites (Khan & Hossain,2022).

2.5 Classification of Nanomaterials based on the Structural Configuration/Composition

NPs can be roughly categorized into four types based on their structural composition: composite, inorganic, carbon-based, and organic/dendrimers:

2.5.1 Organic Nanomaterials

Organic molecules are transformed into organic nanomaterials at the nanoscale. Micelles, ferritin, dendrimers, and liposomes are a few types of organic nanoparticles or polymers.

2.5.2 Inorganic Nanomaterials

Since they don't include carbon atoms, they are referred to as inorganic nanoparticles. Generally speaking, metal-based or metal oxide-based nanomaterials make up inorganic NPs.

2.5.3 Carbon-based Nanomaterials

Graphene, fullerenes, carbon nanotubes, carbon nanofiber, and carbon black are the five primary components of carbon-based nanomaterials. Fullerenes,

which are carbon nanoparticles arranged in spherical and ellipsoidal shapes, are known as Buckyballs.

2.5.4 Composites Nanomaterials

Combinations The components of nanomaterials include nanoparticles mixed with bulk materials, nanoparticles mixed with larger-scale materials, and nanoparticles mixed with other nanoparticles (Khan & Hossain,2022).

2.6 Nanomaterial Classification Based on the Number of Dimensions:

According to their size dimensions, nano-materials are divided into four categories, as illustrated in fig. (1.2): 0D, 1D, 2D, and 3D.

2.6.1 Zero-dimensional nanostructures

Every material's dimensions are measured at the nanoscale. The 0-D dimensions are all smaller than 100 nm. Nanoparticles are the most prevalent type of zero-dimensional nanomaterial

2.6.2 One-dimensional nanostructure

Nanoscale materials are not one-dimensional. This produces nanoparticles that resemble needles. One-dimensional materials include nanowires, nanorods, and nanotubes.

2.6.3 Two-dimensional nanostructures

Two-dimensional materials could be seen as existing outside of the nanoscale. Two-dimensional nanomaterials can take the shape of plates.

2.6.4 Three-dimensional nanostructures

The fact that these materials have three arbitrary dimensions larger than 100 nm directly causes them to differ from one another. Some materials possess characteristics like the presence of structures at the nanoscale or nanocrystalline formations. Nanoscale characteristics of three-dimensional nanomaterials include multi-nanolayers, nanoparticle dispersions, bundles of nanowires and nanotubes, and other nanoscale structures (Mekuye & Abera, 2023).

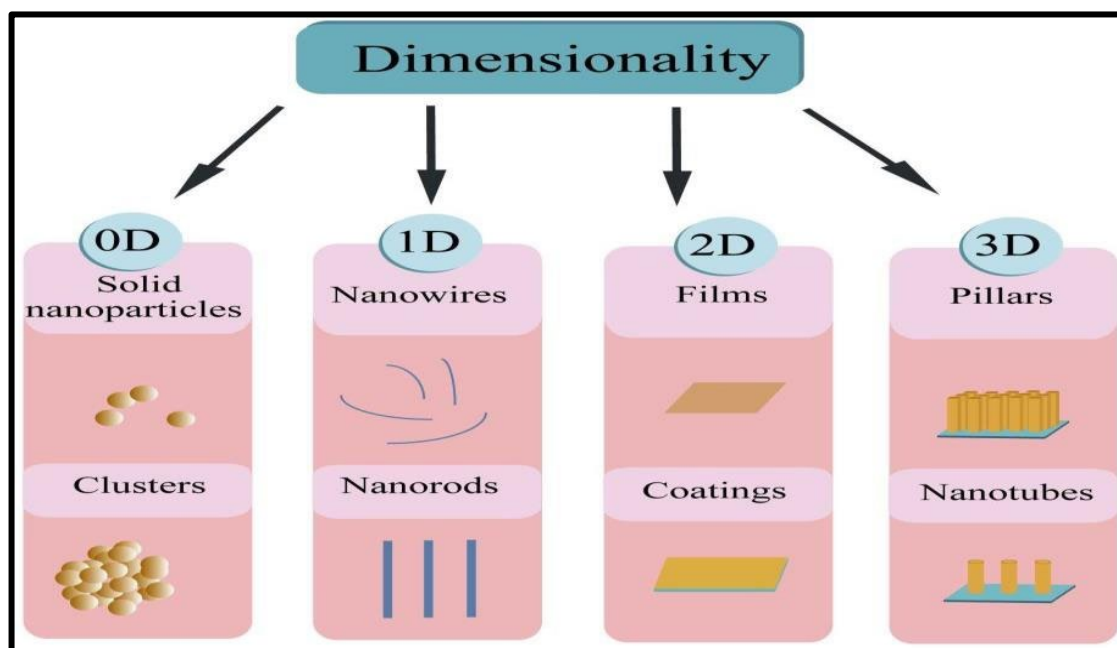


Fig (1.2) Classification of Nanomaterials (a) 0D clusters and spheres, (b) 1D nanofibers, rods, and wires, (c) 2D films, networks, and plates, (d) 3D Bulk Nanomaterial (Bhattacharya *et al.*,2022)

2.7 Nanoparticle Synthesis Methods

2.7.1 Physical Methods

Using a variety of physical processes that modify materials at the nanoscale, physical techniques of nanoparticle production create NPs. These techniques provide exact control over the content, size, and form of the particles (Yadav *et al.*,2023). Some common physical methods include: the melting mixing method, Laser pyrolysis method, Pulsed wire discharge method and high ball milling method Fig (1.3).

2.7.2 Chemical Methods

The most common, prolific, and effective techniques for creating metallic nanoparticles are chemical ones. These techniques don't require complicated equipment and are said to be quick, simple, convenient, and affordable (for large-scale production). Additionally, there is little to no stability loss when the finished nanoparticles are stored for extended periods (Szczyglewska *et al.*,2023). Some common chemical methods include the chemical reduction of metal salts, sol-gel method, micro-emulsion and sono-chemical method Fig (1.3).

2.7.3 Biological Methods

The utilization of biological and green technologies to manufacture different MNPs is becoming more and more popular among the many synthetic methods for MNP preparation that have recently been established, including chemical, photochemical, and thermal processes (Khan et al.,2022). Plant parts, fungi, and bacteria are examples of biogenic sources that efficiently contribute to the stability of NPs Fig (1.3). Because the process can be modified by varying the culture factors, including nutrition, pH, pressure, and temperature, bacteria, yeast, and fungus are used in the environmentally friendly creation of NPs (Yadav et al.,2023). The majority of these techniques are highly costly and entail the use of dangerous and poisonous chemicals that could endanger human health and the environment. Therefore, the use of environmentally benign materials to produce metal nanoparticles is something that materials scientists and nanochemists are looking forward to (Khan *et al.*,2022). The goal of nanobiotechnology is to create nanostructures from living things. Plants have discovered uses in the biological synthesis of nanoparticles, particularly in the synthesis of metal nanoparticles. Because it does not require the complicated process of sustaining cell culture, using plants to synthesis nanoparticles may be more environmentally friendly than other biological techniques. Using plants or their extracts to create nanoparticles extracellularly and controlling their size, shape, and dispersion will make the nanoparticle manufacturing process more beneficial (Khan *et al.*,2022).

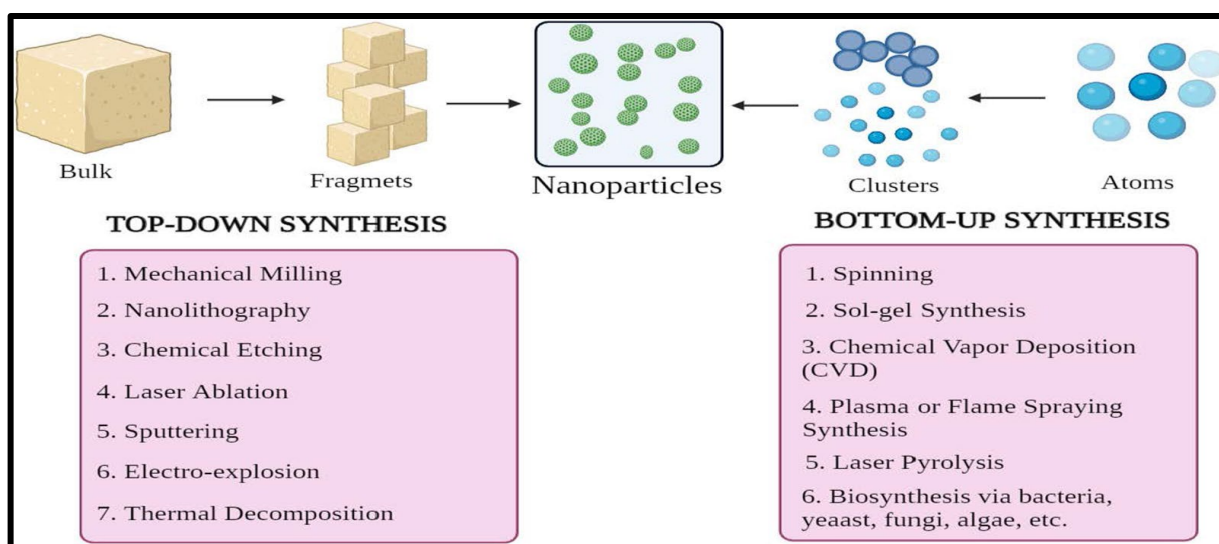


Fig (1.3) Numerous methods of Nanoparticles synthesis (Gavas *et al.*,2021)

2.8 Applications of Biosynthesized NPs

The physicochemical characteristics of NPs—such as their size, form, crystal structure or lack thereof, surface charge, solubility, etc.—will be crucial in determining their applications. NPs materials have several uses and are becoming increasingly significant in both industry and human life (Madkour,2017). For decades, nontechnology has been used in the food industry to enhance the quality, flavour, and texture of foods while shielding them against pathogen infestations. Because nanotechnology inhibits microbial infestations, it extends the shelf life and enhances food storage (Zaib & Iqbal,2019). Researchers are also looking at the potential use of nanomaterials in the food industry, veterinary care, agriculture, and cosmetics. Silver, gold, zinc, selenium, titanium dioxide, and carbon nanotube nanoparticles are among the materials of special interest Fig (1.4). Nanotechnology has several uses in the field of medical bioengineering. The primary application of nanotechnology in this field is in diagnostic testing, where it is employed as a tool for disease diagnosis, imaging, and pharmacological therapy monitoring (mainly the system of drug delivery and disposition in the human body) (Madkour,2017)). The development of nano-polymers has made nanotechnology a crucial component in food processing and packaging. Toxic substances, pollutants, and pathogens in food can be detected using nanosensors (Zaib & Iqbal,2019). In food microbiology, nanomaterials provide a high degree of sensitivity. Nanobiosensors are designed to identify microorganisms in food materials, plants, and food ingredient quantification, alerting suppliers and consumers to the state of food safety. Additionally, it serves as an indicator that responds to environmental changes in storage spaces, microbiological contamination, and product degradation (Zaib & Iqbal,2019).

Nanocomposites, which can perform better electrochemically than single-structured materials, have recently drawn attention for their manufacture and use in supercapacitors. These promising findings indicate a lot of promise for creating high-capacitive energy storage devices for real-world uses., Additionally, nanoparticles are employed in a variety of commercial applications, primarily in food preservatives, pharmaceutical coating materials, and cosmetics (Madkour,2017). Fig (1.4). Also, gold nanoparticles (AuNPs) have been specifically employed in cancer therapy for capillary electrophoresis, protein assay, immunoassay, and cancer cell detection. Gold nanoparticles have generated a lot of interest in the medical field. Biomarkers can be utilized for biological screening exams. Following cellular absorption, they act as precise and potent heaters to eradicate tumours. They can also

cause B cell-chronic lymphocytic leukaemia to undergo apoptosis (Jadoun *et al.*,2021). Because of their small size, silver nanoparticles (AgNPs) may easily pass across the blood-brain cellular barrier and narrow epithelial junctions, making them valuable drug conveyors. Because of their increased surface area-to-volume ratio, it also improve the pharmacokinetics and biodistribution of therapeutic components, which lowers toxicity by allowing them to assemble at the desired location. (Moghaddam *et al.*, 2015). AgNPs are one type of metal nanoparticle that has been extensively studied for use in surgical gloves and covers, antibacterial wound dressings, bed lines, and other applications. They also have several uses in the field of indicative treatments (Purohit *et al.*,2019)

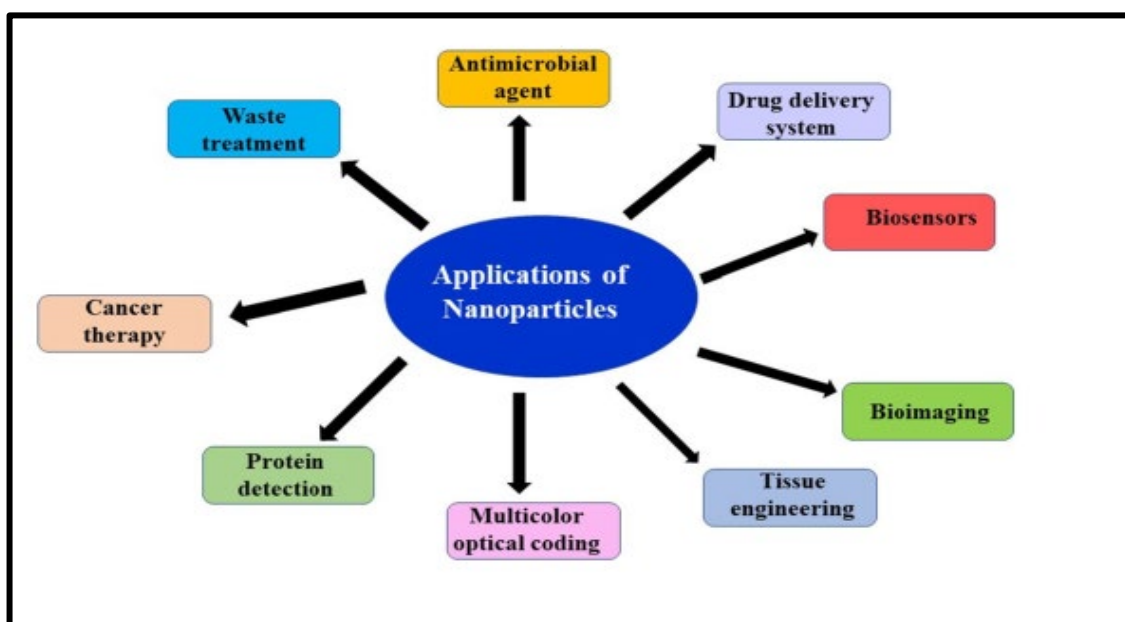


Fig (1.4) Applications of green synthesized nanoparticles in environmental and biomedical fields (Jadoun *et al.*,2021)

2.9 Types of NPs

A new age of scientific discovery has been brought about by nanobiotechnology, where the special qualities of nanomaterials—like gold nanoparticles—have been used for a variety of purposes (Karnwal *et al.*,2024) Noble elements like gold, silver, and palladium in the form of NPs are among the most promising developments in nanotechnology, particularly for the development of bioengineering materials that may be employed as state-of-the-art diagnostic instruments and medical treatment devices for serious illnesses. For instance,

because of their special qualities and numerous uses, silver and gold NPs are often very important in the fields of nanotechnology and materials science (Burlec *et al.*,2023) Over the past few decades, gold nanoparticles (AuNPs) have drawn a lot of attention. Their uses and properties have been studied in a variety of fields, including biology, medicine, and physical and chemistry (Sadiq *et al.*,2024). However, the production of silver nanoparticles has a significant impact on their diverse range of uses. To put it another way, these elements are essential for managing applications of silver nanoparticles. Due to their high electrical and thermal conductivity, silver nanoparticles (NPs) have found application in electronics, where they are found in conductive adhesives, inks, and electronic components (Duman *et al.*,2024). Despite the encouraging antibacterial qualities of Ag and Au NPs, several issues need to be resolved before their full promise in clinical applications can be realized. The emergence of bacterial resistance to silver nanoparticles is one new problem. The effectiveness of silver nanoparticles as antibacterial agents is seriously threatened by this resistance. To combat this, novel approaches are being investigated to prevent the development of resistance, such as the use of Trojan horses, such as proteins (Aguilar-Garay *et al.*,2024). Furthermore, the special properties of AgNPs allow for broad use in a variety of fields, such as electronics, chemical and biological sensors, materials, and pharmaceutical and cosmetic goods (Nguyen *et al.*,2023)

Of these NPs, silver oxide Ag₂O NPs have attracted the greatest attention due to their intriguing characteristics and diverse range of biological activities. Ag₂O nanoparticles, also known as silver oxide nanoparticles, have garnered significant interest recently in many fields due to their distinct physicochemical properties and the vast range of potential uses (Muhammad *et al.*,2023). Strong antibacterial and antifungal properties, biocompatibility, and the capacity to promote electron transfer reactions make Ag₂O nanoparticles very valuable (Gungure *et al.*,2024). Because of these characteristics, Ag₂O nanoparticles are being investigated for a variety of uses, such as gas sensors (Muhammad *et al.*,2023) drug delivery (Thakur *et al.*,2021), and antimicrobial activities (Patel & Joshi,2023)

Therefore, the most researched nanomaterials with intrinsic antibacterial qualities have been metal and metal oxide-based NPs (such as silver, gold, copper, zinc, and all of their oxide derivatives). It should be noted that certain research has shown that different metallic nanoparticles are harmful and aid in the development of antibiotic resistance (Sans-Serramitjana *et al.*,2023). Because metalloid-based

NPs (such tellurium and selenium) are intermediate between metals and non-metals, they can be used in a variety of applications. As a result, they have garnered growing attention. Because of their antioxidant properties, SeNPs may play a useful role in the biomedical area (Bai *et al.*,2017) and anti-cancer properties (Varlamova *et al.*,2021), antimicrobial activity (Truong *et al.*,2021), and immunoregulatory properties (Jin *et al.*,2021). SeNPs have a wide range of effectiveness against bacteria and fungi, according to numerous reports (Lin *et al.*,2021)

2.10 Green Synthesis of NPs

Comparing the green production of nanoparticles using living cells through biological pathways to other biological, physical, and chemical processes, the former is more effective, produces a higher mass, is non-toxic, economical, and more stable (Vijayaram *et al.*,2024). Because it lessens the need for hazardous chemicals and harsh synthetic conditions that are often employed in the manufacture of nanoparticles, green synthesis offers both technical and environmental advantages. This environmentally benign method produces NPs that are appropriate for use in biomedical applications (Pechyen *et al.*,2024). Both unicellular and multicellular organisms have been widely employed as biological agents for the manufacture of metallic nanoparticles. Bacteria, fungi, plant extracts, algae, diatoms, viruses, yeast, and some higher species like earthworms are a few noteworthy examples (Samuel *et al.*,2022). An essential tool for preventing hazardous byproducts through environmentally friendly and sustainable development is a biosynthetic method. A variety of biological structures, including plant extracts, bacteria, yeast, seaweeds, and algae, use the biosynthesis process to create metal and metal oxide nanoparticles (Vijayaram *et al.*,2024).

2.10.1 NPs Biosynthesis by Bacteria

The intracellular and extracellular techniques are the two approaches for NP synthesis that have been documented: Compared to the intracellular approach, the extracellular method is preferred because it is simpler to harvest and purify NPs. Extracellular and intracellular material produced by bacteria serves as a reducing agent when combined with Ag or Au solution to create NPs (Qamar *et al.*,2021). It's an excellent idea to research bacteria. In addition, they grow quickly, are cheap to grow, and are simple to work with. It is simple to regulate growth parameters like temperature, oxygenation, and incubation duration (Pantidos & Horsfall,2014).

In recent work, Srinath and Rai demonstrated how the bacteria *Enterobacter aerogenes* produces pure AuNPs (Srinath, & Rai,2015). Additionally, some of the research that used certain bacterial species to biosynthesize silver nanoparticles (AgNPs) include (Ibrahim & Hateet,2021). (Dewan&Hateet,2023) and in another study selenium nanoparticles (SeNPs) were obtained by bacteria lactic acid bacteria (Stabnikova *et al.*,2023).

Table (1.1) Some types of bacteria produced different NPs

Bacteria	Type	Size (nm)	References
1- <i>Pseudomonas aeruginosa</i>	Te	-	Trutko <i>et al.</i> , 2000
2- <i>Geobacter ferrireducens</i>	Au	-	Kashefi <i>et al.</i> , 2001
3- <i>Escherichia coli</i>	CdS	2-5nm	Sweeney <i>et al.</i> ,2004
4- <i>Staphylococcus epidermidis</i>	Te	-	Calderón <i>et al.</i> ,2006
5- <i>E. coli</i> DH 5α	Au	8-25nm	Du <i>et al.</i> ,2007
6- <i>Shewanella alga</i>	Au	10-20nm	Konishi <i>et al.</i> ,2007
7- <i>Rhodopseudomonas capsulate</i>	Au	10-20nm	He <i>et al.</i> ,2007
8- <i>Geobacter sulfurreducens</i>	Ag	-	Law <i>et al.</i> , 2008
9- <i>Bacillus megaterium</i> D01	Au	2.5nm	Wen <i>et al.</i> ,2009
10- <i>Rhodopseudomonas sphaeroides</i>	PbS	10nm	Bai and Zhang ,2009
11- <i>Lactobacillus</i> sp.	TiO ₂	8-35nm	Jha <i>et al.</i> 2009a
12- <i>Shewanella oneidensis</i>	Fe ₃ O ₄	40-50nm	Perez-Gonzalez <i>et al.</i> 2010
13- <i>Bacillus licheniformis</i>	Ag	-	Vaidyanathan <i>et al.</i> 2010
14- <i>Enterobacter cloacae</i>	Ag	28-122nm	Ahmad <i>et al.</i> ,2010
15- <i>Klebsiella pneumonia</i>	Ag	28-122nm	Ahmad <i>et al.</i> ,2010
16- <i>Escherichia coli</i>	Cd	3-2nm	Bao <i>et al.</i> , 2010
17- <i>Pseudomonas proteolytica</i>	Ag	6-13nm	Shivaji <i>et al.</i> ,2011
18- <i>Lactobacillus casei</i>	Ag	20-50nm	Korbekandi <i>et al.</i> ,2012
19- <i>Actinobacter</i>	Au	13.2nm	Golinska <i>et al.</i> , 2016
20- <i>Klebsiella pneumonia</i>	Au	10-15nm	Prema <i>et al.</i> , 2016
21- <i>Bacillus cereus</i>	Au	40-50nm	Pourali <i>et al.</i> , 2017
22- <i>Bacillus endophyticus</i>	Ag	5.1nm	Gan <i>et al.</i> , 2018
23- <i>Streptomyces spp</i>	Ag	20-50nm	AL Dhabi <i>et al.</i> , 2018
24- <i>Rhodobacter sphaeoides</i>	Au	3-10nm	Italiano <i>et al.</i> , 2018
25- <i>Shewanella loihica</i>	Cu	10-16nm	Lv <i>et al.</i> , 2018
26- <i>Bacillus brevis</i>	Ag	41-68nm	Saravanan <i>et al.</i> , 2018
27- <i>Bacillus marisflav</i>	Au	12-30nm	Nadaf and Kanase, 2019
28- <i>Bacillus siamensis</i>	Ag	25-50nm	Ibrahim <i>et al.</i> , 2019
29- <i>Streptomyces spp</i>	CuO	78-80nm	Hassan <i>et al.</i> , 2019

30- <i>Escherichia coli</i>	Ag	14-19nm	Hashim, 2020
31- <i>Enterococcus faecalis</i>	ZnO	16-96	Kelmani, 2020
32- <i>Staphylococcus lentus</i>	Ag	20-90nm	Ibrahim &Hateet,2021
33- <i>Microbacterium sp</i>	Ag	-	Dewan&Hateet,2022
34- <i>Microbacterium sp</i>	Ag	-	Dewan&Hateet,2023
35- <i>Nocardia asteroides</i>	AuO	-	Hassan <i>et al.</i> ,2023
36- <i>Streptomyces fradia</i>	Pt	-	Makhtoof&Hateet,2024

2.10.2 NPs Biosynthesis by Fungi

All of the biological reactions that an organism performs can be combined to form its metabolism. Usually limited to tiny molecules, metabolites are the products and intermediates of metabolism (Thirumurugan *et al.*,2018). Complex metabolic processes in microorganisms rely on substrates, cofactors, enzymes, gene control, and intermediates to produce final products (Conrado *et al.*,2022). Enzymes, fermented foods, animal feed, antibiotics, pharmaceutical products, and pigments are just a few examples of the microbiological groups of fungi and their products that have greatly benefited humans and several biotechnological industries (Shankar & Sharma,2022). Numerous fungal species have shown encouraging traits as biological materials for AuNP production. Depending on the microbiological site of AuNPs production, the biosynthesis pathway may be extracellular or intracellular (Brandelli & Veras,2023). Gold ion absorption by the fungal cell wall by proteins, polysaccharides, or electric absorption, as well as gold ion reduction by enzymes, proteins, and other cytoplasmic redox mediators in the cytoplasm or cell wall, are necessary for the processes of intracellular AuNPs formation (Xu *et al.*,2024).

The metabolites outside of fungal cells, such as proteins, peptides, enzymes, and phenolic metabolites, are primarily responsible for the extracellular synthesis of AuNPs (Xu *et al.*,2024). Although the significance of AuNPs has grown recently, there are fewer examples of their synthesis by fungus than those made of AgNPs. Unlike the bulk form of gold, AuNPs are reactive due to their small size, which makes them perfect for usage as catalysts and precursors in electronics applications (Pantidos & Horsfall,2014). According to Clarence *et al.*, AuNPs were synthesized utilizing *Fusarium solani*, and intracellular AuNPs were found to be localized on the mycelia's surface by the biological reduction of AuCl₄ (Clarence *et al.*,2020) Vahabi *et al.* used *Aspergillus fumigatus* to create extra-cellular AgNPs that ranged in size from 5 to 25 nm (Vahabi *et al.*,2011). Research has also been

done on the production of SeNPs from a particular fungus. For instance, research has shown that the fungus *Fusarium semitectum* may generate selenium nanoparticles, which can subsequently be utilized as antimicrobial and anti-cancer medications (Abbas & Abou Baker,2020). This study found two fungus isolates: *Rhizopus arrhizus* and *Penicillium citrinum*. According to the results, SeNPs were generated in consistent spherical shapes, with the majority of them being between 50 and 80 nm in size (Gharieb *et al.*,2023).

Table (1.2) Some types of fungi produced different NPs

Fungi	Type	Size (nm)	References
1- <i>Verticillium</i>	Ag	21-25nm	Mukherjee <i>et al.</i> ,2001
2- <i>Aspergillus fumigates</i>	Ag	5-25nm	Bhainsa &Souza,2006
3- <i>Fusarium semitectum</i>	Ag	10-60nm	Basavaraja <i>et al.</i> ,2007
4- <i>Saccharomycescerevisiae</i>	Sb ₂ O ₃	2-10nm	Jha <i>et al.</i> , 2009
5- <i>Fusarium solani</i>	Ag	3-35nm	Ingle <i>et al.</i> ,2009
6- <i>Penicillium fellutanum</i>	Ag	5-25nm	Kathiresan <i>et al.</i> ,2009
7- <i>Rhizopus nigricans</i>	Ag	35-40nm	Ravindra & Rajasab,2014
8- <i>Pencillium verrucosum</i>	Ag	3-24nm	kamalakannan <i>et al.</i> ,2014
9- <i>Pencillium notatum</i>	Ag	30-40nm	Desai &Datta, 2015
10- <i>Magnusiomyces ingens</i>	Au	10-80nm	Zhang <i>et al.</i> , 2016
11- <i>Aspergillus spp</i>	Au	4-29nm	Shen <i>et al.</i> , 2017
12- <i>Trichoderma harzianum</i>	Au	32-44nm	Tripathi <i>et al.</i> , 2018
13- <i>Chaetomium globosum</i>	Au,Ag	6-40nm	Singh <i>et al.</i> , 2018a
14- <i>Pleurotus ostreatus</i>	Au	10-30nm	El Domany <i>et al.</i> ,2018
15- <i>Thermoascus thermophilus</i>	Au	10nm	Molnar <i>et al.</i> , 2018
16- <i>Fusarium oxysporum</i>	Ag	21-37nm	Ahmed <i>et al.</i> , 2018
17- <i>Trichoderma hamatum</i>	Au	5-30nm	Abdel-Kareem & Zohri,2018
18- <i>Fusarium oxysporum</i>	Au	10-25nm	Pourali <i>et al.</i> , 2018
19- <i>Aspergillus niger</i>	ZnO	53-69nm	Kalpana <i>et al.</i> , 2018
20- <i>Fusarium semitectum</i>	Se	40-80nm	Abbas & Abou Baker,2020
21- <i>Penicillium citrinum</i> (MEBPOO1)	Au	-	Alewi &Hateet,2022
22- <i>Penicillium citrinum</i>	Se	50-80nm	Gharieb <i>et al.</i> ,2023
23- <i>Rhizopus arrhizus</i>	Se	-	Gharieb <i>et al.</i> ,2023
24- <i>Aspergillus fumigatus</i>	Au	-	Alewi &Hateet,2023

2.10.3 NPs Biosynthesis by Plants

Secondary metabolites from plants are extremely important goods from an economic standpoint. These are high-value chemicals used in things like medications, dyes, pesticides, tastes, and scents. Numerous secondary metabolites found in plants, including flavonoids, alkaloids, terpenoids, and tannins, have been shown to possess antibacterial qualities in vitro (Thirumurugan *et al.*,2018) . The ability of bacteria and fungi to synthesize metallic nanoparticles has been the subject of much research in recent decades, while plants have received less attention in this regard. A growing amount of research has been conducted in the last ten years on the environmentally friendly synthesis of metallic NPs utilizing plants or plant extracts (Pantidos & Horsfall,2014) Since gold nanoparticles are superior to other metallic nanoparticles in terms of their exceptional medical and nonmedical qualities and applications, research (Shahriari *et al.*,2019) Clean, fresh *Allium noeanum* leaves Reut. Ex Regel leaves have been utilized for their cytotoxicity, antioxidant, and antibacterial qualities as well as for the creation of gold NPs

In studies including (Bharadwaj *et al.*,2021),(Diksha *et al.*,2023) gold nanoparticles were manufactured from some types of plants. Silver nanoparticles (AgNPs) were synthesized by green approach from methanolic leaf extract of *Blighia sapida* and used in antioxidant activity (Akintola *et al.*,2020). Al Sufyani *et al.* discussed the production of silver nanoparticles using aqueous *Olea chrysophylla* and *Lavandula dentata* leaf extracts and the change of colour to dark brown of AgNPs then characterization revealed their crystalline shape with a mean size of 284.5 nm (Al Sufyani *et al.*,2019). Numerous studies have also examined the production of selenium nanoparticles from specific plants or plant extracts. For example, one study used a solution of selenium acid (H₂SeO₃) in conjunction with a plant leaf extract from *Withania somnifera* to produce green synthesis. when this combination was agitated, Se NPs coupled with secondary metabolites of *W. somnifera* were dispersed (Alagesan & Venugopal,2019).In another study, several plants have been already reported for the preparation of SeNPs (Pyrzynska & Sentkowska,2021).

Table (1.3) Some types of Plants produced different NPs

Plants	Type	Size (nm)	References
1- <i>Pelargonium roseum</i> (<i>rose geranium</i>)	Au	2-27nm	Shankar <i>et al.</i> ,2003

2- <i>Aloe barbadensis</i> Miller (<i>Aloe vera</i>)	Au, Ag	-	Chandran <i>et al.</i> ,2006
3- <i>Cinnamomum camphora</i> (<i>camphor tree</i>)	Au, Ag	55-80nm	Huang <i>et al.</i> ,2007
4- <i>Coriandrum sativum</i> (<i>coriander</i>)	Au	6-57nm	Narayanan& Sakthivel,2008
5- <i>Acalypha indica</i>	Ag	20-30nm	Krishnaraj <i>et al.</i> ,2009
6- <i>Brassica juncea</i> (<i>mustard</i>) Silver	Ag	2-35nm	Haverkamp& Marshall,2009
7- <i>Pear fruit extract</i>	Au	-	Ghodake <i>et al.</i> ,2009
8- <i>Gardenia jasminoides</i> Ellis (<i>gardenia</i>)	Pd	-	Jia <i>et al.</i> ,2009
9- <i>Syzygium aromaticum</i> (<i>clove buds</i>)	Au	5-100nm	Raghunandan <i>et al.</i> ,2010
10- <i>Tanacetum vulgare</i> (<i>tansy fruit</i>)	Au, Ag	11nm	Dubey <i>et al.</i> ,2010
11- <i>Garcinia mangostana</i> (<i>mangosteen</i>)	Ag	10-30nm	Veerasamy <i>et al.</i> ,2010
12- <i>Terminalia catappa</i> (<i>almond</i>)	Au	10-35nm	Ankamwar,2010
13- <i>Cycas sp. (cycas)</i>	Ag	2-6nm	Jha &Prasad,2010
14- <i>Nelumbo nucifera</i> (<i>lotus</i>)	Ag	25-80nm	Santhoshkumar <i>et al.</i> ,2011
15- <i>Tragia involucrate</i>	Pt	10nm	Selvi <i>et al.</i> ,2020
16- <i>Nigella sativa L</i>	Pt	1-6nm	Aygun <i>et al.</i> ,2020
17- <i>Mentha arvensis</i>	TiO	20-70nm	Ahmad <i>et al.</i> ,2020
18- <i>Croton sparsiflorus</i>	Au	16-17nm	Boomi <i>et al.</i> ,2020
19- <i>Litsea cubeba</i>	Au	8-18nm	Doan <i>et al.</i> ,2020
20- <i>Desmodium gangeticum</i>	Au	-	Ghosh <i>et al.</i> ,2020
21- <i>Elaeagnus umbellata</i>	Ag	40nm	Ali <i>et al.</i> ,2020
22- <i>Dionaea muscipula</i>	Ag	5-10nm	Banasiuk <i>et al.</i> ,2020
23- <i>Malus domestica</i>	Ag	16nm	Kazlagić <i>et al.</i> ,2020
24- <i>Reishi Mushroom</i>	Ag	-	Aygün <i>et al.</i> ,2020
25- <i>Cestrum nocturnum</i>	Ag	20nm	Keshari <i>et al.</i> ,2020
26- <i>Urtica dioica</i>	ZnO	20-22nm	Bayrami <i>et al.</i> ,2020
27-Lemon peel extract	TiO	-	Nabi <i>et al.</i> ,2020

2.11 Bacterial Pathogenesis

The immunological status of the host and the microbial species involved in the exposure are two important elements that determine a microorganism's

pathogenicity, or its capacity to cause disease. Microbial pathogenicity is a complex phenomenon, driven by a multifaceted interplay of genetic and molecular determinants. These determinants, encompassing virulence factors and resistance mechanisms, play crucial roles in the essential processes of disease establishment, progression, and dissemination (Biondo,2022). Zoonotic transmission plays a significant role in the emergence of infectious diseases affecting human populations. A substantial proportion, estimated at 75%, of newly identified infectious diseases have their origins in animal reservoirs. Furthermore, approximately 60% of all known human infectious diseases are attributable to zoonotic pathogens transmitted from both domestic and wild animal sources. (Salyer *et al.*,2017). Furthermore, climate change may make a significant number of dangerous diseases and their routes of transmission worse, endangering human health (Mora *et al.*,2022)

The majority of bacterial infections still have poorly understood pathogenetic pathways, and the lack of knowledge about host-microbe interactions and the intricate mechanisms by which infection is established is a significant barrier to the creation of novel medications and vaccines. Bacteria can cause disease in their hosts by a variety of methods, some of which are species-specific or species-neutral (Wilson *et a.*,2002). This clarifies the variety of target cells, infection modes, and molecular processes that underlie bacterial disease. A common characteristic of many bacterial infections is the acquisition of virulence and antibiotic-resistance genes, which can be passed horizontally to other bacteria via mobile genetic elements (such as plasmids and transposons) (Deng *et al.*,2019).

2.12 Virulence Factors of Bacterial Pathogenesis

"Virulence" is the ability of an organism to infect its host and spread disease. With the help of substances known as virulence factors, the bacterium enters the host's cells. These components fit into one of three groups: membrane-related, cytosolic, or secretory. The bacteria can quickly adapt by changing its physiology, metabolism, and morphology thanks to cytosolic factors. The virulence factors linked to the membrane let the bacteria adhere to and escape the host cell (Suleiman, 2018). The essential components that allow germs to create an infection, get past human defences, and cause illness are known as virulence factors. These components can be broadly categorized into two groups: those that promote colonization and those that aid in tissue damage. Toxins, proteases, and lipases are factors that cause tissue damage, while adhesins, pili, and capsules are factors that

promote colonization (Abdulateef *et al.*,2023). A common Gram-negative bacterium in the environment, *Pseudomonas aeruginosa* typically lives in soil, water, plants, and people (Wu and Li, 2015) The virulence factors of *P. aeruginosa* have been carefully investigated and are categorized into three basic categories, including bacterial surface structures, secreted factors and bacterial cell-to-cell interaction (Liao *et al.*,2022). One of the most significant nosocomial pathogens, *Acinetobacter baumannii*, can cause infections such as meningitis, pneumonia, urinary tract infections, septicemia, and wound infections.

Numerous virulence factors, such as outer membrane proteins, lipopolysaccharide, capsule, phospholipase, nutrient-acquisition systems, efflux pumps, protein secretion systems, quorum sensing, and biofilm formation, are in charge of the disease and high mortality of *A. baumannii*. These virulence factors support antimicrobial resistance and pathogen survival under harsh settings (Dehbanipour & Ghalavand,2022). An opportunistic Gram-negative human bacterium called *Serratia marcescens* can lead to several nosocomial diseases, including infections of the respiratory, urinary, and wound systems. The generation of virulence factors that can harm human cells increases this capacity. In addition to swimming and swarming motilities and biofilm formation, *S. marcescens* uses the quorum sensing (QS) system to control the production of prodigiosin pigment and virulence components like proteases (Abbas & Hegazy,2017)

2.13 Medical Applications of NPs

2.13.1 Antimicrobial Activity

Utilizing nanoparticles as antimicrobial agents could circumvent bacterial resistance mechanisms because of their direct contact with the bacterial cell wall, which confers a microbicidal effect without requiring cell penetration (Fernando *et al.*,2018). MNPs are a good choice for this purpose because of their high surface-to-volume ratio, which increases the possibility of contact with the bacterial surface, and their antibacterial nature. As resistant strains and their infections increase, there is an inevitable need for a new antibacterial agent that is inexpensive, has few side effects, and is strong (Hosseini *et al.*,2016). When Rajan *et al.* examined the antibacterial properties of AuNPs made by *Elettaria cardamomum*, they found that the generated AuNPs were more effective against *S. aureus* than against *E. coli* and *P. aeruginosa* (Rajan *et al.*,2017). According to another study, (AgNPs) produced by *Microbacterium sp.* showed toxic effects on both gram-

negative and positive bacteria (Dewan & Hateet,2022). Furthermore, tellurium and selenium nanoparticles inhibit the formation of biofilms and have antibacterial qualities.

The nanoparticles effectively inhibited the growth of *S. aureus* ATCC 25923, *Pseudomonas aeruginosa* PAO1, and *E. coli* JM109 (Zonaro *et al.*,2015).In the study (Dharmaraj *et al.*,2021). Ag₂ONPs synthesized by *Bacillus paramycoides* were used as effective antimicrobials. The low surface-to-volume ratio of the NPs can boost the antibacterial activity allowing increased contact of the nanomaterial with the surrounding environment (Fernando *et al.*,2018). The following processes underlie NPs' antimicrobial activity: direct attachment to the cell membrane, instability and modification of the membrane's permeability, release of metal ions, production of (ROS), and modification of signal transduction pathways (Dakal *et al.*, 2016; Susanti *et al.*, 2022).

2.13.2 The Cancer

Cancer is regarded as a major health concern to everyone worldwide and is one of the main causes of the rising death rate in many countries, according to the World Health Organization's World Cancer Report (Sung *et al.*,2021). Cancer is the leading cause of premature death and lowers life expectancy in many nations as the world's population ages and grows (Cao *et al.*,2021). While lung and breast cancers are the major causes of cancer-related mortality in men and women, respectively, lung, liver, and stomach cancers are the three most fatal malignancies in the overall population (Mattiuzzi & Lippi,2019).

2.13.3 Liver and Colon Cancer

As the most frequent cause of cancer deaths around the globe and fifth most prevalent in the United States, liver cancer is the only one of the top five deadliest cancers to have an annual percentage increase in occurrence (Anwanwan *et al.*,2020). Its incidence rates have been rising gradually in several countries. The world's highest incidence rates of liver cancer are seen in Asia and Africa Chronic infections with the hepatitis B and hepatitis C viruses are responsible for around three-quarters (73.4%) of hepatic cellular carcinoma cases globally (Elzoghby,2019). The goal of liver cancer screening is to find tumours before symptoms show up. As with any other disease, screening those believed to be at risk for the specific cancer is cost-effective.Before screening for primary liver

cancer, HCC screening must be completed. Hepatocellular carcinoma, the fifth most common cancer in men and the seventh in women is on the rise in Western countries (Cucchetti *et al.*,2013). Colorectal cancer (CCR) is the leading cause of gastrointestinal cancer-related deaths, the second leading cause of cancer-related deaths globally, and the third most frequent disease in both men and women. Poor eating habits, smoking, intestinal inflammatory illness, polyps, genetic factors, and ageing are all associated with an increased chance of acquiring this malignancy (Granados-Romero *et al.*,2017). The development of screening programs, changes in disease incidence, and advancements in therapy have all contributed to a change in the primary causes of cancer-related mortality. Although it was relatively uncommon before 1950, colorectal cancer is today a common malignancy in Western nations, contributing to about 10% of all cancer-related deaths (Kuipers *et al.*,2015).

2.13.4 Anticancer Activity

The anticancer characteristics of biological NPs have been explained by three ideas. First, a high level of ROS is necessary for the apoptotic pathway, which results in oxidative stress and DNA fragmentation in the cancerous cell (Singh *et al.*,2014). Second, cell chemistry functions are caused by interference between proteins and DNA. Thirdly, biological NPs' interaction with cell membranes results in changes in cell permeability and mitochondrial dysfunction (Lim *et al.*,2011, Sunita *et al.*,2015). Caspase 3, Caspase 9, and Bax expression levels were upregulated in the pancreatic cancer cell lines (PANC-1) treated with gold nanoparticles derived from *Scutellaria barbata*, while Bid and Bcl-2 expression was downregulated (Wang *et al.*,2019). According to another study (BalaKumaran *et al.*,2022), among six different cancer cell lines evaluated, AgNPs showed fairly substantial cytotoxicity against MCF-7 cells with an IC₅₀ value of 2.90 µg/ mL, whereas, AuNPs showed the strongest activity against HepG2 cells (IC₅₀: 25.79 µg/mL). Furthermore, the supplied dose, particle size, and chemical makeup are the main determinants of selenium nanoparticles' pharmacological activity. Additionally, several studies have demonstrated that because these nanoparticles are not harmful to non-cancerous cells, their administration is safe. The most pertinent antecedents of selenium nanoparticles' anticancer potential in prostate, breast, cervical, lung, liver, and colorectal cancer cell lines are covered (Martínez-Esquivias *et al.*,2022).

2.14 Cancer Treatment with Nanotechnology

Globally, nanotechnology is receiving a lot of attention for treating cancer. Nanobiotechnology promotes the integration of therapies and diagnostics, which is an essential part of a tailored approach to treating cancer. Nanomedicine uses nanoparticles to help diagnose and cure a variety of illnesses, including cancer (Chaturvedi *et al.*,2019). Specifically, organic and inorganic nanoparticles with a variety of modes of action, such as metallic gold and silver nanoparticles, quantum dots, and graphene, are being investigated in the context of cancer treatment. Their use may also be extended into diagnostic applications, for instance, higher cellular absorption, enhanced reactive oxygen species generation, and functionalization characteristics for more targeted delivery (Pavelić *et al.*,2023). One essential feature of nano-carriers for drug delivery is their ability to preferentially target cancer cells, which increases therapeutic efficiency while shielding healthy cells from damage (Yao *et al.*,2020).

Many metal nanoparticles (NPs) have been utilized to treat cancer. Botteon *et al.* revealed that gold NPs were biosynthesised using Brazilian red propolis (BRP), a bee product (Botteon *et al.*,2021). When biosynthetic gold nanoparticles were applied to T24 bladder cancer and PC-3 prostate cancer cell lines, they demonstrated significant in vitro lethal effects (Bray *et al.*, 2018). According to (Muhammad *et al.*,2021), functionalized paclitaxel nanocrystals with silver NPs increase the overall anti-cancer activity of human cancer cells. To target tumours, nanocrystals combining inorganic silver nanoparticles and the organic anti-cancer medication paclitaxel were created. Additionally, NPs loaded with Paclitaxel, a common medication used to treat prostate cancer, are one of the techniques that involve the use of nanoparticles in cancer treatment (Sahoo *et al.*,2004). The coupling of nanospheres (spherical NPs) with targeting moieties significantly boosts a treatment's efficacy, according to one of the key implications to be made from these findings.

2.15 Physical Characterization of NPs

2.15.1 UV-Vis Spectroscopy

The highly conjugated structure, chemical makeup, and presence of transition metal ions of a substance dictate the wavelength (WL) at which its molecules absorb visible light. UV-Vis spectroscopy uses visible and near-ultraviolet (NUV)

light to analyze molecules undergoing electronic changes (Forough & Farhadi,2010).

2.15.2 Infrared Fourier transform spectroscopy (FTIR)

Two types of vibratory spectroscopy that are useful for analyzing the structural characteristics of nanoparticles are Raman spectroscopy and infrared spectroscopy, commonly known as Fourier transform (FT-IR). Apart from core nanoparticles, infrared spectroscopy is commonly employed to ascertain the properties of many kinds of nanoparticles, including metal nanoparticles and carbon nanomaterials. (Merck, 2020).

2.15.3 Zeta potential analysis

The electrochemical equilibrium between particles and liquids, such as in nanoparticle (NP) colloidal solutions, is expressed by the zeta potential, a parameter that finds use in chemical production, medicine, and pharmaceuticals. ZP determination of NPs is necessary for accurate NP characterization (Lunardi *et al.*,2021).

2.15.4 X-ray Diffraction (XRD)

Utilizing X-ray diffraction (XRD) techniques, which were popular and very useful nondestructive characterization tools, the physical characteristics, crystallographic structure, and chemical makeup of materials were investigated. A variety of crystalline phasing structural characteristics, such as phase composition, grain size, strain, and defect structure, can also be described using it (Sharma *et al.*, 2012).

2.15.5 Fe-SEM and energy-dispersive spectroscopy (EDX)

The restricted capacity of TEM to examine the ultrastructure of vast regions and quantities of biological samples is its drawback. Modern field-emission scanning electron microscopy (FE-SEM) with high-sensitivity detection can get around this restriction by producing TEM-like pictures from the flat surfaces of biological specimens embedded in resin (Lewczuk & Szyryńska,2021). Energy dispersive spectroscopy was used to examine a sample's surface analysis and elemental characterization. Analyzing the X-rays of various energies that are released from the sample when an electron beam strikes its constituent atoms is the

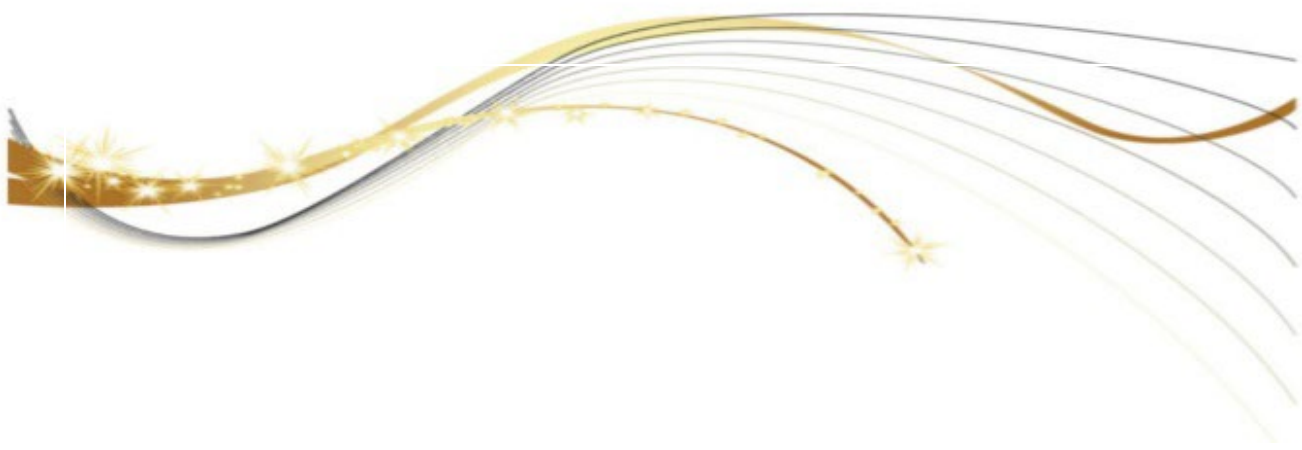
basic concept. By examining the surface of the sample, one can quickly ascertain the quantity and makeup of metal nanoparticles (Smuleac *et al.*, 2013).

2.15.6 Transmission Electron Microscopy (TEM)

In transmission electron microscopy, or TEM, an electron beam is passed through an incredibly thin object and interacts with it during the process. This technique uses energetic electrons to offer information about the composition, morphology, and crystallography of samples. It is widely utilized in nanotechnology and biology and is excellent in observing metal nanoparticles (Cooper *et al.*, 2016).

2.15.7 Atomic Force Microscopy (AFM)

AFM is an advanced nanoscope technology used to describe nanoparticles and examine the surfaces of nanomaterials in three dimensions. Because AFM images can be acquired in an aqueous media, they are an invaluable resource for studying NP behaviour in a biological setting (Bhosale *et al.*, 2014).



Chapter two

Materials and Methods

2. Materials and Methods

2.1. Materials

2.1.1. Equipment and Apparatus

Table (2.1): Apparatus Used During the Study Period

No	The Apparatus	Company / origin
1	Autoclave	Hirayama/Japan
2	Atomic force microscope (AFM)	NT-MDT/ Russia
3	Biosafety	Lab Tech/France
4	Centrifuge	Hittich/Germany
5	CO ₂ incubator	Memmert/Germany
6	Digital gel documentation	Shownic/Korea
7	Electrophoresis	Consort/Belgium
8	FTIR	Zenith lab/China
9	Hot plate with a magnetic stirrer	Heidolph/Germany
10	incubator	Human Lab/Korea
11	Laminar flow hood	K & K Scientific Supplier/Korea
12	Light Microscope	Olympus/Japan
13	Microwave	Shownic/Korea
14	Oven	Memmert/Germany
15	Refrigerator	Vistal/Poland
16	SEM	Zenith lab/China
17	Sensitive Balance	Sartorius/Germany
18	Shaking Incubator	Zenith lab/China
19	TEM	GFR/Germany
20	Thermo cycler appartus	Prime/UK
21	UV-visible spectroscopy	Shimadzu/Japan
22	Water distillatory	GFR/Germany
23	Water path	Memmert/Germany
24	X-Ray diffraction	Phillips/Holland
25	Zeta potential	GFR/Germany

Table (2.2) Equipment Used During the Study Period

No	The Equipment	Company/Origin
1	Standard wire loop	Himedia/India
7	Flask	Iso Lab/Germany
8	Beaker	General/USA
9	Cell culture plate	Thermo Fisher Scientific/US
10	Disposable Syringes	Superstar/India
11	Test tube	ALS/Canada
12	Benzen burne	Gallenkamp/ England
13	Petri Dishes	Bio zek medical/Holland
4	Epindroff	Bio neer/Korea
3	Filter paper	Watman No.1/UK
2	Gloves	Broche/ Malaysia
6	Micropipettes 0.5-10 μ L, 10-100 μ L, 100- 1000 μ L	Dragon/China
5	Screw cap bottles	Pyrex/England

2.1.2. Culture Media

Table (2.3):List of culture Media used in the current study

No	Culture Media	Amount
1	Nutrient Agar	28 g in 1000-ml D.W
2	Mueller Hinton Agar	38 g in 1000-ml D.W
3	Nutrient Broth	13 g in 1000-ml D.W
4	Mackonky agar,	51.5 g in 1000-ml D.W
5	Blood agar	40 g in 1000-ml D.W

6	MGYP broth	45 g in 1000-ml D.W
---	------------	---------------------

2.1.3. Biological and chemical materials

Table (2.4): List of chemicals used in corrent Study

No	Chemicals	Company	Origin
1	Agar powder	KR	Chile
2	Ethanol 70%	BDH	England
3	Oligo Primers	Macrogen	(South Korea)
4	Gentamicin disks	Liofilchem s.r.i	Italy
5	Agarose powder	Bioneer	Canada
6	Deionization water	Ajax	Australia
7	Absolute ethanol	RBL	Spain
8	DMSO	Santa Cruz	USA
9	HauCl ₄ .3H ₂ O	Sigma	USA
10	AgNO ₃	Sigma	USA
11	Na ₂ SeO ₃	Avonchem	UK
12	DNA Extraction Kit	Geneaid	Taiwan
13	Green Master mix 2X	Promega	USA
14	Loading Dye	Promega	USA
15	Orange Diamond Dye Tm	APM	Canada
16	TAE buffer	Bioneer	Canada
17	Nuclease free water	Promega	USA
18	Green safe dye	Promega	USA

19	PBS	Promega	USA
20	Trypsin/veresin enzyme	Bioneer	Canada
21	Trypan Blue stain	Promega	USA
22	crystal violet stain	Promega	USA

2.2 Methods

2.2.1 Samples Collection

Ten bacterial samples were collected between January to April from different sources (blood, wounds, burns, and urine). Table (2.5) shows the process of collecting clinical samples according to the basic guidelines and instructions. The samples were obtained from some hospitals, including Al-Sader Hospital, Al-Zahrawi Hospital, and Children and Maternity Hospital.

Table (2.5) Clinical samples collection

Code	Specimine	Container	Primary plating medium	Direct examination
H1	Blood	Blood culture media (pottel)	Mackonky agar, Blood agar	Gram stain
H2	Wound	Swab	Mackonky agar, Blood agar	Gram stain
H3	Burns	Swab	Mackonky agar, Blood agar	Gram stain
H4	Urine	Swab	Mackonky agar, Blood agar	Gram stain
H5	Wound	Swab	Mackonky agar, Blood agar	Gram stain
H6	Burns	Swab	Mackonky agar, Blood agar	Gram stain
H7	Wound	Swab	Mackonky agar, Blood agar	Gram stain
H8	Urine	Swab	Mackonky agar, Blood agar	Gram stain
H9	Burns	Swab	Mackonky agar, Blood agar	Gram stain
H10	Urine	Swab	Mackonky agar, Blood agar	Gram stain

2.2.2 Isolation of Pathogenic bacteria

Four types of bacterial isolates were selected for the current study. After collecting the samples, the following steps were carried out:

1-The sample was cultured using a 1:100 ml (loop) for the two samples (blood + urine). At the same time, a direct swab was used for the two samples (wounds + burns) on the media (Mackonky agar, Blood agar) using Petri dishes.

2-The culture media were incubated for 24-48 hours at a temperature of 37°C.

3-After incubation and growth of bacteria on the above-mentioned culture media, the isolates was directly examined using a Gram stain to determine whether the bacteria were Gram-positive or negative.

4-Then the genus and type of bacteria were determined using the VITEK-2 system, in addition to molecular diagnosis using the PCR technique.

5-Isolates were purified by streaking on NA to produce pure isolates (Sirisha *et al.*, 2017).

6-For additional research, all isolates were kept on nutrient agar slants (Dash & Payyappilli, 2016).

2.2.3 identification of Pathogenic bacteria

2.2.3.1 VITEK-2 System

The Vitek-2 system was accomplished at Children and Maternity Hospital according to Bitew *et al.*, 2017. To identify the bacteria, the Vitek 2 system Gram-negative identification test (GNI) card or Gram-positive identification test (GPI) cards were used. A sterile loop was used to transfer enough colonies of a pure culture and to suspend the bacteria in a test tube containing 3.0 mL of 0.45% sterile saline. The turbidity of this suspension was adjusted to 0.5–0.63 McFarland. The McFarland turbidity was measured by the DensiCHEK Plus Meter. After that, a test tube containing the bacterial suspension was placed into a special rack (cassette) and the identification card was placed in the adjoining orifice. For the identification of bacteria, Vitek-2 plastic rack was transferred to the Vitek-2 automated instrument and after 24 h the result of bacterial identification was obtained.

2.2.3.2 Molecular identification

2.2.3.1 Extraction of bacterial genomic DNA

The genomic DNA was extracted from all bacterial isolates grown on nutrient agar plates by using Presto™ MinigDNA bacteria kit according to the manufacturer's instructions. The genomic DNA was stored at -20° C.

2.2.3.2 Confirmation of the presence of extracted DNA

A conventional 0.8% (w/v) agarose gel was used to check the presence of the extracted template DNA. The agarose solution was prepared by dissolving 0.2g of agarose powder in 25 mL TBE buffer (1X), gently mixed, and heated to boiling point in the microwave oven for 3 min until the solution became clear. After the mixture had cooled to 50-60 °C., 2 µL of green safe dye was added and mixed carefully. To create the wells, the comb was placed at one end of the pre-prepared gel box, and the agarose solution containing green safe dye was poured into it, and left until solidification. The comb was then carefully removed from the box, and the gel was transferred to the electrophoresis tank, where the diluted buffer solution was poured into it to cover the gel's surface approximately 3 to 4 mm. 1:3µL of each template DNA and 2 µL of the promophenol dye (loading dye) were mixed and loaded into agarose gel pits using a micropipette. Then the electrodes were linked in their specified positions, and the running was carried out for 30 min at 120 mA 80 V. Finally the results of gel electrophoresis were visualized by gel documentation system (Lee *et al.*, 2012).

2.2.3.3 Amplification of 16S rDNA gene

All the isolated bacteria were identified by the 16S rDNA gene (~1500 bp). Amplification of 16S rDNA using thermocycler was done by universal 27 F forward primer (5'-AGAGTTTGATCCTGGCTCAG -3') and 1492 R reverse primer (5'-GGTTACCTTGTTACGACTT-3'). The reaction mixture was carried out in a volume of 25µL, where the template DNA, primers (10 pmol), and master mix are shown in Table (2.6).

Table (2.6) PCR Reaction for amplification of 16 srDNA gene

Reagents	Volume µl
Master Mix	13 µl
Primer forward	1 µl
Primer reverse	1 µl
DNA template	3 µl

Free water	7 μ l
Total	25 μl

To amplify 16S rDNA gene fragments, the PCR program was carried out according to Table (2.7).

Table (2.7) PCR program for amplification of the 16S rDNA gene.

Steps	Temperature	Time	No. of cycles
Initial denaturation	96 °C	3 min	1
Denaturation	96°C	30 sec	27
Annealing	52°C	25 sec	
Elongation	72°C	15 sec	
Final Elongation	72 °C	10 min	1

2.2.3.4 Electrophoresis of PCR Products

The amplified DNA fragments were separated using an electrophoresis apparatus on 1% agarose gel (stained with 2 μ L of green safe dye) for 45 min at 120 mA 80V using 1x TBE buffer. In agarose gel wells, 5 μ L of PCR product and DNA ladder were loaded. Finally, the results of gel electrophoresis were visualized using a gel documentation system.

2.2.3.5 Sequencing of 16S rDNA gene

Each sample was labelled and sent to a Macrogen biotechnology company (South Korea). Purification of the PCR product and analysis of the sequence of forward and reverse 16S rDNA gene were done by the same company. The sequence results were then compared with the ready gene sequences to the National Center for Biotechnology Information (NCBI) website by using the Basic Local Alignment Search Tool (BLAST) and analyzed to detect the closest match for the bacterial isolates.

2.2.4 Preparation of (HAuCl₄.3H₂O, AgNO₃, Na₂SeO₃)

1-HAuCl₄.3H₂O: 0.0786g of gold chloride was dissolved in 1000 ml of sterilized deionized water according to the law of molarity and in dark conditions to obtain a solution of gold chloride with a concentration of (2Mm).

2-AgNO₃: 0.01698g of silver nitrate was dissolved in 1000 ml of sterilized deionized water according to the law of molarity and in dark conditions to obtain a solution of AgNO₃ with a concentration of (1Mm).

3-Na₂SeO₃: 0.034g of Sodium selenate was dissolved in 1000 ml of sterilized deionized water according to the law of molarity to obtain a solution of Na₂SeO₃ with a concentration of (2Mm).

2.2.5 Biosynthesis of NPs

This method was carried out, with minor adjustments, by Singh *et al.*, (2015).

1- All of the recovered bacteria were cultivated in flasks that contained 100 ml NB, and incubated for 24 h at 37 °C in an orbital shaker at 150 rpm,

2- To obtain the supernatant, the cultures were centrifuged for 10 minutes at 6000 rpm.

3- 100 ml of a solution of HAuCl₄.3H₂O, AgNO₃, and Na₂SeO₃ (2 mM, 1 mM, and 2 mM) was combined with the supernatant (50 ml) of each isolate in a 200 mL flask. The flasks were then covered with foil and incubated at 37 °C for 24 h for AuNPs, 48 h for SeNPs, and 72 h for AgNPs at 150 rpm.

4- The control was a supernatant.

2.2.6 Characterization of NPs

The most often used techniques for figuring out NPs' characteristics were physical and biological characterizations.

2.2.6.1 Physical Characterization

2.2.6.1.1 UV- vis Spectroscopy

To confirm that NPs were formed, a Uv–vis spectral was performed at 300–800 nm. The treated and untreated solutions were centrifuged at 2000 rpm for 5 minutes. While treated supernatants are utilized to track their Uv- vis absorbance.

2.2.6.1.2 FTIR

The purpose of the FTIR study was to determine whether the produced NPs contained functional groups that would aid in the biosynthesis process. The powdered materials were measured at a resolution of 4 cm⁻¹ in the 400–4000 cm⁻¹ range using the FTIR spectrometer.

2.2.6.1.3 Zeta potential

Using a zeta potential analyzer device, the stability of the NPs was evaluated. The samples were centrifuged for this examination, and the NPs were measured at 25.2 °C (the holder's temperature) between -200 and +200 mv.

2.2.6.1.4 XRD

The XRD of NPs produced by bacteria was measured using the X'pert Pro X-ray diffractometer. The diffraction pattern of the powdered form of generated NPs was recorded from 10° to 80° (2 theta) with a step size of 0.050° using Cu K-Alpha radiation ($k = 1.54060 \text{ \AA}$) operating at 40 kV and 30 mA. The average crystalline size of the NPs was determined using Scherer's equation.

2.2.6.1.5 Fe-SEM and EDX

Fe-SEM was used to examine the morphological characteristics of the NPs produced by bacteria. Before being examined by SEM, a tiny drop of NPs suspensions was added to the slide and given time to dry. The magnification at which the microscope operated varied (Saleh & Alwan, 2020). All mid-energy (1–20 keV) X-rays collected during any given analysis period are displayed simultaneously by the EDX detection system, and the energy of the X-rays is reproduced as a spectrum, which is a histogram representation of the number of counts against X-ray energy .

2.2.6.1.6 TEM

TEM was used to analyze the shape, size, and distribution of NPs. The TEM grids were prepared by transferring the NP suspensions onto carbon-coated copper grids. The grids were allowed to air dry before imaging, and TEM was used to capture individual pictures at 200 kV.

2.2.6.1.7 AFM

The size and morphology of NPs were characterized by the AFM device. Bio-fabricated nanoparticles were applied in thin layers to sterile glass coverslips before AFM scanning, and they were allowed to cure at room temperature.

2.2.6.2 Biological Activity

The biosynthesized NPs in this work were characterized using antibacterial and anticancer activities.

2.2.6.2.1 Antibacterial Activity of NPs

By employing the Agar disc diffusion method, the NPs' anti-bacterial activity in this work was tested against two pathogenic bacterial strains, Gram-positive *S. aureus* and Gram-negative *E.coli*, isolated from clinical specimens. VITEK-2 was used for identification. Where both kinds of harmful bacteria were subcultured on nutrient agar transfer media and kept for 24 hours at 37 °C. After that, sterile swabs were used to swab individual standardized suspensions of each teste bacteria (1.5×10^8 cells/ml) by McFarland standard 0.5N (CLSI) onto sterile Muller Hinton agar plates. The plates were then allowed to stand for ten minutes. Following tablet preparation, the tablets are submerged in the produced NPs solution for one to two hours, after which we insert Au, Ag, Ag₂O₃ and SeNPs discs. To ensure contact, the discs were gently pressed down. The plates were either incubated right away or within 30 minutes. The inhibitory zone in Petri dishes was measured in millimetres after a 24-hour incubation period at 37°C (Abdul-Hassan,2016). As a control gentamicin disc (10 µg) was used to compare with (AuNPs, AgNPs, Ag₂O₃NPs, and SeNPs) discs.

2.2.6.2.2 Anticancer Activity of Synthesized NPs

The method (Capes-Davi & Freshney,2021) was used to evaluate the toxicity of different concentrations of the synthesized NPs in the current study against human liver cancer cells HepG2, human colon cancer cells HT-29, and normal cell lines

mouse embryo fibroblast cells (MEF). Five different concentrations (10, 20, 40, 80, 160 µg/ml) of each NPs biosynthesized were used.

1-Growth of HT -29, HepG2 Cancer Cell Lines and MEF

The method (Capes-Davi & Freshney,2021) was used to grow cancerous line cells as follows:

- 1- Cells of each of the lines were placed in a culture container with a diameter of 25 cm² containing RBMI-1640 culture medium and 10% calf B serum.
- 2- The containers containing the cell suspension and culture medium were incubated in a 5% CO₂ incubator at 37°C for 24 hours.
- 3- After a day of incubation, and when it was confirmed that there was growth in the cell culture and that it was free of contamination, secondary cultures were conducted for it.
- 4- The cells were examined using an inverted microscope to ensure their viability, freedom from contamination, and growth to the required number of approximately 500 to 800 thousand cells/ml.
- 5- The cells were transferred to the growth booth and the used culture medium was disposed of.
- 6- The cells were washed with PBS solution and then discarded, and the process was repeated twice for 10 minutes each time.
- 7- A sufficient amount of trypsin/veresin enzyme was added to the cells and incubated for 30-60 seconds at 37°C and monitored until they changed from a monolayer of cells to single cells, then the enzyme was stopped by adding a new culture medium containing serum.
- 8- The cells were collected in centrifugal tubes and placed in a centrifuge at 2000 rpm/min for 10 minutes at room temperature, to precipitate the cells and get rid of the trypsin and the used culture medium.
- 9- The filtrate was discarded and the cells were suspended in a fresh culture medium containing 10% serum.

10- Examine the number of cells by taking a specific volume of the cell suspension and adding to it the same volume of Trypan Blue stain to determine the number of cells and their vitality by using a Hemacytometer slide, according to the equation:

$$C = N \times 10^4 \times F \text{ \textbackslash ml} \dots\dots\dots(2.1)$$

Since:-

C = number of cells in one ml of solution

N = number of cells in the slide

F = dilution factor

10^4 = Slide Dimensions

11- The percentage of cell vitality in the sample was also calculated by using a Hemacytometer slide according to the equation:

$$\text{Live cell viability} = (\text{live cells}) \ \ (\text{dead cells}) \times 100 \dots\dots\dots(2.2)$$

12- The cell suspension was distributed in new containers and then incubated in a 5% CO₂ incubator at 37°C for 24 h.

2-Cytotoxic assay of biosynthesized NPs in cancer cell line Under sterile conditions, a filter unit with a diameter of 0.22 μm was employed to sterilize the Au, Ag, Ag₂O₃, and Se NPs at concentrations of 10 and 20, 40, 80, and 160 μg/ml. After the preparation process was finished, all of the prepared concentrations were used right away.

- 1- Prepare the cell suspension by treating the contents of a 25 cm² tissue culture container with trypsin/versine solution after emptying the old culture medium and gently moving the bottle, then incubating in the incubator at a temperature of 37 °C for 10 minutes, then 20 ml of the culture medium containing serum was added to it. The cell suspensions were mixed well and 0.2 ml was transferred to each hole of the flat-bottomed plate for tissue culture by using an automatic fine pipette.
- 2- The plate was left in the incubator at a temperature of 37 °C for 24 hours until the cells adhered to the hole, after which the old culture medium was disposed of in the holes and 0.2 ml of the previously prepared concentrations of the extract was added with three replicates for each concentration, in addition to that three replicates were made For control (cell suspension only) plates were incubated at 37°C.
- 3- After 24 hours of exposure time, remove the plate from the incubator and add crystal violet stain solution to all holes containing the cells at a rate of 100 µl for each hole.
- 4- The plate was returned to the incubator for 20 minutes, after which it was taken out, its contents were removed and the cells were washed with water until the excess stain was removed, as the living cells take the stain while the dead ones do not.
- 5- The results were read by using the ELISA with a wavelength of 492 nm

The inhibiting ratio was calculated according to the equation:

$$\text{Percentage of cell inhibition} = \left(\frac{\text{absorbance reading of control cells} - \text{absorbance reading of treated cells for each concentration}}{\text{absorbance reading of control cells}} \right) \times 100 \dots \dots (2.3)$$

2.2.7 Statistical analysis

The ANOVA test and the GraphPad Prism Version 6 analysis system were used to statistically examine the findings. The Duncan Multiplex experiment was used to compare the means with significant.



Chapter three

RESULTS AND

DISCUSSION



3. Results and Discussion

3.1 Isolation of Bacteria

Four types of bacterial isolates were selected for the current study. Table (3.1) shows the colony characteristics of the bacterial species.

Table (3.1) Bacterial colonies properties.

code	Specimine	Gram stain	Mackonky agar	blood agar	Size	Morphology
H1	Blood	Gram-negative	gray to white	No hemolysis	1-2 mm	soft, non-mucous, slightly transparent
H2	Wound	Gram-negative	colourless	partial hemolysis	2-3 mm	With a smooth or mucous surface
H3	Burns	Gram-negative	colourless	partial hemolysis	2-3 mm	With a smooth or mucous surface
H4	Urine	Gram-negative	colourless	partial hemolysis	1-3 mm	Rod-shaped, convex circular with smooth edges

3.2 Identification of bacteria

The results of the VITEK-2 showed that the isolates (H1, H2, H3, H4) were identical to bacteria (*Acinetobacter baumannii*, *Pseudomonas aeruginosa*, *Pseudomonas aeruginosa*, *Serratia marcescens*) respectively, and at the same time, these results were consistent with the results of molecular diagnosis. DNA was extracted from pathogenic bacteria currently under study, and the results using PCR showed that the primers amplified the gene sequence and the locations of the amplified bands appeared between (1000-1500pb) Fig (3.1).

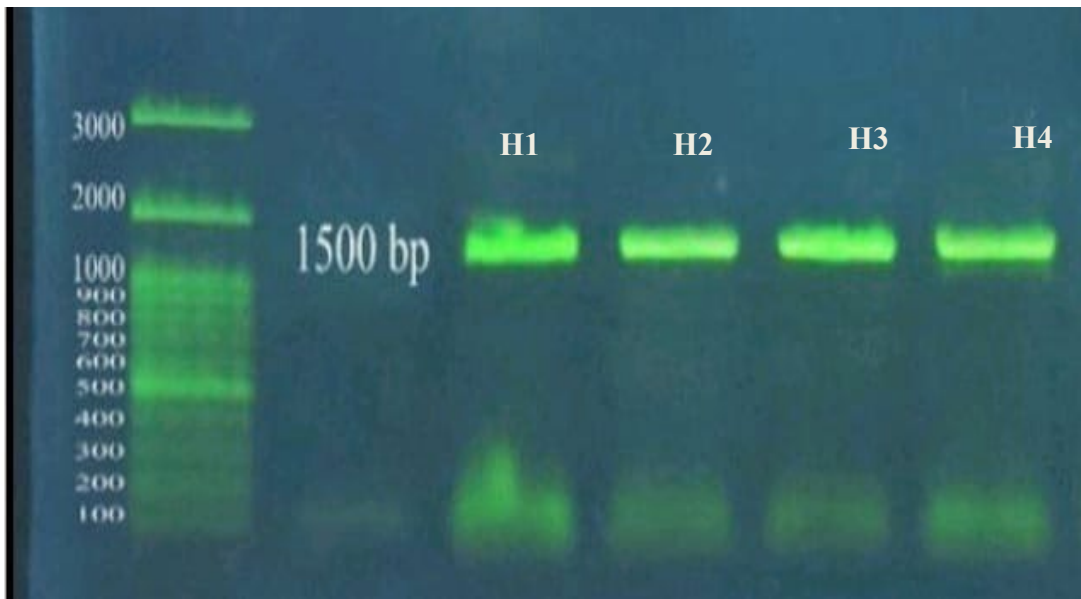


Fig (3.1) Gel electrophoresis of the 16S rDNA gene using primers amplified appeared between (1000-1500pb)

The results of the analysis of the sequence of the nitrogenous bases of the genetic material DNA that the isolates H2, H3, and H4 were 99% identical to *Pseudomonas aeruginosa* *Pseudomonas aeruginosa* *Serratia marcescens* and were compared and registered in the GenBank while the isolate H1 was 100% identical to *Acinetobacter baumannii* Table (3.2).

Table (3.2) shows isolated strains and their accession number.

Code	Closed bacteria	Reference copy (NCBI)	Percent identify	Accession number
H1	<i>Acinetobacter baumannii</i>	LN611358	100%	-
H2	<i>Pseudomonas aeruginosa</i>	PP762162	99%	LC815917
H3	<i>Pseudomonas aeruginosa</i>	PP762162	99%	LC815921
H4	<i>Serratia marcescens</i>	CP053572	99%	LC815918

3.3 Biosynthesis of NPs

The results of the current study showed the ability of all bacterial strains isolated from the previously mentioned sources to biosynthesize each of the Au, Ag, Ag₂O₃ and Se NPs after growing on fermentation cultures. After daily monitoring of the fermentation cultures, a color change was observed in the filtrate of the isolate *A. baumannii* after 24 h of incubation at 37°C when treated with gold tetrachloride salt (HAuCl₄), as it showed a colour change from transparent yellow to dark red as initial evidence of its ability to synthesize AuNPs Fig (3.2,), Table (3.3) while no colour change was shown in the filtrates of the other bacterial isolates when treated with salt. This result is consistent with the study (Kang *et al.*,2023) when they observed the presence of dark-red AuNPs.

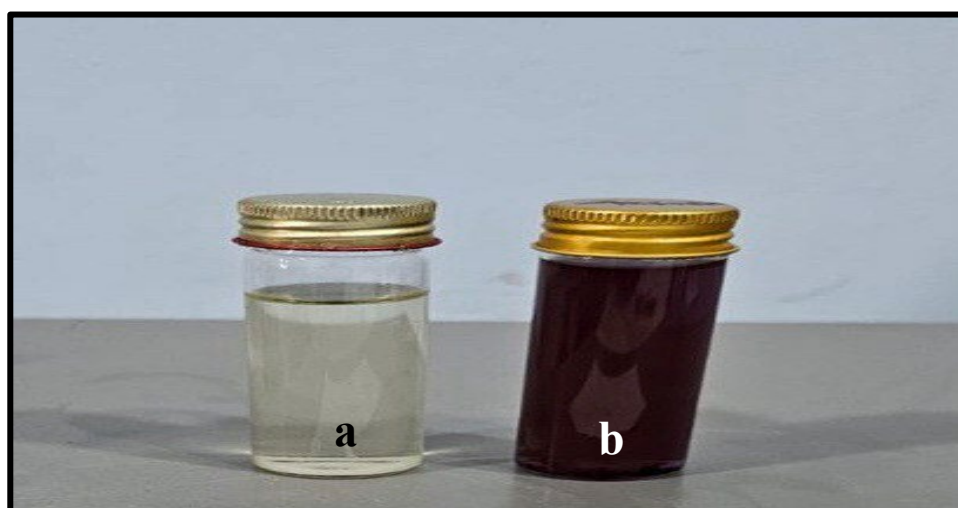


Fig (3.2) Shows the incubation of *A. baumannii* with HAuCl₄ salt for AuNPs. The color changed from transparent yellow to dark red a) without salt b) with salt

As for the filtrates of the two isolates *P.aeruginosa* and *P.aeruginosa*, they showed a colour change from transparent yellow to dark brown after 72 hours of incubation after being treated with silver nitrate salt (AgNO₃) as preliminary evidence of the ability of the bacteria *P.aeruginosa* to synthesize AgNPs Fig (3.3), Table (3.3) and the ability of the bacteria *P.aeruginosa* to synthesize Ag₂O₃NPs Fig (3.4), Table (3.3). (Ibrahim & Hateet,2021) and (Dewan & Hateet,2023) confirmed the

biosynthesis process of AgNPs through the color change of the particles which acquired a dark brown colour after a 72 h incubation period.

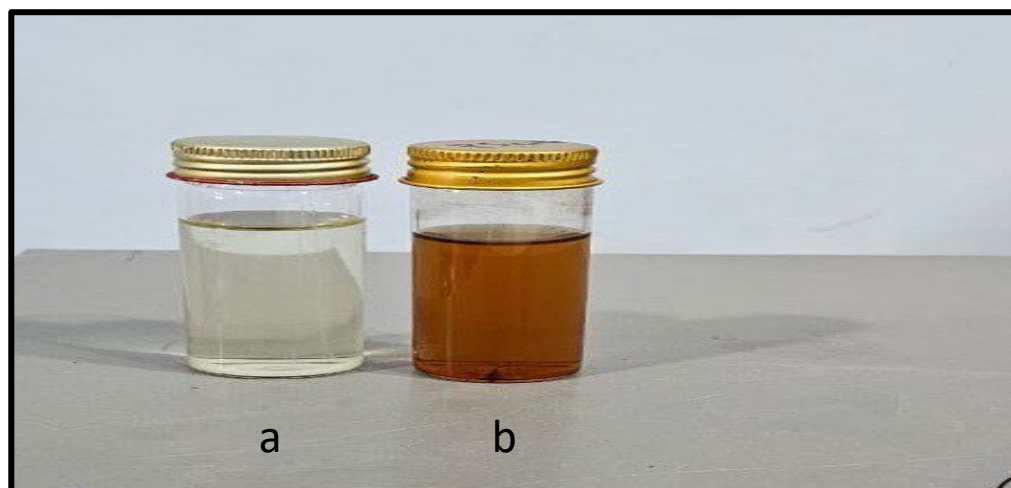


Fig (3.3) Shows the incubation of *P.aeruginosa* with AgNO_3 salt for AgNPs. The color changed from transparent yellow to dark brown a) without salt b) with salt

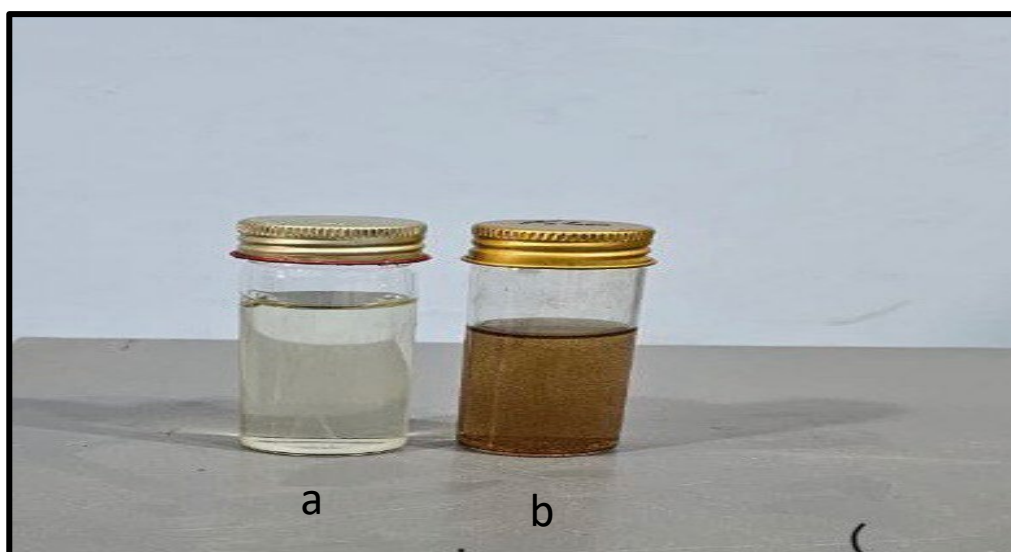


Fig (3.4) Shows the incubation of *P.aeruginosa* with AgNO_3 salt for Ag_2O_3 NPs. The color changed from transparent yellow to dark brown a) without salt b) with salt

The filtrate of the isolate *S.marcescens* showed a colour change from transparent yellow to light orange after incubation for 48 hours when treated with sodium selenate salt (Na_2SeO_3) as preliminary evidence of the ability of the bacteria to biosynthesize SeNPs Fig (3.5), Table (3.3) while no colour change was observed

for the filtrates of the other isolates when treated with salt. In a study (Shoeibi&Mashreghi,2017), it was confirmed that SeNPs were synthesized after the color change.

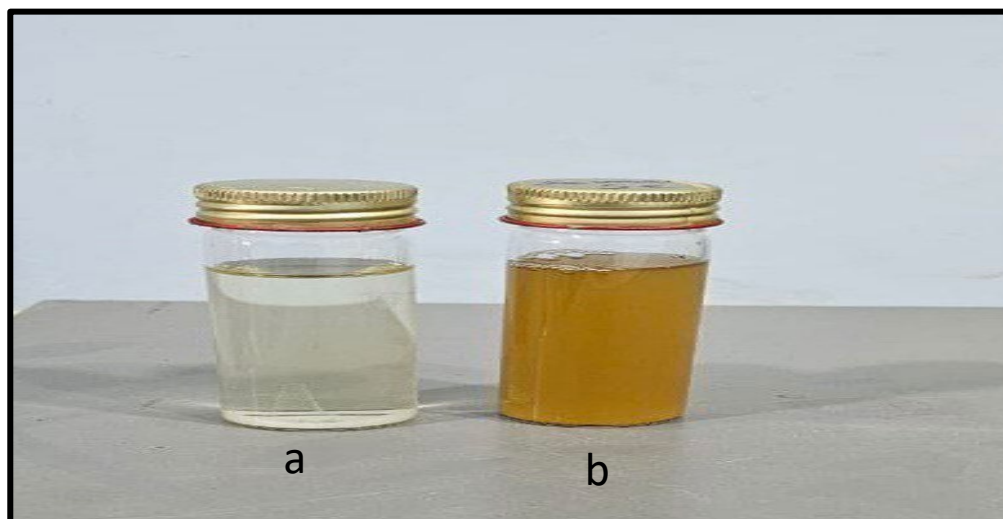


Fig (3.5) Shows the incubation of *S.marcescens* with Na_2SeO_3 salt for SeNPs. The color changed from transparent yellow to light orange a) without salt b) with salt

The colour change in the reaction mixture might be explained by the surface plasmon resonance (SPR) of the NPs suspension, providing an initial and visible directory for NPs biosynthesis (Syed *et al.*,2016; Sidhu & Nehra,2020). According to Chang *et al* (2021) research on AuNP synthesis, the quick reduction of gold ions using an aqueous extract of *Cannabis sativa* leaves led to uniform nucleation of gold metals, which in turn produced tiny AuNPs.

Table (3.3) NPs with chang colour, media and hours of incubation

Bacteria	NPs	Colour	Media	Hours of incubation
<i>A. baumannii</i>	Au	dark Red	N.B	24 h
<i>P. aeruginosa</i>	Ag	dark brown	MGYP	72 h
<i>P. aeruginosa</i>	Ag_2O_3	dark brown	MGYP	72 h
<i>S. marcescens</i>	Se	Light orange	N.B	48 h

3.4 Characterization of Synthesized NPs

3.4.1 Physical characterization

3.4.1.1 UV-Visible

The presence of the synthesized NPs in the present study was confirmed by some tests, including UV-Visible. The peaks at 560 nm wavelength confirmed the production of AuNPs synthesized from *A. baumannii* after incubation for 24 h Fig (3.6), as the study (Srinath & Rai,2015) showed the surface plasmon resonance (SPR) of AuNPs usually ranges from 510 to 560 nm. where the UV spectrum of AuNPs synthesized from *Enterobacter aerogenes* filtrate was determined at a peak of 540 nm.

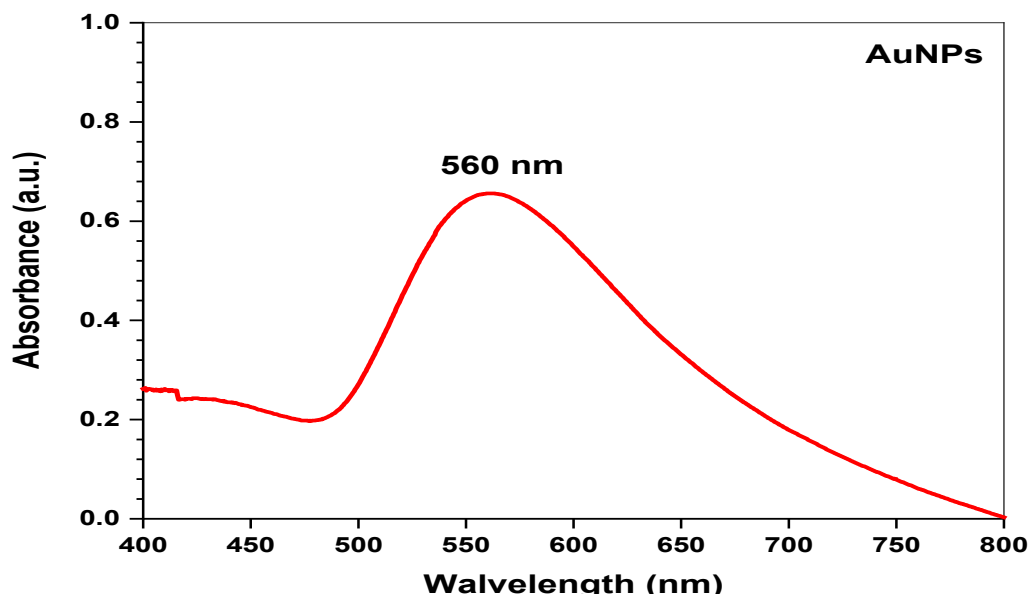


Fig (3.6) Uv-visible of AuNPs produced by *A. baumannii*

While the peaks at 426 nm and 430 nm confirmed the production of AgNPs and Ag₂O₃NPs synthesized from *P. aeruginosa*, and *P. aeruginosa* respectively after incubation for 72 h Fig (3.7), Fig (3.8). In the study (Ibrahim&, Hateet, 2021), where the UV spectrum of AgNPs synthesized from *Staphylococcus lentus* filtrate was recorded after 72 hours of interaction at about 400 nm, which is a feature of colloidal silver. In another study (Minhas *et al.*,2023) the surface plasmon resonance peak of Ag₂O₃NPs synthesized by *Nodularia haraviana* appeared at 428nm. The appearance of absorption bands in the visible region is due to the surface oscillation of the conduction electron plasmon, which is coupled through

the surface with the external electromagnetic fields. This is one of the most important optical properties of nanoparticles that differ from their bulk metal (Ogarev *et al.*, 2018)

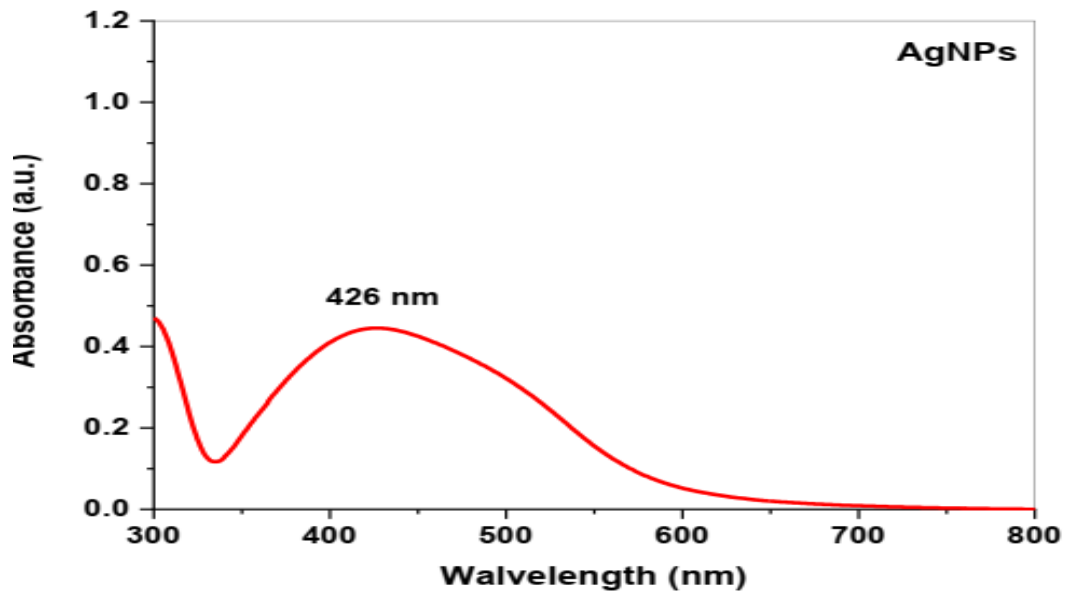


Fig (3.7) Uv-visible of AgNPs produced by *P. aeruginosa*

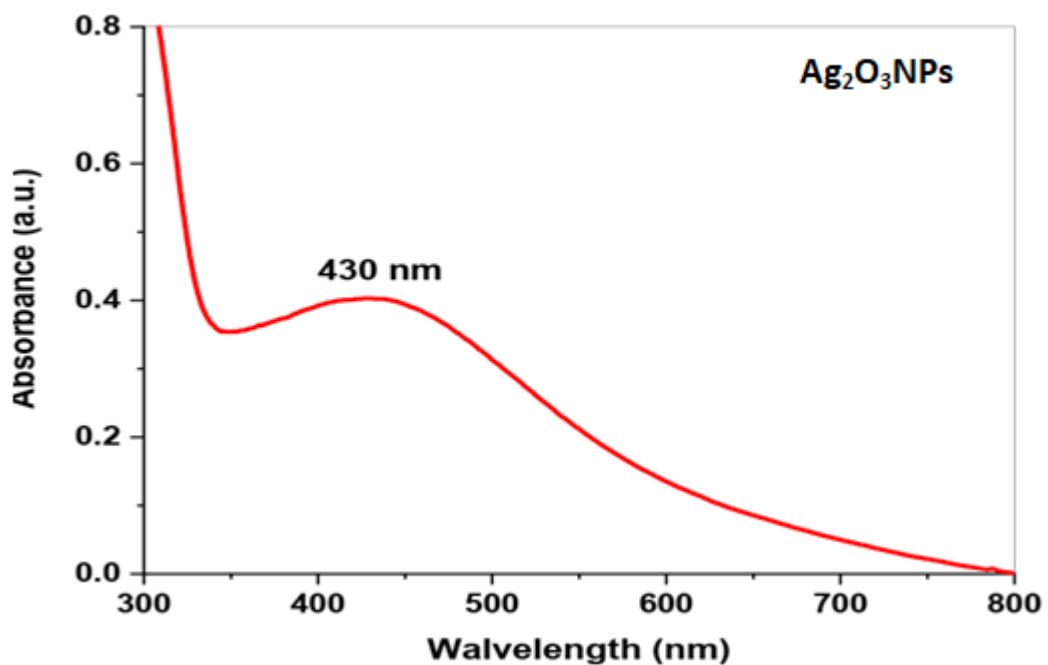


Fig (3.8) Uv-visible of Ag₂O₃NPs produced by *P. aeruginosa*

As for the production of SeNPs synthesized from *S.marcescens* after incubation for 48 h, according to the absorbance scan, observing a strong plasmon resonance peak at 298 nm Fig (3.9) confirmed the presence of selenium in the samples (Ghaderi *et al.*,2022). According to Shoeibi & Mashreghi,2017 SeNPs produced by *E. Faecalis* had the largest absorption peak at the ideal 24-hour period with a sodium selenite concentration of 0.19 mM, and the lowest absorption peak occurred at a concentration of 2.97 mM (Shoeibi & Mashreghi,2017).

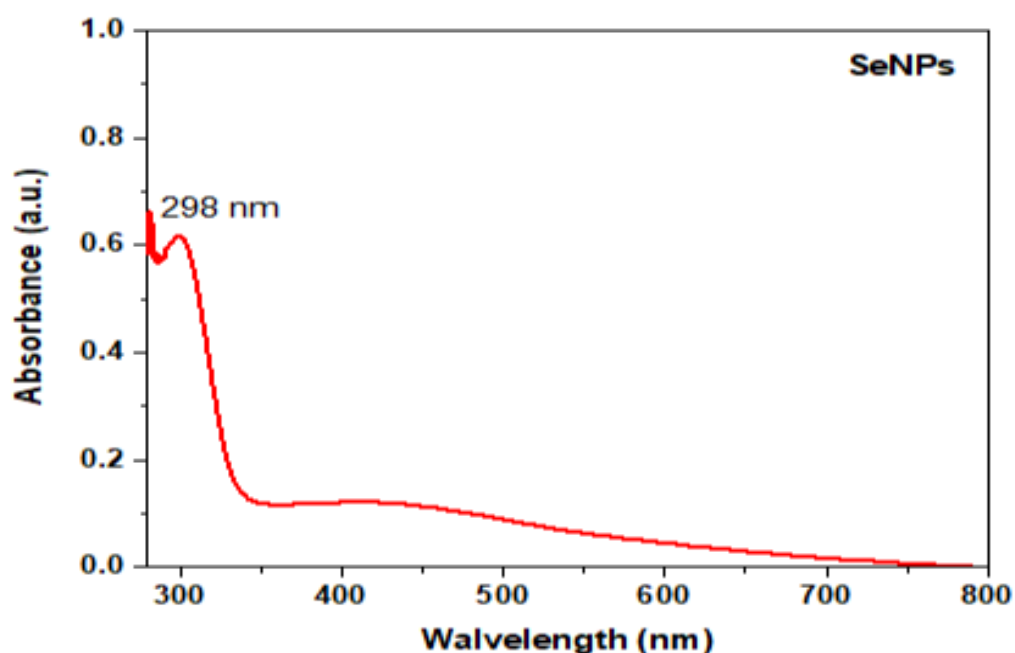


Fig (3.9) Uv-visible of SeNPs produced by *S.marcescens*

Table (3.4) Uv-visible wave length of NPs

Bacteria	NPs	Wave Length
<i>A. baumannii</i>	Au	560 nm
<i>P. aeruginosa</i>	Ag	426 nm
<i>P. aeruginosa</i>	Ag ₂ O ₃	430 nm
<i>S. marcescens</i>	Se	298 nm

3.4.1.2 Fourier transform infrared spectroscopy (FTIR)

The functional groups associated with the nanoparticles were identified according to the reference table (Merck, 2020). The FTIR data confirmed that all the synthesized nanoparticles were surrounded by distinct and functional molecules and possessed three similar functional groups for AuNPs, AgNPs, Ag₂O₃NPs, SeNPs peaks at 3294, 3302, 3327, 3326 (O-H stretching) respectively, while peaks at 2105, 2155, 2091, 2173 (C-C) and 1637 (C=C stretching) which might be due to the presence of aggregates (Alcohol, Alkyne, Alkene) respectively. Fig (3.10) and Table (3.5), Fig (3.11) and Table (3.6), Fig (3.12) and Table (3.7), Fig (3.13) and Table (3.8)

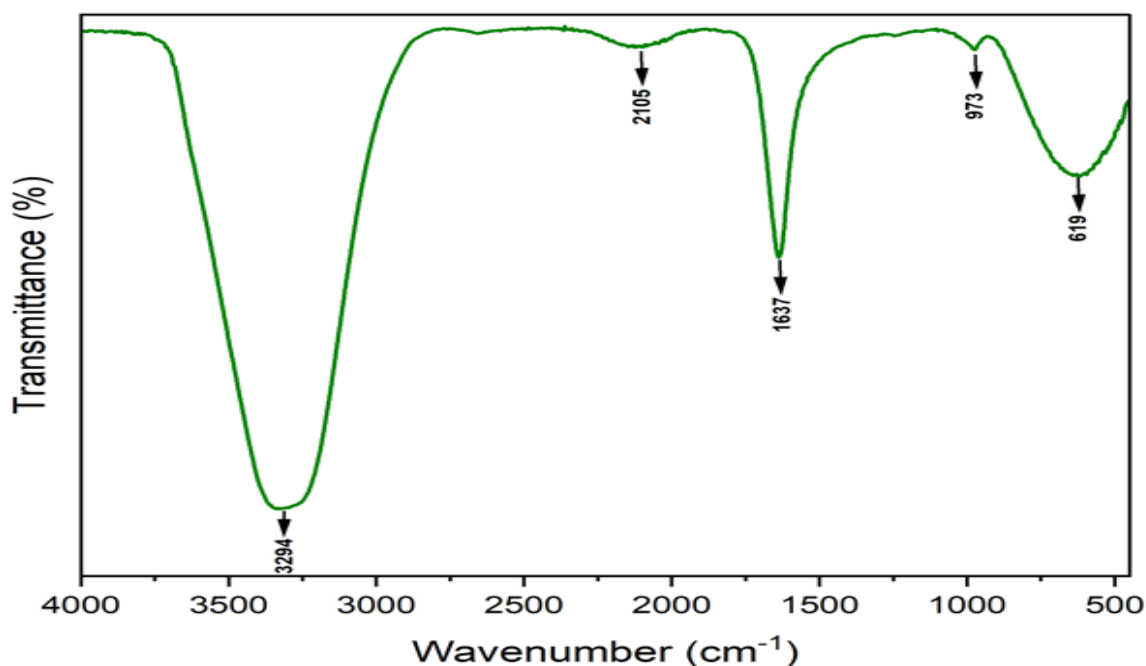


Fig (3.10) FTIR analysis of AuNPs produced by *A. baumannii*

Table (3.5) The various bands and Functional groups of AuNPs

Wave number cm ⁻¹	Bands	Functional group
3294	O-H	Alcohol
2105	C-C	Alkyne
1637	C=O C=C	Alkene

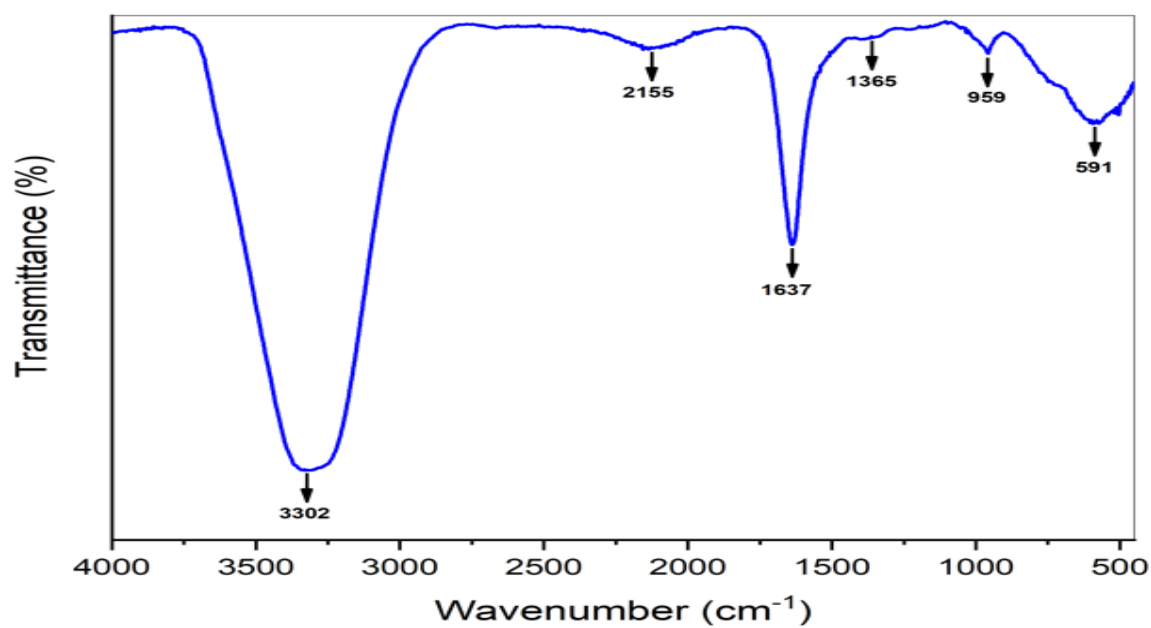


Fig (3.11) FTIR analysis of AgNPs produced by *P. aeruginosa*

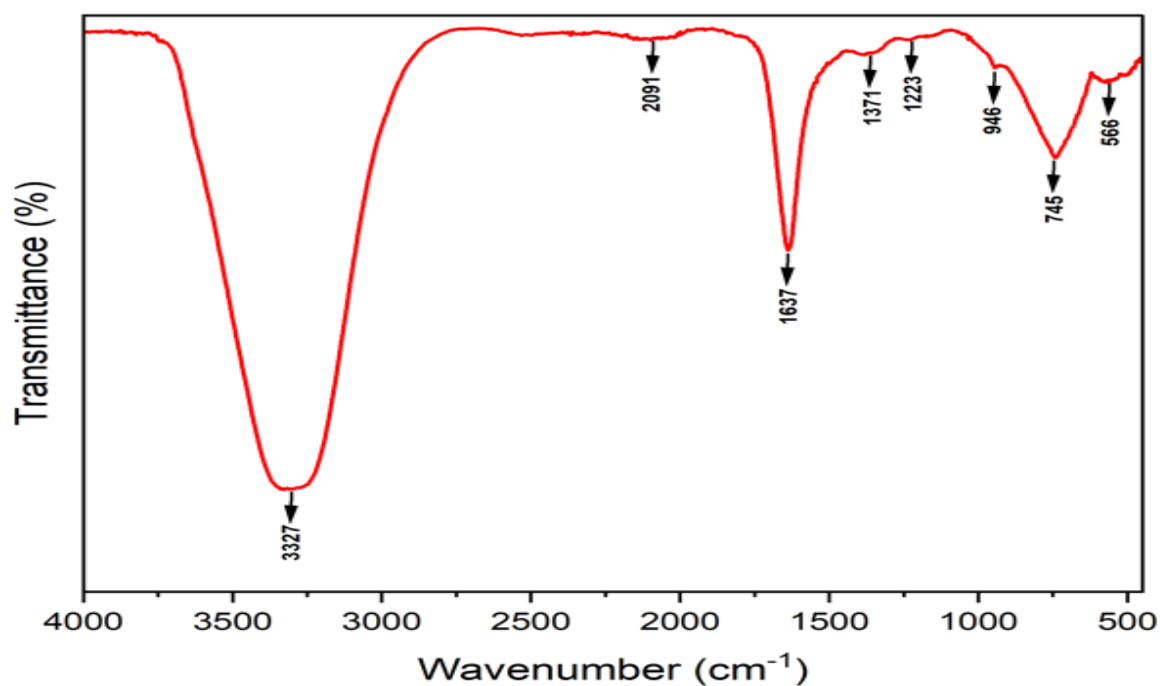


Fig (3.12) FTIR analysis of Ag_2O_3 NPs produced by *P. aeruginosa*

Table (3.6) The various bands and Functional groups of AgNPs, Ag₂O₃NPs

Wave number cm ⁻¹	Bands	Functional group
3302	O-H	Alcohol
2155	C-C	Alkyne
1637	C=O C=C	Carbonyle
1365	C-H	Alkene
959	C=O	Alkene
591	C-I	halo compound

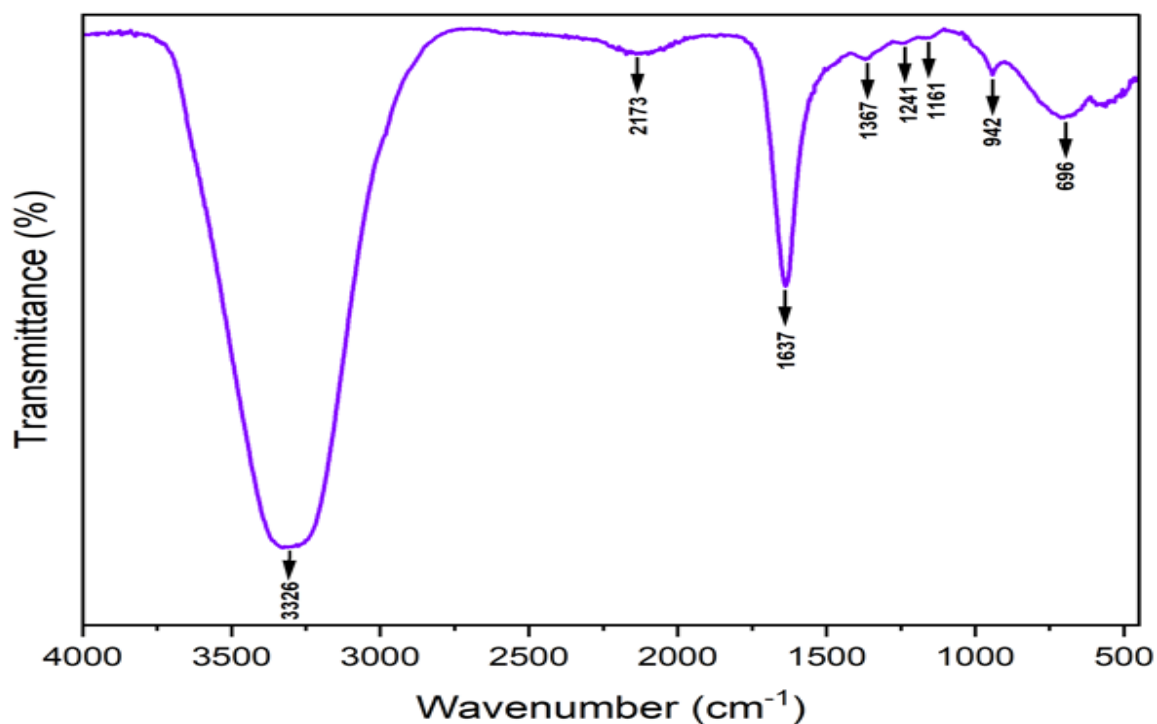
Fig (3.13) FTIR analysis of SeNPs produced by *S. marcescens*

Table (3.7) The various bands and Functional groups of SeNPs

Wave number cm^{-1}	Bands	Functional group
3326	O-H	Alcohol
2173	C-C	Alkyne
1637	C=O C=C	Carbonyle
1367	C-H	Alkene
1241	C-N	Amine
1161	S=O	Sulfone
942	C=C	Alkene
696	C=C	Alkene

(Tabassum *et al.*, 2024) indicated that the FTIR spectrum at peak (1616) is attributed to C=C stretching vibrations which indicate the presence of double bonds between carbon atoms and the presence of unsaturated organic compounds or aromatic rings. A study by (Menon *et al.*, 2020) showed that the peak is located at peak 3372 within the functional groups of amines (N=H) which may be due to the presence of urea or peptides. (Alfryyan *et al.*, 2022) indicated these results may be the contribution of proteins and other molecules in the bio-reduction process and the stability of NPs.

3.4.1.3 Zeta potential analysis

The zeta value of AuNPs synthesized from *A. baumannii* was determined to be (-13mv) Fig (3.14). The electrical potential of measuring the zeta potential difference indicates the stability of the colloidal solution. If the particles have a high positive or negative value, these particles will separate from each other and thus there will

be no aggregation or clumping with each other (El-Saadony *et al.*,2019) while the zeta value of AgNPs and Ag₂O₃NPs synthesized from *P. aeruginosa* was (14.5mv, 0.95mv) respectively, Fig (3.15), (3.16). As for the zeta value of SeNPs synthesized from *S. marcescens*, it was (-19.8mv) Fig (3.17). The more negative/positive charge on the surface of the nanoparticles is important for long-term stability, as it prevents the particles from agglomerating in the medium (Pallavi *et al.*, 2022). Since SeNPs showed a greater negative result than AgNPs and AuNPs, they are more stable among the particles, while AgNPs and Ag₂O₃NPs showed a positive result.

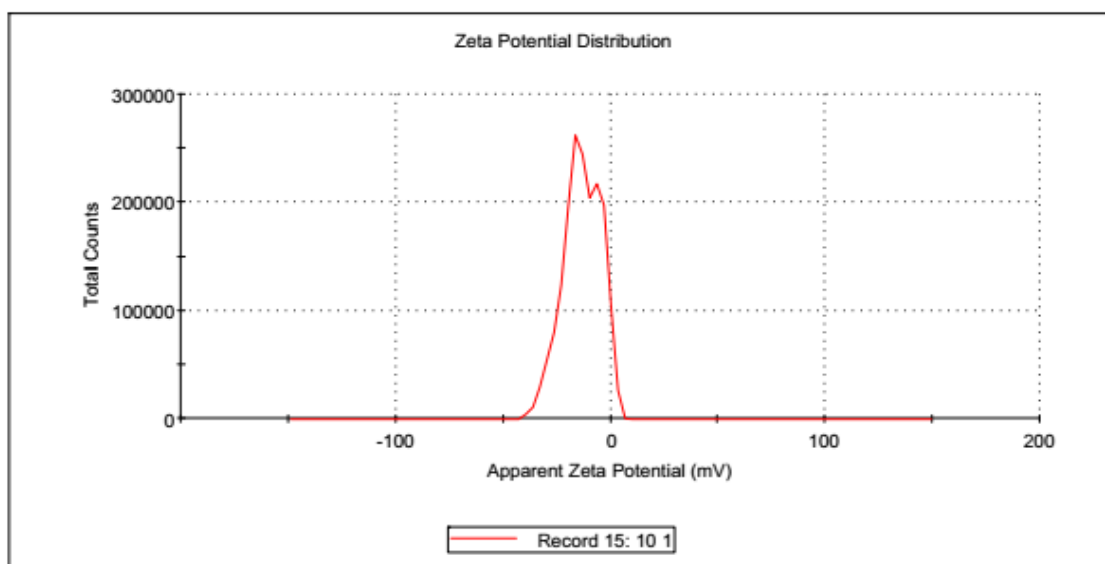


Fig (3.14) zeta value of AuNPs produced by *A. baumannii*

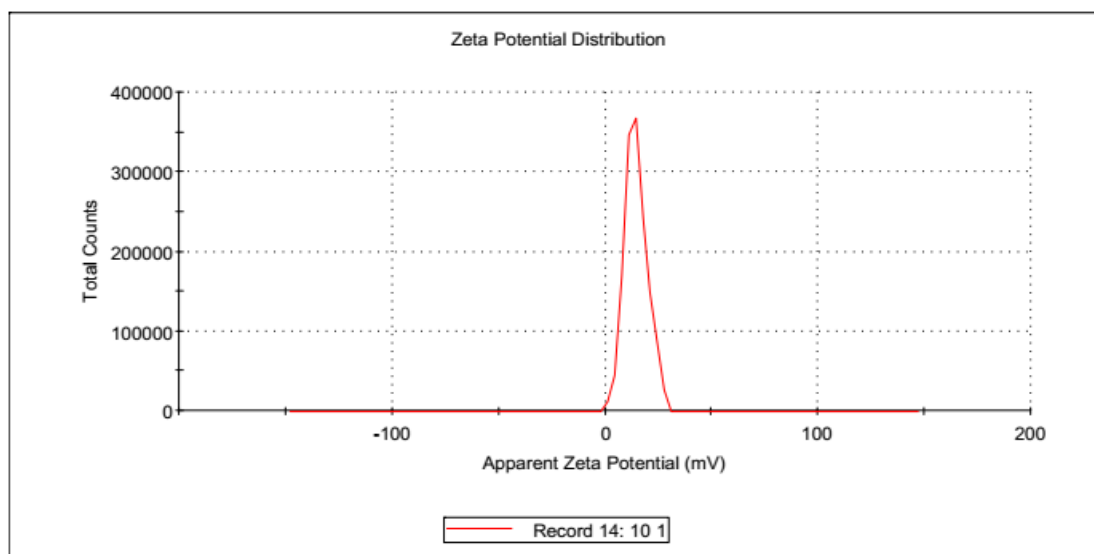
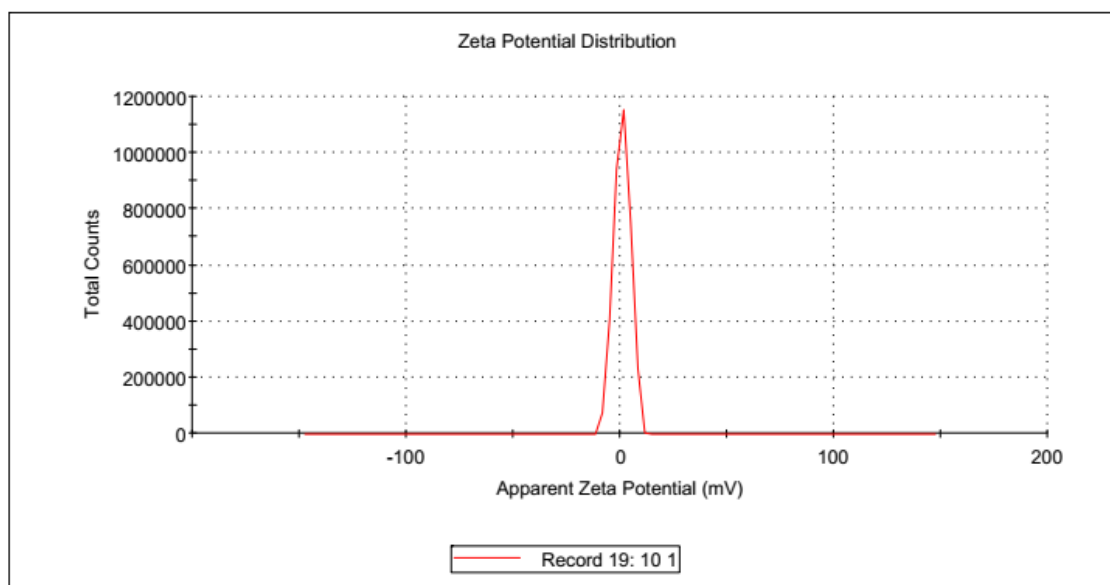
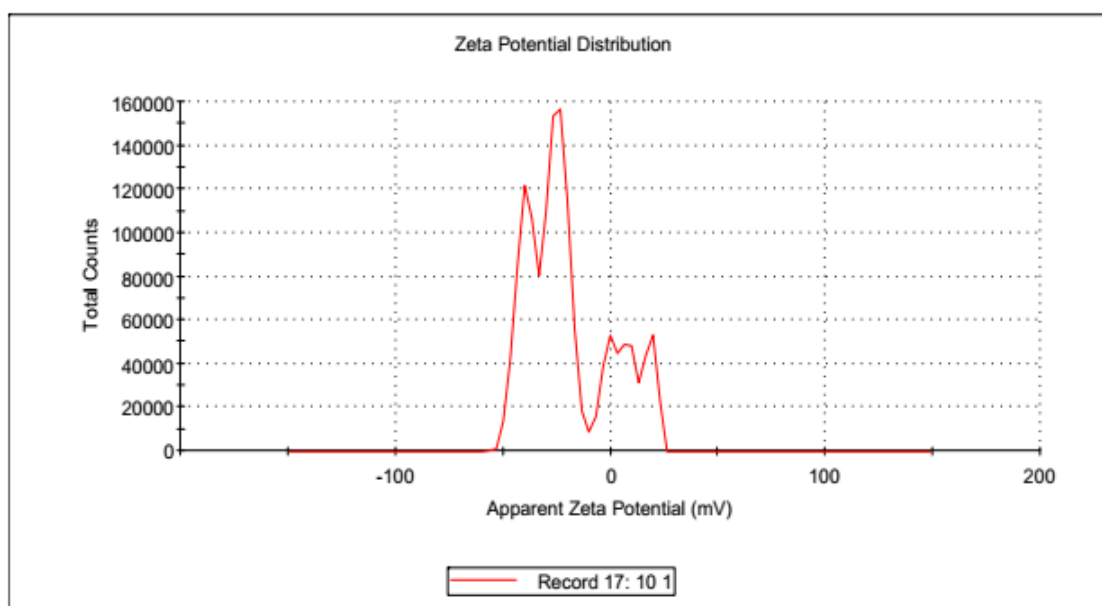


Fig (3.15) zeta value of AgNPs produced by *P. aeruginosa*Fig (3.16) zeta value of Ag₂O₃NPs produced by *P. aeruginosa*Fig (3.17) zeta value of SeNPs produced by *S. marcescens*

3.4.1.4 XRD analysis

The results of the current study showed that the X-ray spectrum of the peaks obtained was consistent with Bragg reflections at a value of 2 theta and finding the average size of the nanoparticles using the Debye-Schärer equation. Fig (3.18)

shows the XRD spectrum of AuNPs created from the filtrate *A. baumannii* four Bragg reflections (111) (200) (220) (311) at a value of 2 theta for angles (38.18) (44.39) (64.57) (77.54) respectively, referring to JCPDS data file No. 00-004-0784 as a standard reference for AuNPs, indicating that they are particles. The crystalline nature tends to have a cubic structure and the average particle size using the Debye-Schwarr equation was 22.6 nm, Table (3.8). This is consistent with (Sunderam *et al.*,2019).

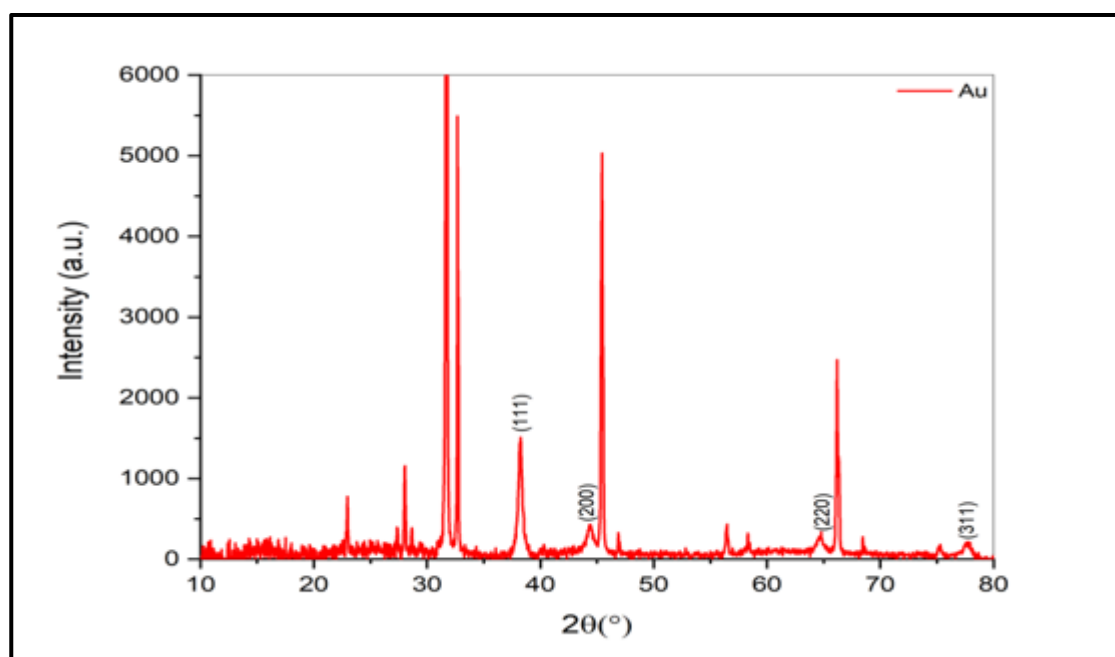


Fig (3.18) XRD analysis of AuNPs produced by *A. baumannii*

Table (3.8) Debye-Schwarr equation of AuNPs

2 theta	theta (deg)	theta (rad)	Cos theta	FWHM (β) (deg)	FWHM (rad)	D
38.236	19.11801	0.33350306	0.9449014	0.25584	0.004462987	32.86633
44.357	22.1785	0.38689161	0.92608636	0.374804	0.006538248	22.89024
64.676	32.338175	0.5641215	0.84505864	0.51168	0.008925973	18.37472
77.549	38.774375	0.67639743	0.77983294	0.614016	0.010711168	16.593
D-average						22.6811

Fig (3.19) shows the XRD spectrum of AgNPs synthesized from the filtrate *P. aeruginosa* where it showed Bragg reflection peaks (111) (200) at 2 theta for angles (38.11) (43.27) respectively based on JCPDS data file No. 00-004- 0783 which indicates that the AgNPs are crystalline and have a structure similar to that of AuNPs (cubic) and their average size is 34.5nm, Table (3.9). In a study (Dewan & Hateet,2023) the X-ray spectrum showed that AgNPs are FCC (face-centered and cubic) and are spherical and created crystalline. XRD was used in another investigation to identify the crystalline phase and structure of AgNPs. AgNPs' distinctive diffraction peaks at 2θ were found to be 29.8°, 33.2°, 36.5°, 47.8°, 52.7°, 5.0°, 61.6°, 69.9°, 71.8°, and 87.3° (Tabassum *et al.*,2024).

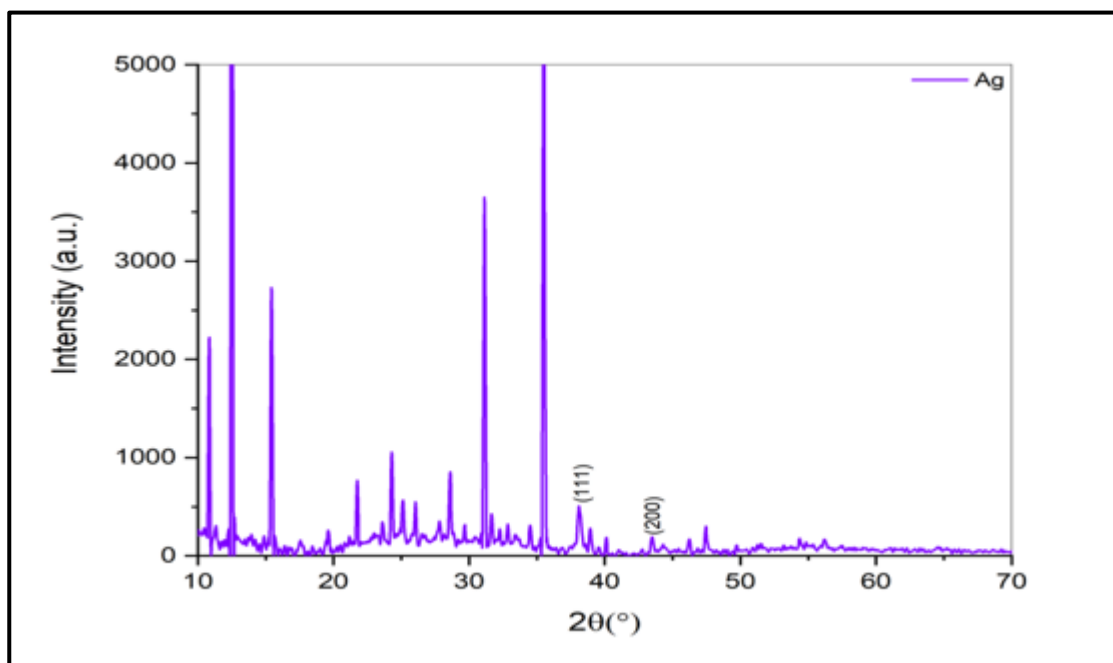


Fig (3.19) XRD analysis of AgNPs produced by *P. aeruginos*

Table (3.9) Debye-Schwarr equation of AgNPs

2 theta	theta (deg)	thata (rad)	Cos theta	FWHM (β) (deg)	FWHM (rad)	D
38.09	19.045235	0.33223354	0.94531622	0.307008	0.005355584	27.37659
43.496	21.74818	0.37938492	0.92889261	0.204672	0.003570389	41.79094
D-average						34.5838

Fig (3.20) shows the XRD spectrum of Ag_2O_3 NPs synthesized from the filtrate *P. aeruginosa* where the peaks agree with Bragg reflections (111) (211) (221) at 2θ for angles (31.57) (45.25) (56.22) respectively and they can be considered as crystalline particles and have a cubic structure and the average its size is 53.7 nm, Table (3.10) according to JCPDS data file No. 76-1393. This result can be considered completely consistent with what was reached by (Pradheesh *et al.*,2020) and in the study (Gungure *et al.*,2024) when recording the XRD from 20° to 80° angles, the crystallite peak positions were noted. The planes of (110), (111), (200), (220), and (311) correspond to the spherical phase of Ag_2O NPs at 29.30° , 38.0° , 45.04° , 65.14° , and 76.32° , respectively. This means Every sample had spherical structures and strong crystallinity in a single phase of Ag_2O NPs.

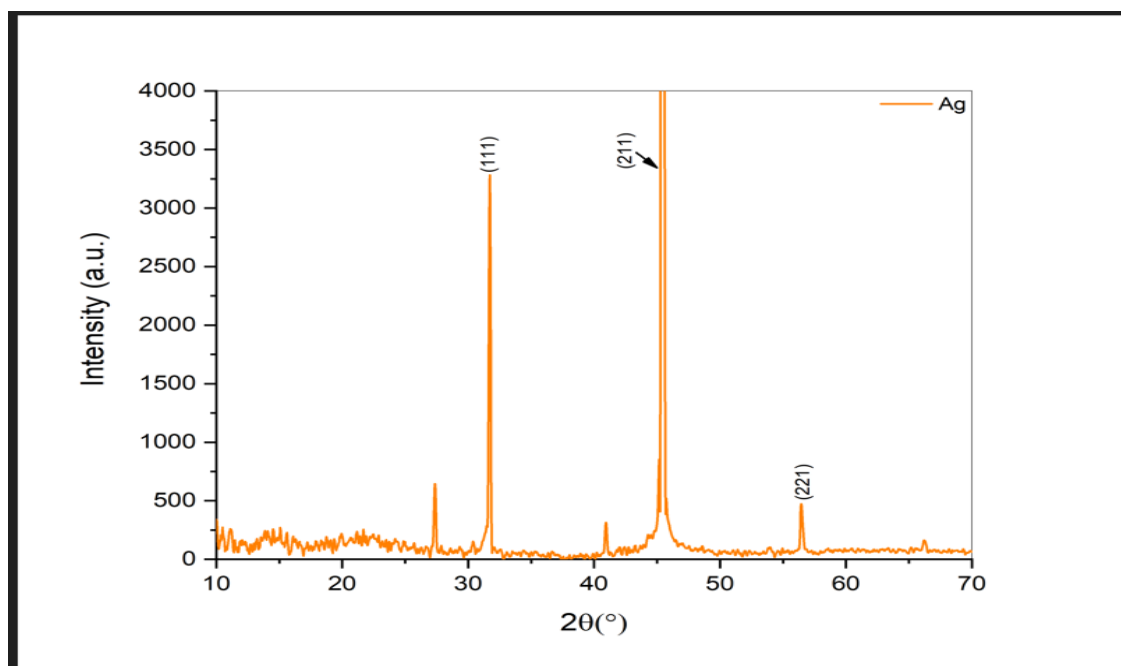


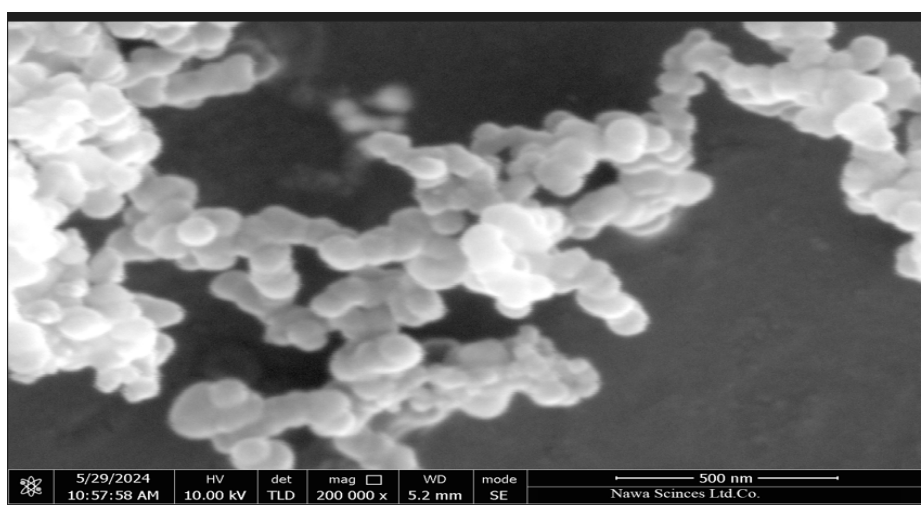
Fig (3.20) XRD analysis of Ag_2O_3 NPs produced by *P. aeruginosa*

Table (3.10) Debye-Schwarr equation of Ag₂ONPs

2 theta	theta (deg)	thata (rad)	Cos theta	FWHM (β) (deg)	FWHM ((rad)	D
31.703	15.851655	0.27652332	0.96201043	0.12792	0.002231493	64.56362
45.395	22.697425	0.39594397	0.92263291	0.12792	0.002231493	67.31916
56.485	28.24256	0.49267577	0.88107042	0.307008	0.005355584	29.37283
D-average						53.7519

3.4.1.5 Fe-SEM analysis

Most of the images showed the morphology of the mentioned nanoparticles, which had uniform nanostructures with average size at different magnifications. Fig (3.21) shows Fe-SEM images of AuNPs synthesized from *A. baumannii* filtrate with a spherical shape and a scale bar of 500 nm and different sizes ranging from (43-91nm) and an average of 68nm Fig (3.22). The outcomes of a prior work demonstrated the successful synthesis of AuNPs with a spherical morphology, where the bio-synthesised AuNPs are homogeneous, uniform, and well-dispersed. Additionally, a propensity for aggregation is noted for artificial NPs while their size was ranged from 10-50nm (Chang *et al.*,2021).

Fig (3.21) Fe-SEM image of AuNPs Produced by *A. baumannii*

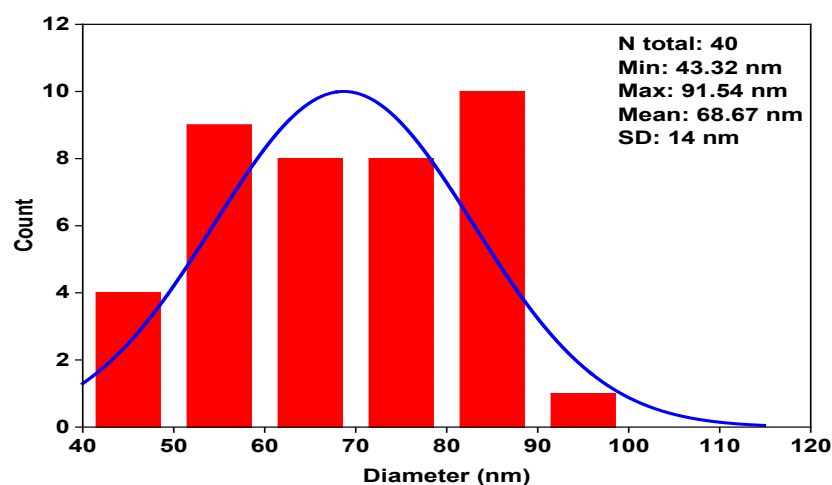


Fig (3.22) The histogram of the size distribution of AuNPs Produced by *A. baumannii*

While Fig (3.23) shows Fe-SEM images of AgNPs synthesized from *P. aeruginosa* filtrate also with a spherical shape and sizes ranging from (18-309nm) and an average of 45nm Fig (3.24).As Fig (3.25) shows some clusters of Ag₂O₃NPs synthesized from *P. aeruginosa* filtrate and almost spherical shapes and have nano sizes ranging from (25-351nm) and an average of 45nm Fig(3.26). In a study by (Dewan & Hateet,2023), the absence of direct contact between the AgNPs even within the aggregates indicated that they were crystalline in structure and had been stabilized by a capping agent. The microscopy analysis of biogenic AgNPs made by the two strains revealed homogenous, well-dispersed AgNPs, with the most common shape being spherical. With size between 41.55 nm and 44.51 nm. As demonstrated by (Gungure *et al.*,2024), the mean crystalline size of Ag₂O NPs was found to be 61.25 nm, and their typical surface morphology is spherical shapes of various sizes (20–100 nm). Additionally, accumulations of distinct Ag₂O NPs were discovered. While the findings of (Ibrahim&Hateet,2021) showed that there were spherically shaped particles with sizes ranging from 20.4 to 93.04 nm. Generally speaking, the function of NPs had a significant impact on the size and shape of the monodispersed particles.

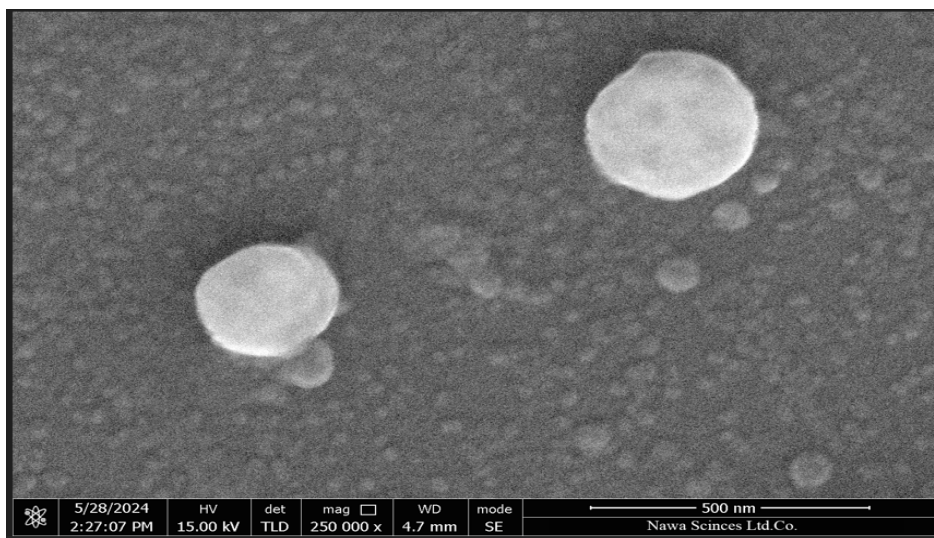


Fig (3.23) Fe-SEM image of AgNPs Produced by *P. aeruginosa*

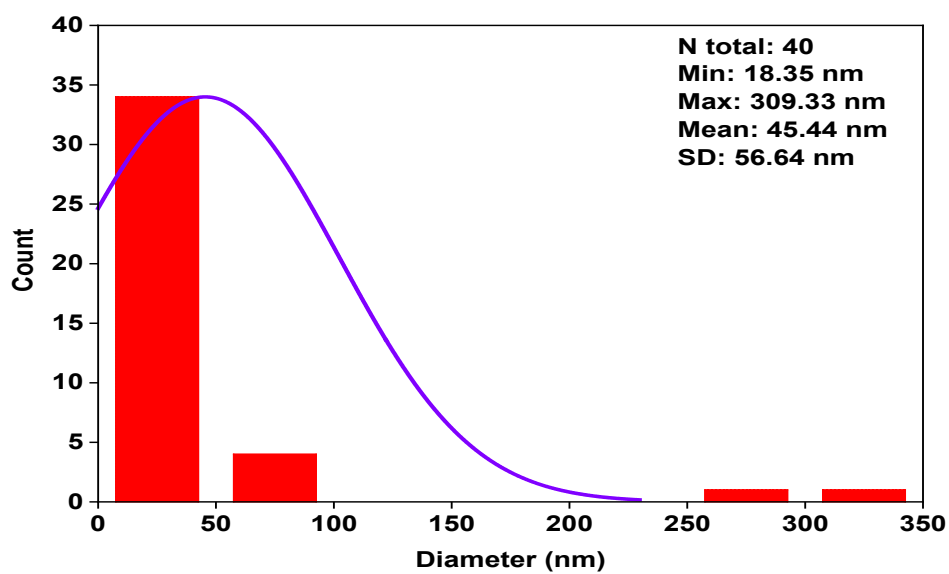


Fig (3.24) The histogram of the size distribution of AgNPs Produced by *P. aeruginosa*

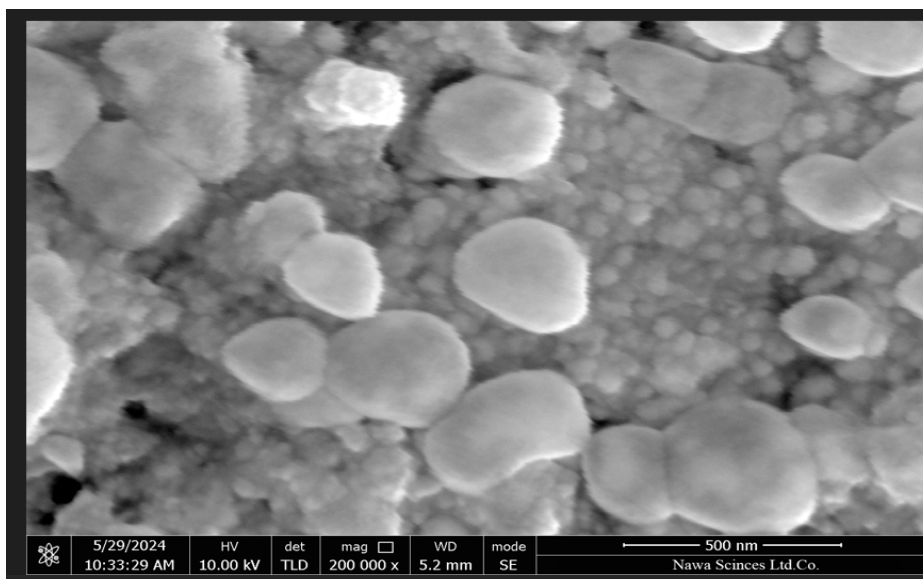


Fig (3.25) Fe-SEM image Ag₂ ONPs Produced by *P. aeruginosa*

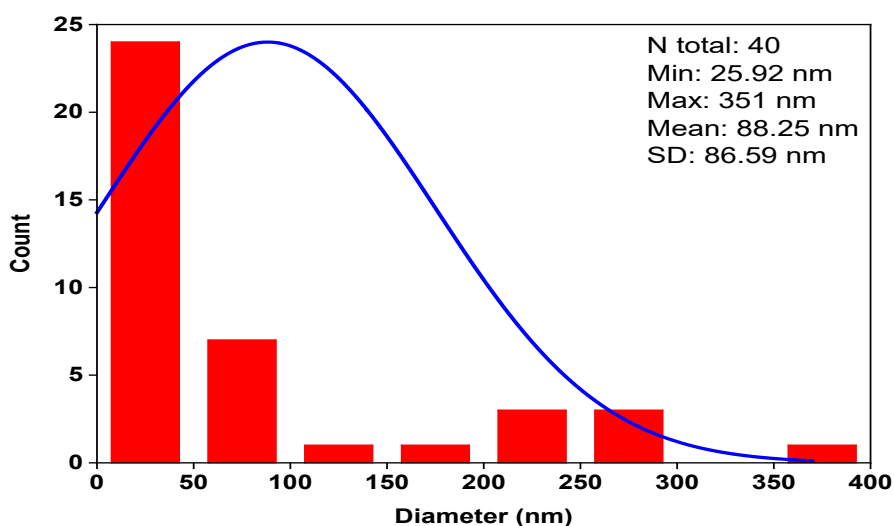


Fig (3.26) The histogram of the size distribution of Ag₂ ONPs Produced by *P. aeruginosa*

while SeNPs synthesized from *S. marcescens* filtrate were characterized by having semi-spherical shapes and undefined structures with some clusters and a scale bar of 500 nm Fig(3.27) and had nano sizes ranging from (35-203nm) and an average of 92nm, Fig (3.28). Similarly, the findings by (Salah *et al.*,2024) released SEM of Se NPs that dispersed as bright particles with a uniform surface distribution. Cittrarasu *et al.* used the green synthesis approach to generate SeNPs,

and they used FE-SEM to examine their size and morphological features. The findings demonstrated that the produced SeNPs have an average size of 55.9 nm and a consistent spherical shape (Cittrarasu *et al.*,2021)

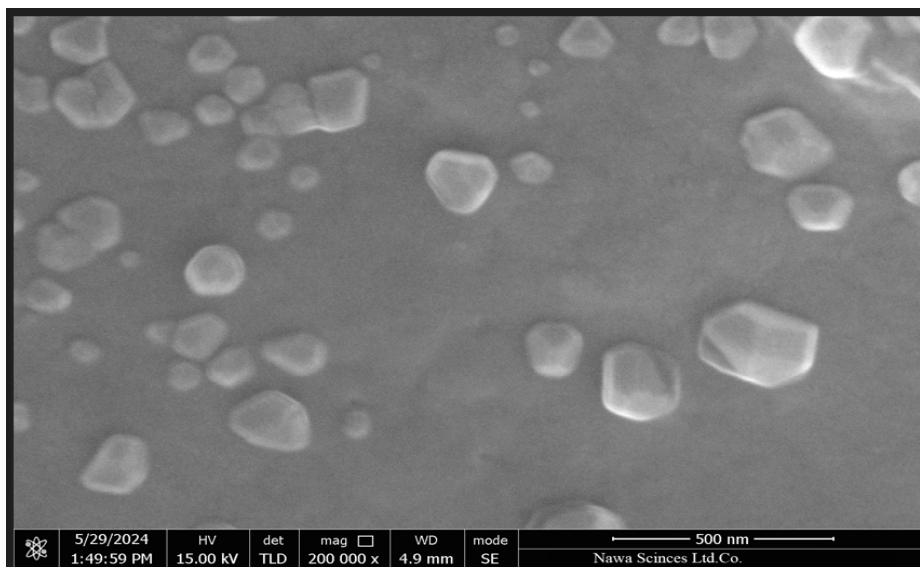


Fig (3.27) Fe-SEM image of SeNPs Produced by *S. marcescens*

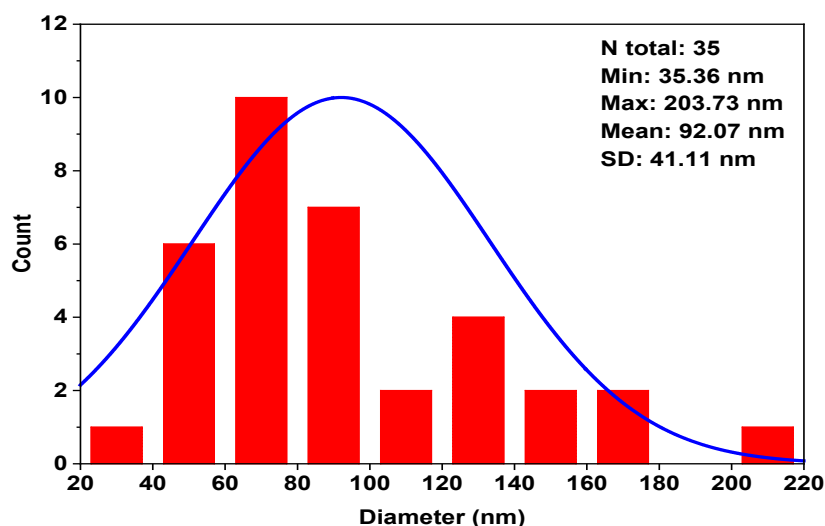


Fig (3.28) The histogram of the size distribution of SeNPs Produced by *S. marcescens*

It was observed that the AuNPs were in groups but were not in direct contact with each other, which indicates that they are more stable than other particles, this is consistent with what he has reached (Hatipoğlu,2021). As (Amendola *et al.*,2017)

revealed the tiny NPs diameter provides a rationale that aligns with the findings of the UV-visible optical absorption analysis, which tracked light absorption in the ultraviolet spectrum. This absorption shows how NPs interact with UV light and is consistent with their modest size.

3.4.1.6 EDX-Mapping analysis

According to the EdX data we obtained, it was confirmed that the NPs synthesized in our study contain (Au, Ag, Ag₂O₃ and Se) in their composition. In other words, the strong signal from (Au, Ag, Ag₂O₃ and Se) atoms indicates the success of the biosynthesis process of the mentioned NPs. To identify and link unique X-rays based on their wavelength and intensity to the presence of certain elements and their concentration in a sample, the elemental structure of NPs is examined using EDX spectroscopy, which is also used to validate the created samples (Salah *et al.*,2024). It can be said that the peaks seen in Fig (3.29), (3.30), (3.31), and (3.32) are due to the chemicals present in the bacterial extracts, and the presence of signals such as oxygen, carbon, and silicon, chloride, etc Table (3.11). May have arisen from organic biomolecules or phenolic compounds on the surface of the NPs (Hatipoğlu,2021). (Minhas *et al.*,2023) indicated the presence of other elements, such as O, S, C, and Na, with percentages of 23.63%, 1.27%, 1.84%, and 2.14%, respectively, was also revealed by the quantitative analysis, which further confirmed a high content of silver (65.38%) in the sample synthesized by *Nodularia haraviana*. It is possible that these elements were present because of some salt or protein residue in the strain isolates. In another study the silver (Ag) portion of the EDX spectrum showed a broad signal, while the oxygen (O) region showed smaller signals means that rather than AgNPs, the EDX spectrum data show the creation of Ag₂ONPs (Dharmaraj *et al.*, 2021). The presence of selenium in the solutions tested by the EDX test has also been confirmed in many previous studies, including (Sowndarya *et al.*,2017; Haddadian *et al.*,2022; Nassar *et al.*,2023)

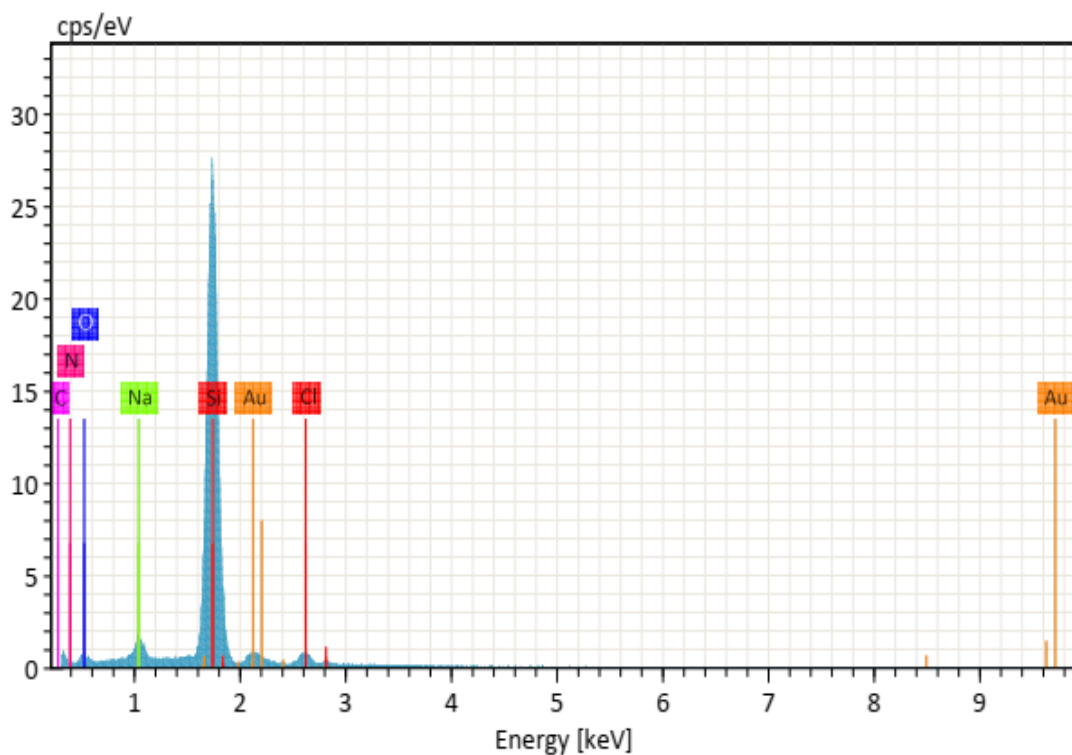


Fig (3.29) EDX analysis of AuNPs produced by *A. baumannii*

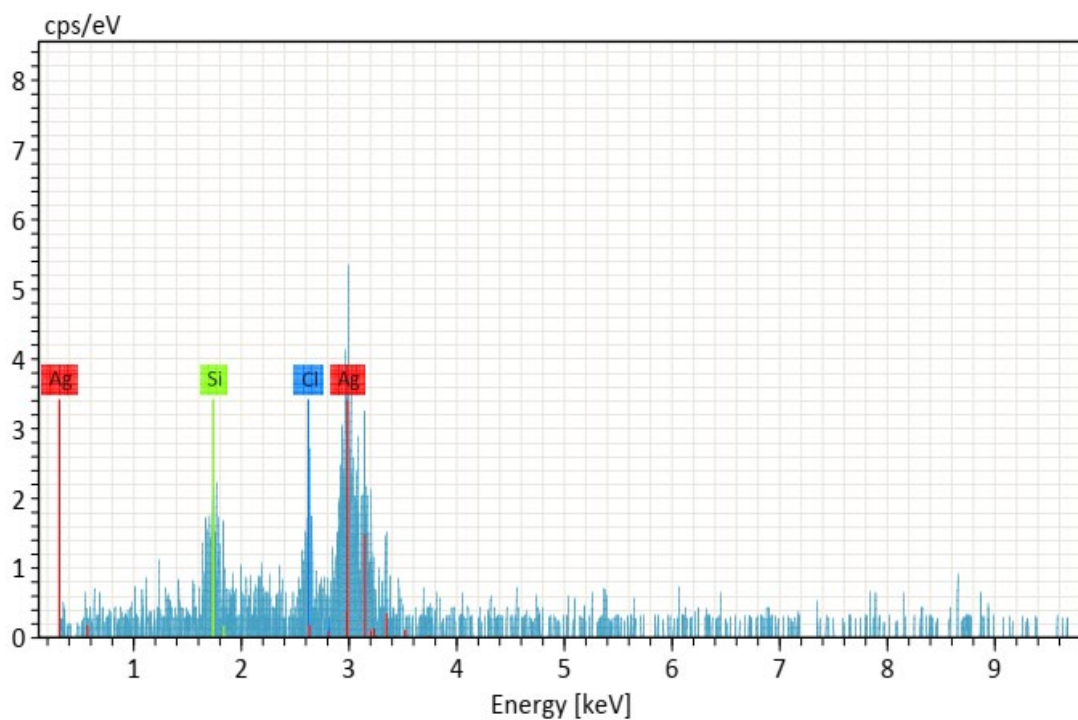


Fig (3.30) EDX analysis of AgNPs produced by *P. aeruginosa*

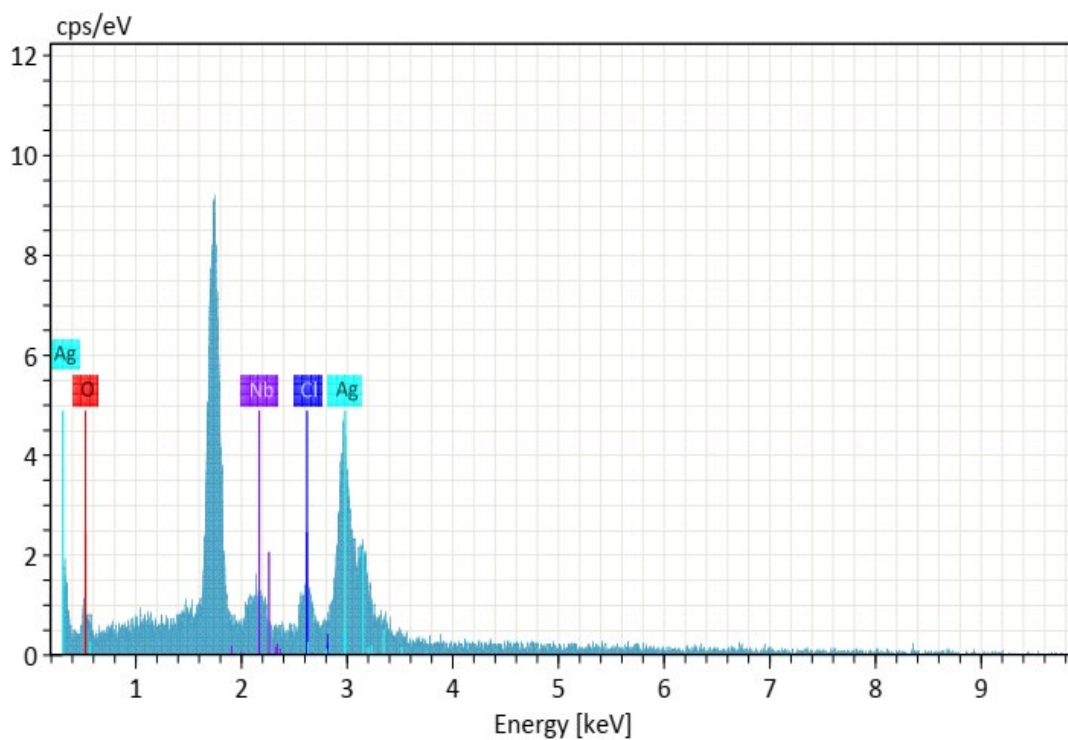


Fig (3.31) EDX analysis of Ag₂ONPs produced by *P. aeruginosa*

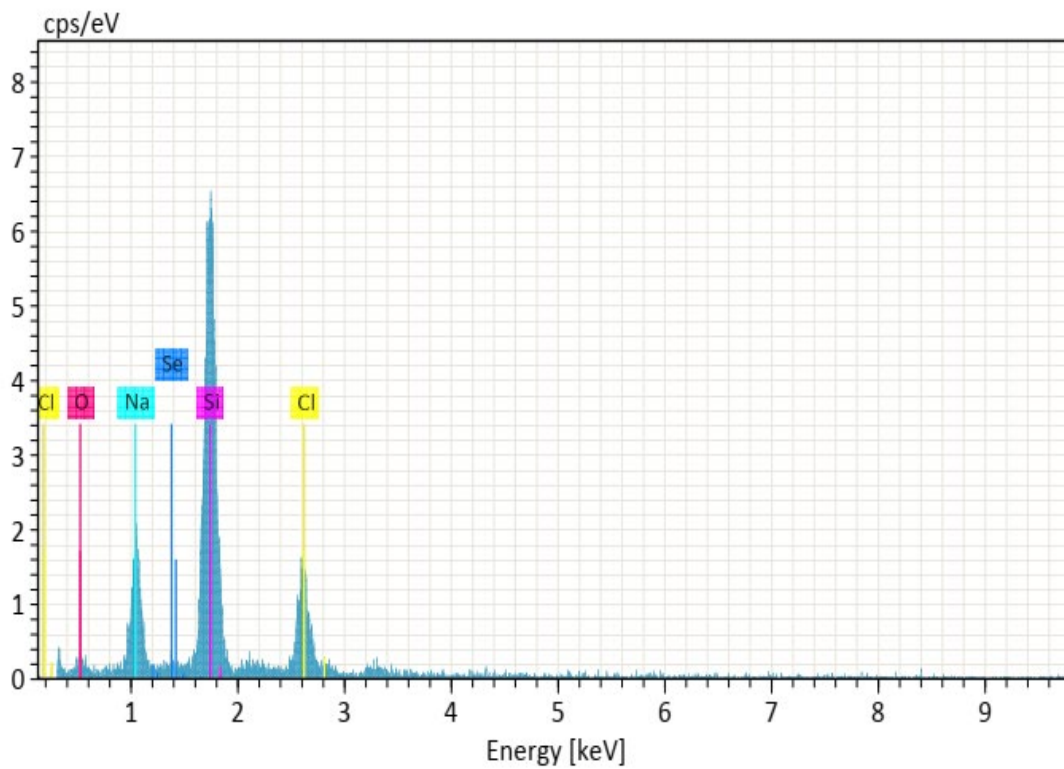
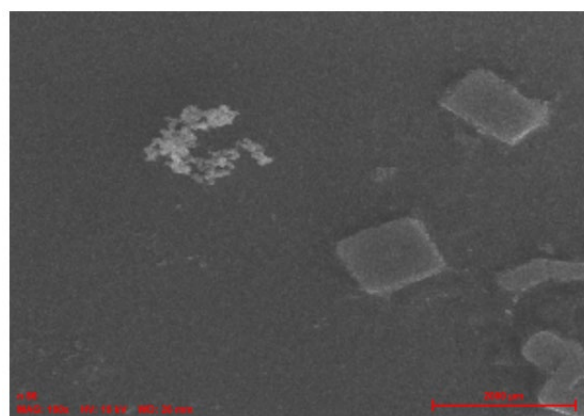
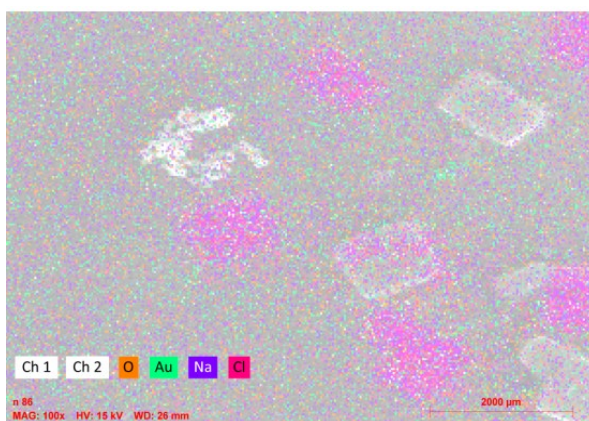


Fig (3.32) EDX analysis of SeNPs produced by *S. marcescens*

Table (3.11) Elemental ratios present in NPs by EDX analysis

Element	Mass%				Atom%			
	Au	Ag	Ag ₂ O ₃	Se	Au	Ag	Ag ₂ O ₃	Se
⁶ C	0				0			
⁷ N	8.14				21.38			
⁸ O	4.26		5.17	8.33	9.78		25.19	13.82
¹¹ Na	2.11			21.34	3.38			24.64
¹⁴ Si	47.55	10.19	16.14	46.04	62.27	27.15	44.84	43.52
¹⁷ Cl	2.16	7.44	1.9	23.88	2.24	15.71	4	17.88
⁷⁹ Au	5.02				0.94			
⁴⁷ Ag		82.37	32.05			57.14	23.18	
⁴¹ Nb			3.13				2.62	
³⁴ Se				0.4				0.14
Total	69.24	100	58.39	100	100	100	99.83	100

Fig (3.33) (3.34) (3.35) (3.36) show EDX-Mapping images of NPs (Au, Ag, Ag₂O₃, and Se) respectively, which show a map of the distribution of atoms for each element of the NPs, where it demonstrated that the atoms are uniformly distributed throughout each sample's map. We discover that the atoms are uniformly scattered across the sample's surface, indicating that the atoms take up multiple locations within the sample, providing a large area for spreading, which is one of the properties of nanomaterials, as they are of the smallest sizes and have a wide surface area (Alsohaimi *et al.*,2020; Ferraa *et al.*,2021)



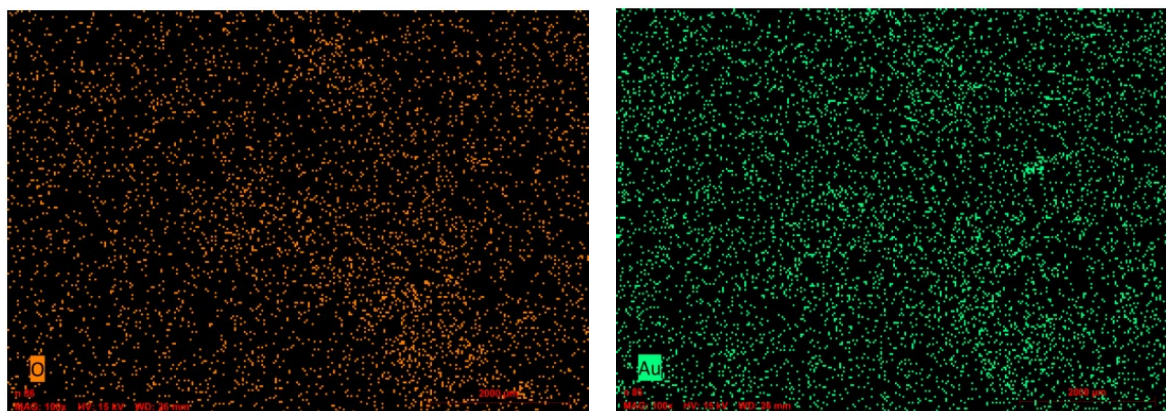


Fig (3.33) EDX-Mapping image of AuNPs produced by *A. baumannii*

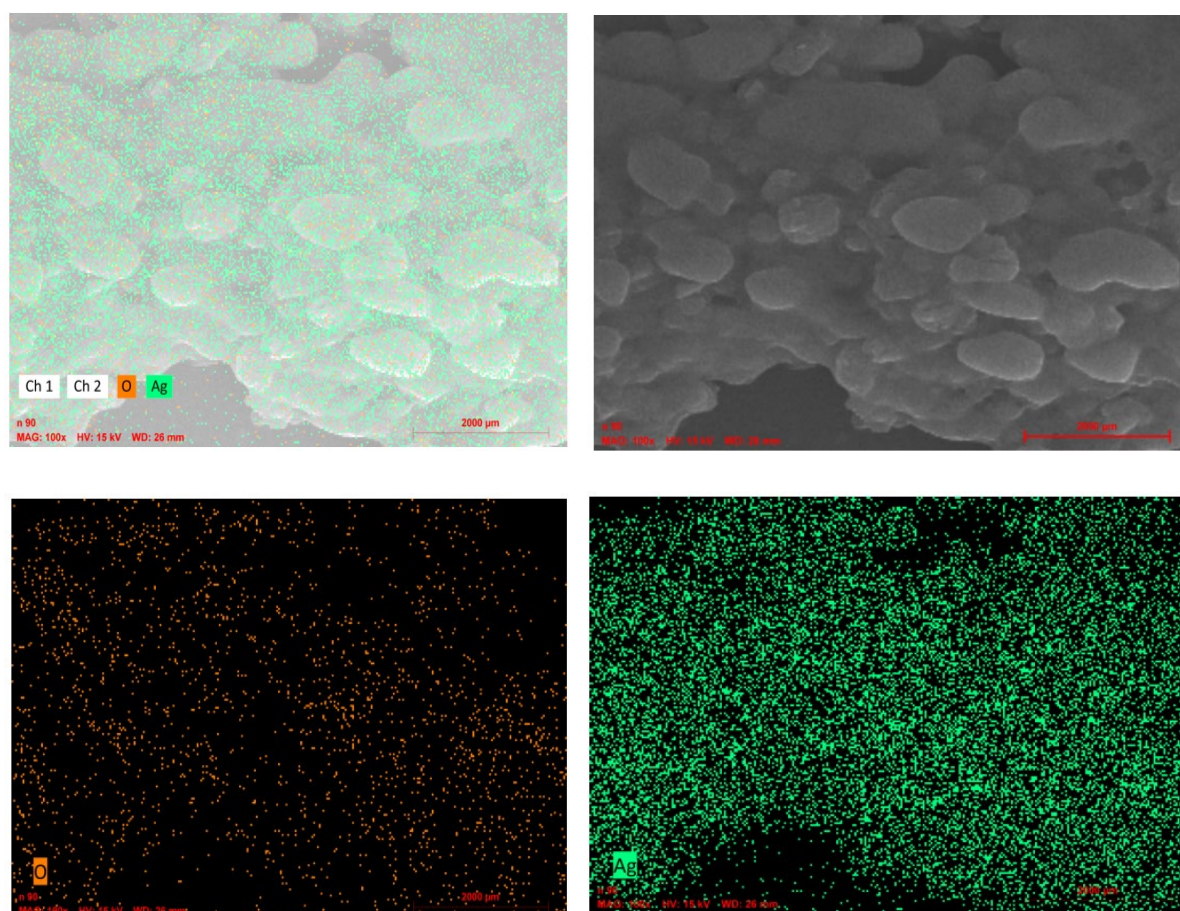


Fig (3.34) EDX-Mapping image of AgNPs produced by *P. aeruginosa*

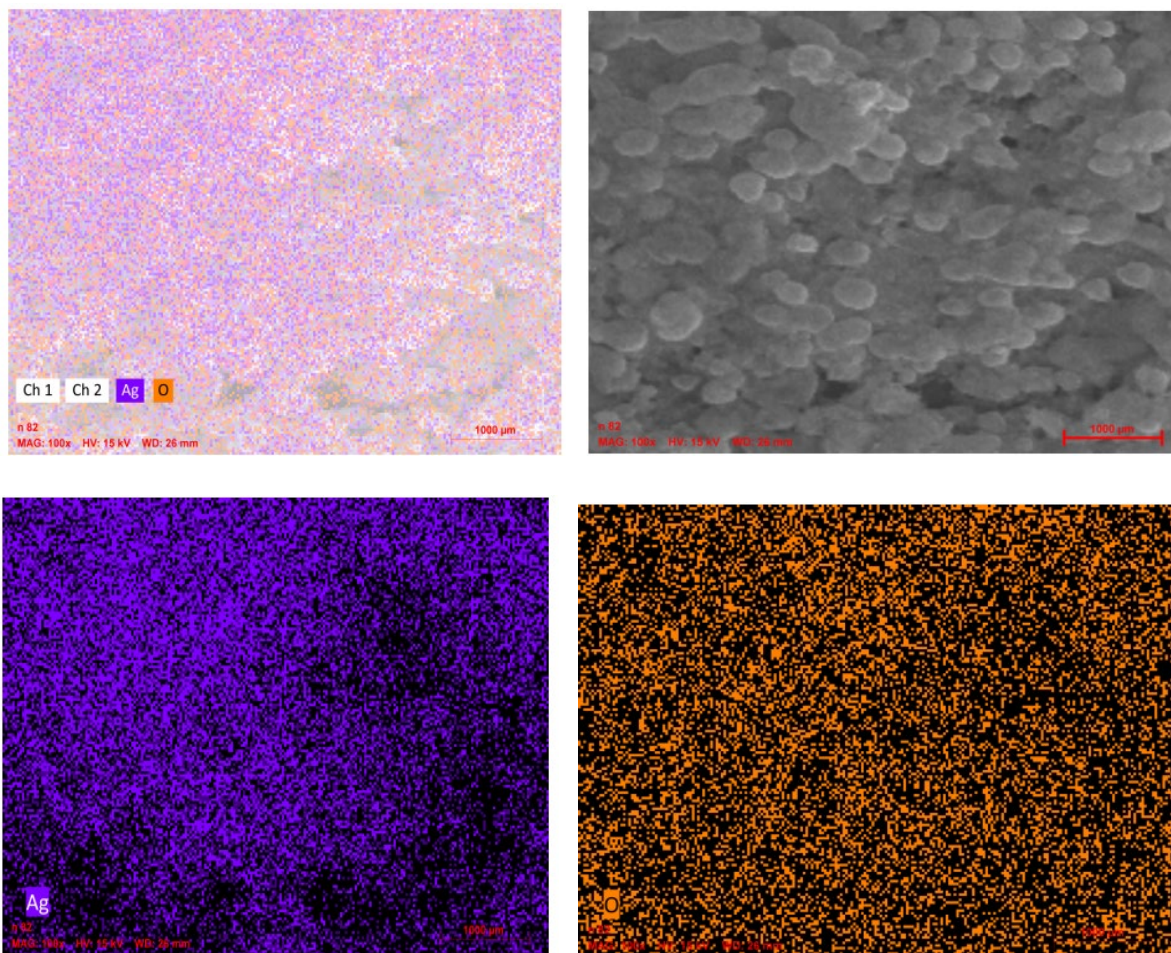
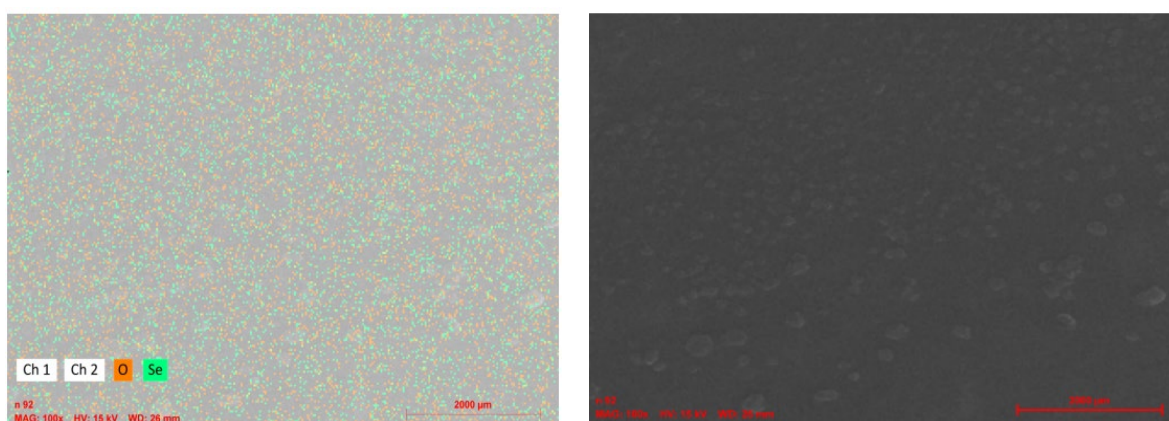


Fig (3.35) EDX-Mapping image of Ag₂ONPs produced by *P. aeruginosa*



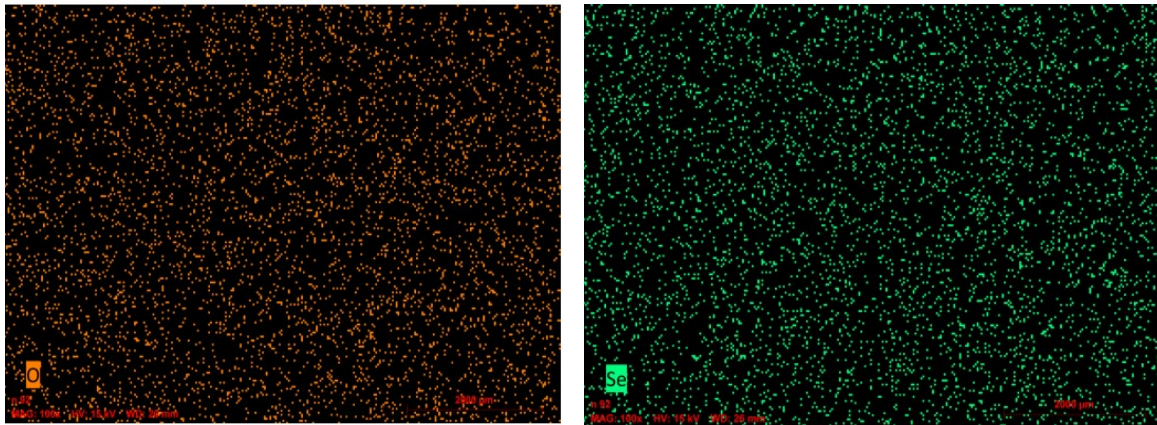


Fig (3.36) EDX-Mapping image of SeNPs produced by *S. marcescens*

3.4.1.7 Transmission electron microscope (TEM) analysis

Regarding the results of TEM analysis of the NPs manufactured in the current study, In Fig (3.37) the TEM shows images at different magnifications of the sample prepared from the bacterial filtrate *A. baumannii* where the presence of spherical AuNPs of small size ranging between (12-37 nm) and an average of 22.96 nm Fig(3.38) with a dark colour indicating the formation of AuNPs was observed. Similar results were reported in the study (Hatipoğlu,2021). also validated the TEM findings for *Aspergillus fumigatus*-biosynthesized AuNPs. In areas where AuNPs are not dispersed, the majority are spherical, range in size from 13 to 40 nm, and have an estimated average diameter of 23 nm (Alewi& Hateet,2022)

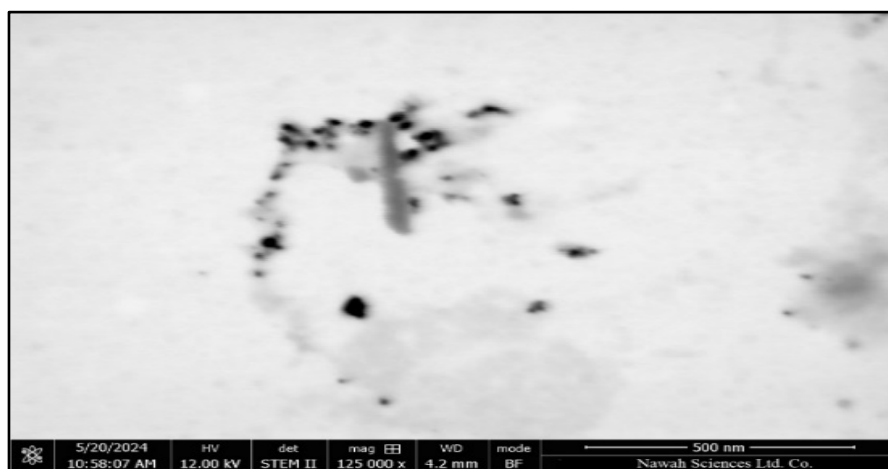


Fig (3.37) TEM image of AuNPs Produced by *A. baumannii*

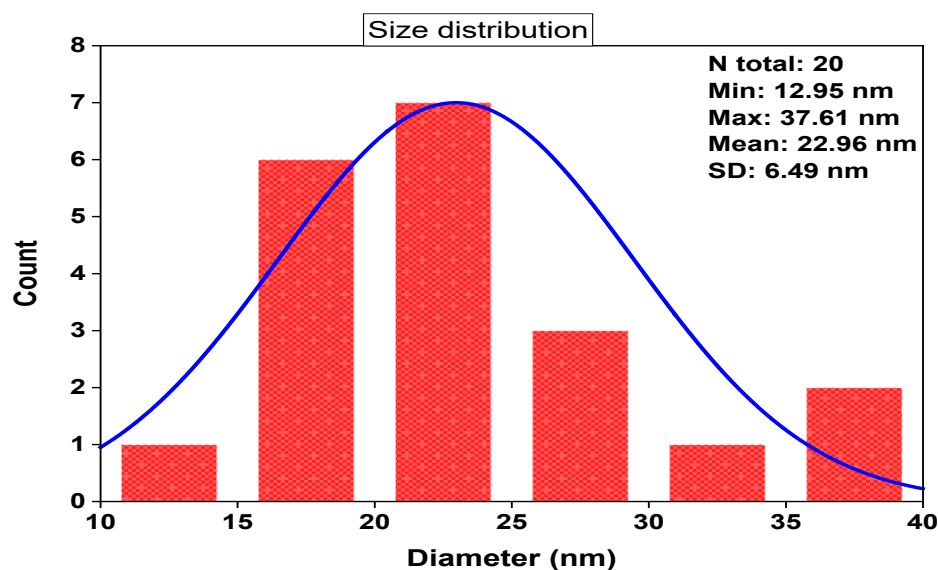


Fig (3.38) The histogram of the size distribution of AuNPs Produced by *A. baumannii*

In Fig (3.39) where we notice the presence of AgNPs synthesized from *P. aeruginosa* with a semi-spherical shape and some of them are close to the spherical shape and their nano size ranges from 10-81nm and an average of 29.61 nm Fig(3.40). This result can be considered in agreement with the study (Wypij *et al.*,2021) when the TEM analysis showed spherical and polydispersed of AgNPs with a size range of 3–36 nm. The highly dense AgNPs produced by the BO leaves further supported the formation of AgNPs, according to the TEM results in the study (Ansar *et al.*, 2020). Additionally demonstrates the development of comparatively uniformly distributed, spherical nanoparticles with an average diameter of 20 nm.

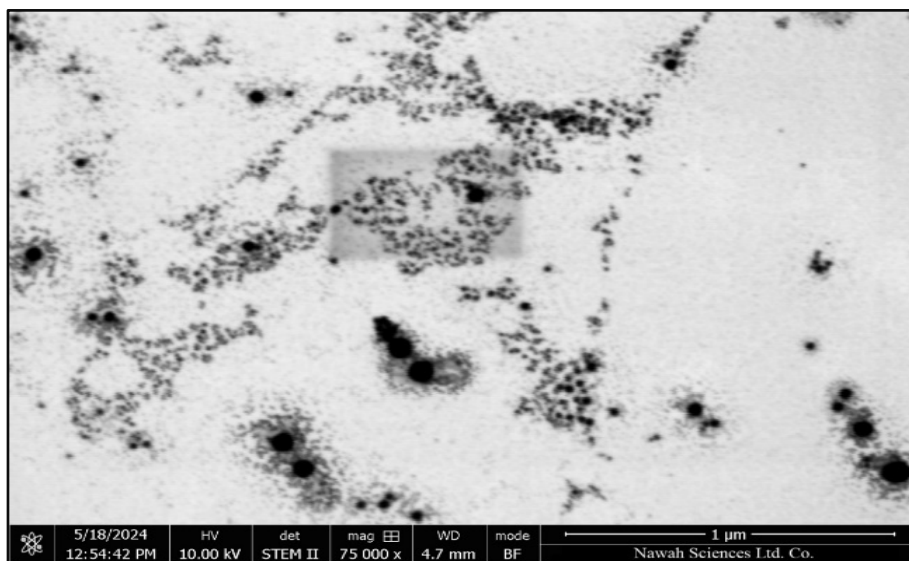


Fig (3.39) TEM image of AgNPs Produced by *P. aeruginosa*

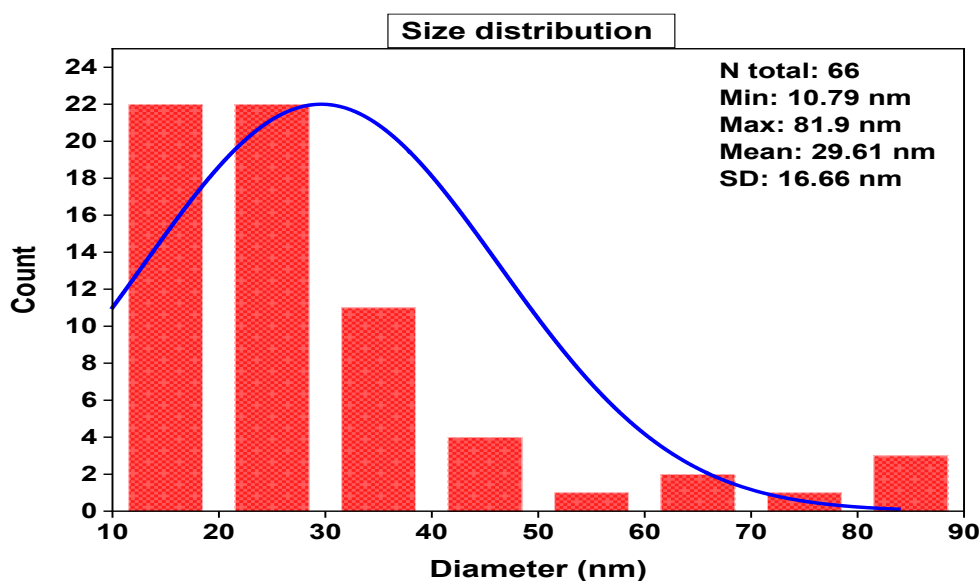


Fig (3.40) The histogram of the size distribution of AgNPs Produced by *P. aeruginosa*

The Ag_2O_3 NPs synthesized by *P. aeruginosa* shown in the Fig (3.41) were in the form of spaced particles and with very small sizes ranging between (9-30 nm) and an average of 17.23 nm Fig(3.42) similarly to (El-Sapagh *et al.*,2024) According to (Dharmaraj *et al.*, 2021), the TEM revealed that the NPs were spherical, somewhat consistent in size, and ranged in size from 25 to 70 nm. Although Ag_2O_3 NPs were produced similarly (Gungure *et al.*, 2024), TEM results verified the spherical

distribution of Ag₂O NPs, which were found to range in size from 20 nm to 80 nm with diameter 54.4 nm, which is also supported by the results of XRD and SEM.

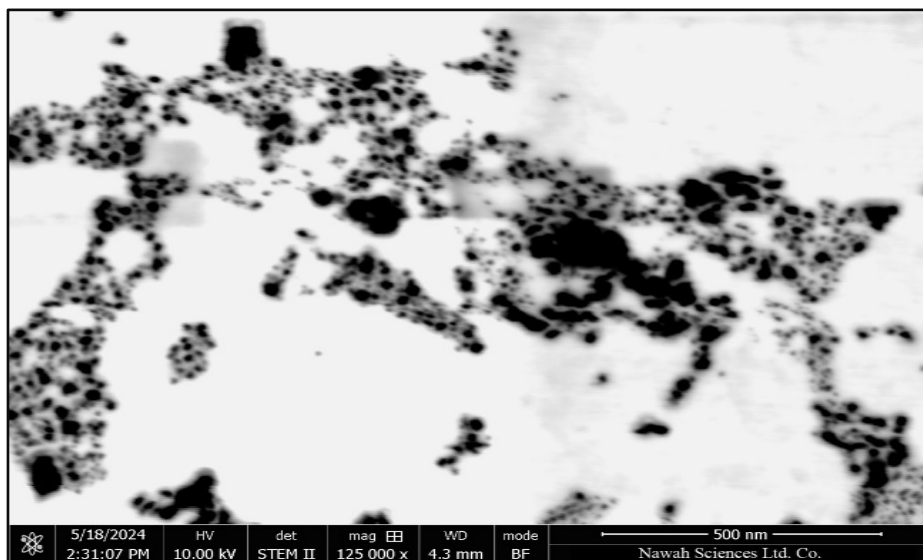


Fig (3.41) TEM image of Ag₂ONPs Produced by *P. aeruginosa*

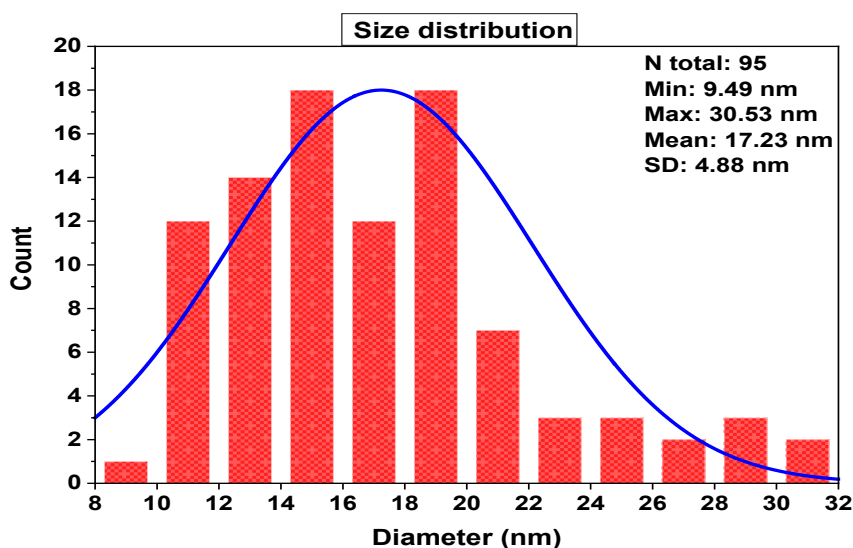


Fig (3.42) The histogram of the size distribution of Ag₂ONPs Produced by *P. aeruginosa*

While the SeNPs synthesized by *S. marcescens* were regular spherical particles without clumps of very small size (dimensions less than 100 nm) Fig (3.43) and the size of them ranging from 40-64nm and an average of 51nm Fig (3.44). A previous

study used a similar methodology to characterize the size and shape of biosynthesized SeNPs and indicated a regular spherical shape for particles with an average between 50 and 80nm (Gharieb *et al.*,2023). Also, the measurements we obtained through TEM measurement are in complete agreement with the crystal sizes of the mentioned nanoparticles measured through X-ray diffraction using the Debye-Scherrer equation (Alsohaimi *et al.*,2020). When comparing the production of SeNPs intracellularly and extracellularly in the study (Zhang *et al.*,2019) , the TEM results verified that both SeNPs were spherical and had a consistent size distribution. However, compared to internal SeNPs, external SeNPs were larger. It was determined that the average size of extracellular and intracellular SeNPs was 212.65 and 45.19 nm, respectively.

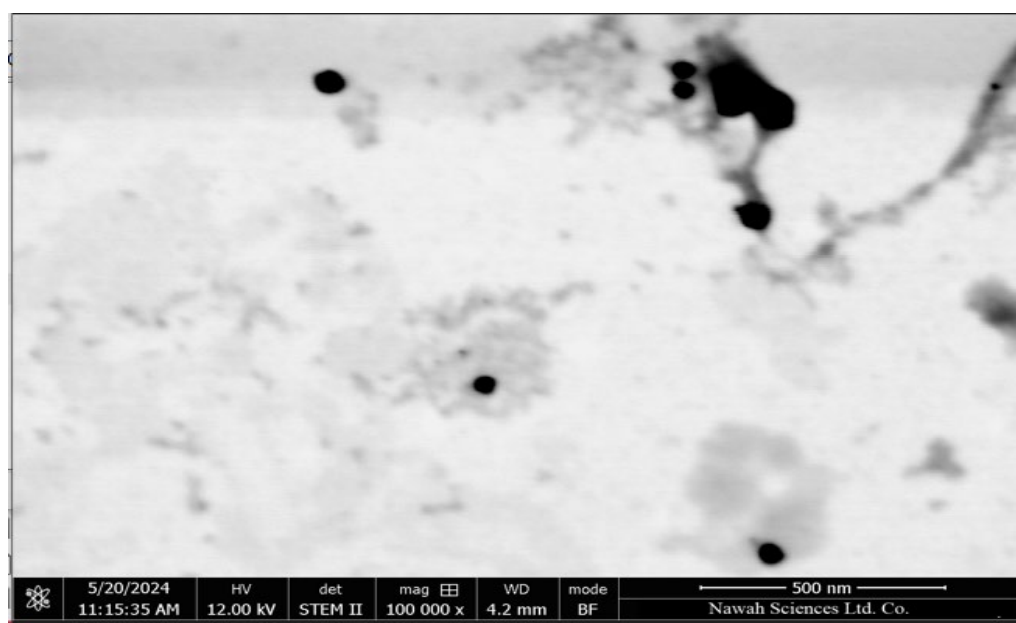


Fig (3.43) TEM image of SeNPs Produced by *S. marcescens*

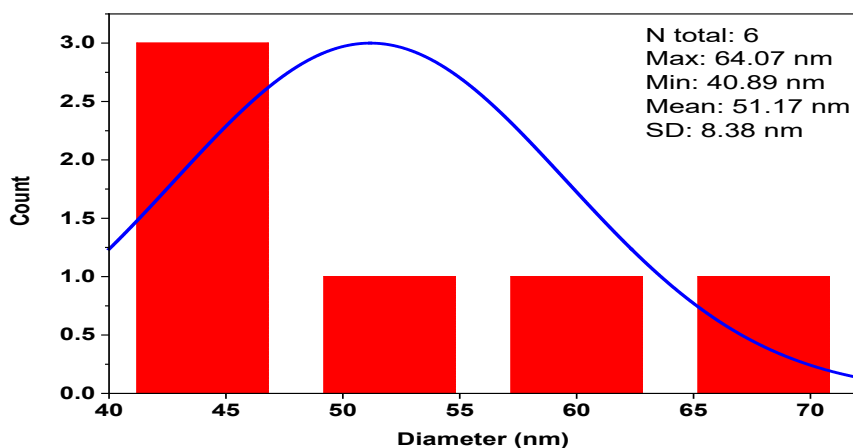


Fig (3.44) The histogram of the size distribution of SeNPs Produced by *S.marcescens*

3.4.1.8 Atomic force microscopy (AFM)

The surface of the NPs was studied in our study using the atomic force microscope (AFM), where Fig (3.45) shows two- and three-dimensional images of the surface of AuNPs synthesized from *A. baumannii* where they had a mean diameter of about (59nm) and less than 100 nm. The AFM images in Fig (3.46) revealed two- and three-dimensional images of the surface of the AgNPs synthesized from *P. aeruginosa* where they had a mean diameter of about (51nm). As in Fig (3.47) two- and three-dimensional images of AFM for Ag₂O₃NPs synthesized from *P. aeruginosa* as the images show a uniform distribution where they had a mean diameter of about (75nm). While the atomic force microscope images of the SeNPs synthesized from *S. marcescens* are shown in Fig (3.48) where two- and three-dimensional images of the surface showed a homogeneous distribution with the presence of multiple clusters and they had a mean diameter of about (121nm). Additionally, the spherical shape and uniform distribution of the bio-synthesized NPs produced by TEM and Fe-SEM micrographs were demonstrated by 2D and 3D AFM images. The surface of the NPs is considered rough based on AFM images because it contains peaks of different dimensions. The

presence of surface roughness of the bio-synthetic NPs in the study leads to an increase in the effectiveness of killing bacteria and cancer cells, as surface roughness increases the mechanical stress on bacteria and cancer cells, which leads to damage to the cell walls and thus their death (Rutherford *et al.*,2015). This type of quantitative analysis is useful for studying and understanding surfaces and their applications such as nanotechnology, electronics, energy, etc (Salman & abd,2021)

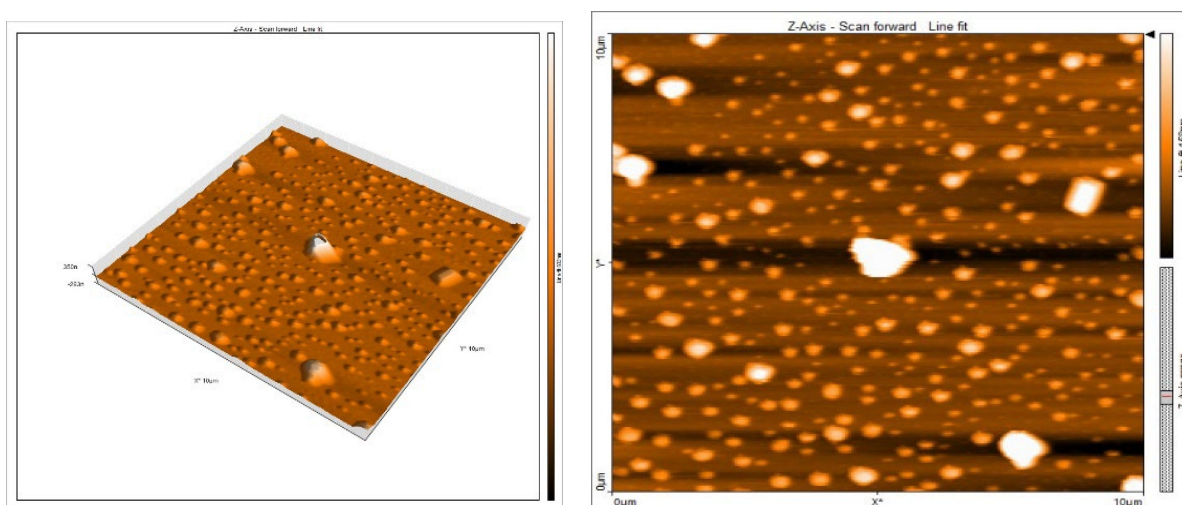


Fig (3.45) AFM image (three-dimensional) of AuNPs produced by *A. baumannii*

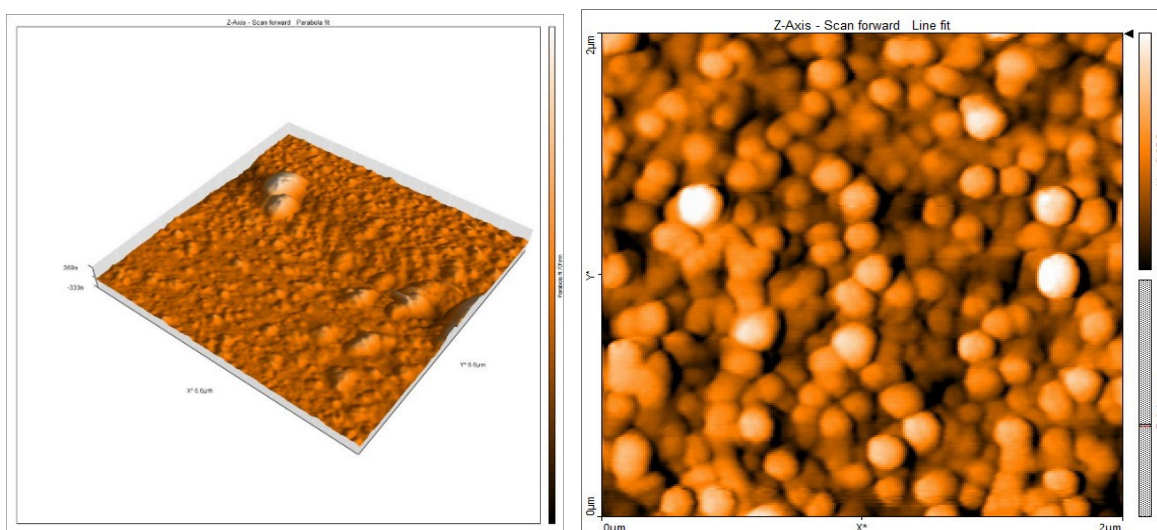


Fig (3.46) AFM image (three-dimensional) of AgNPs produced by *P. aeruginosa*

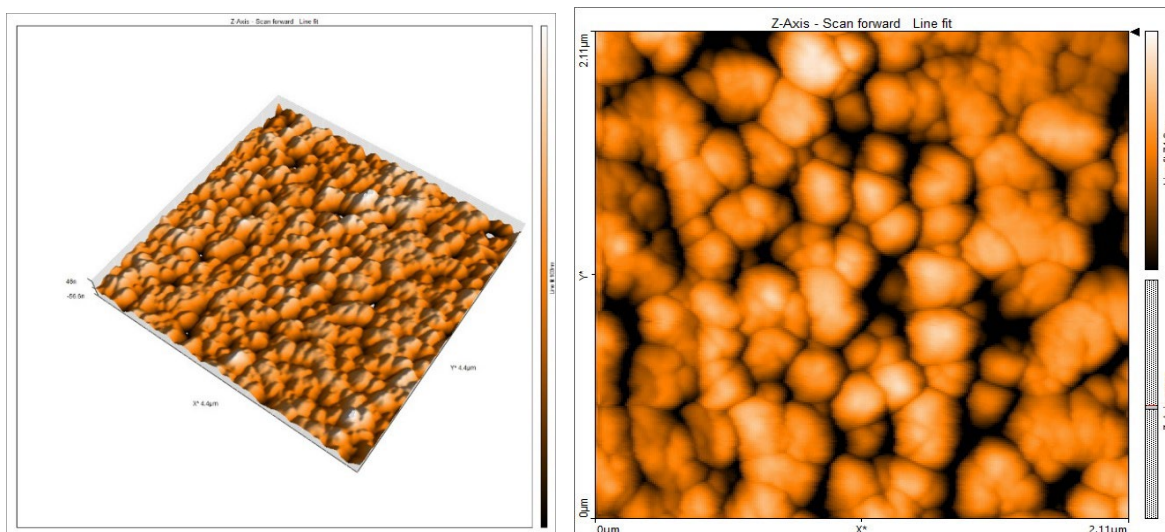


Fig (3.47) AFM image (three-dimensional) of Ag₂ONPs produced by *P. aeruginosa*

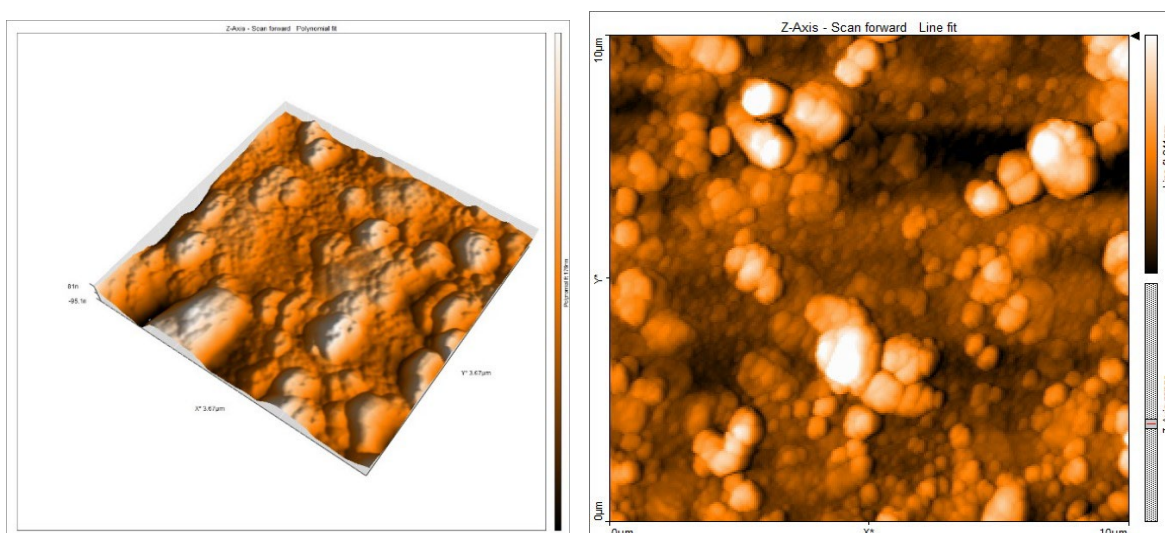


Fig (3.48) AFM image (three-dimensional) of SeNPs produced by *S. marcescens*

3.4.2 Biological Characterization of NPs

3.4.2.1 Antibacterial Activity

The results shown in the table below (3.12) showed good inhibitory activity of the NPs against the two bacterial isolates. Where biosynthesized (Au, Ag, Ag₂O₃, Se NPs) from (*A.baumannii*, *P. aeruginosa*, *P. aeruginosa*, *S. marcescens*) showed growth inhibition zones with diameters of (20, 19, 23, and 16 mm) respectively on *E.coli* Fig (3.50), Fig(3.51) while the growth inhibition zones were (24, 23, 22, 24

mm) respectively on *S. aureus* Fig (3.52), Fig (3.53) while the growth inhibition zone diameter of the antibiotic gentamycin was 20 mm on both positive and negative isolates Fig (3.54). The current study revealed that there was some statistically significant (P value less than 0.05) between NPs and type agent *E.coli*, *S. aureus* Table 3.13 Fig (3.49).

Table (3.12) Inhibition zone diameter of NPs and Gentamysin on *S. aureus*, *E. coli*

NPS	<i>S. aureus</i>	<i>E. coli</i>	F test - P value	LSD
Au	24 mm	20 mm	5.347 0.02	2.51
Ag	23 mm	19 mm		
Ag ₂ O ₃	22 mm	23 mm		
Se	24 mm	16 mm		
Gentamysin	20 mm	20 mm		

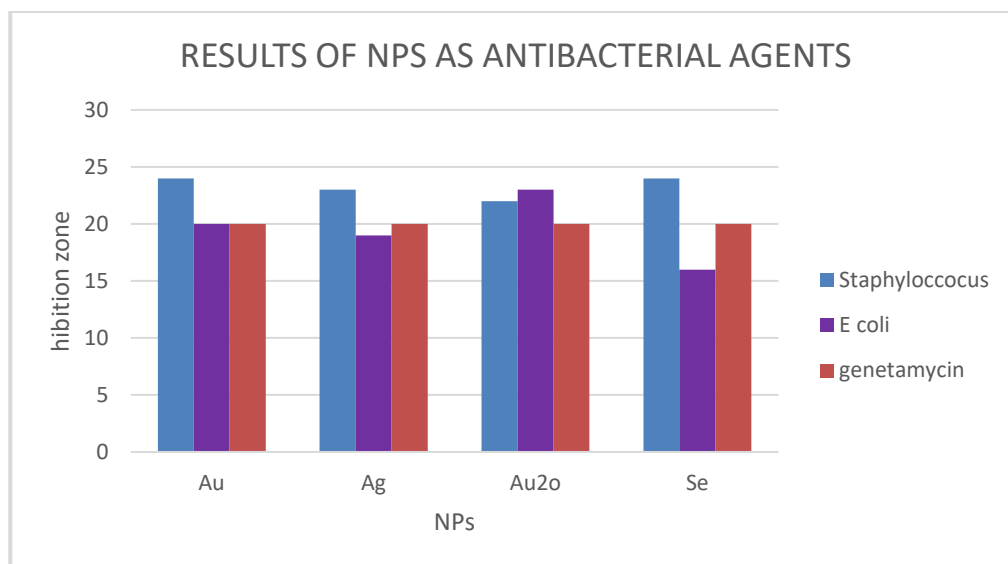


Fig (3.49) Result of NPs as Antibacterial agents

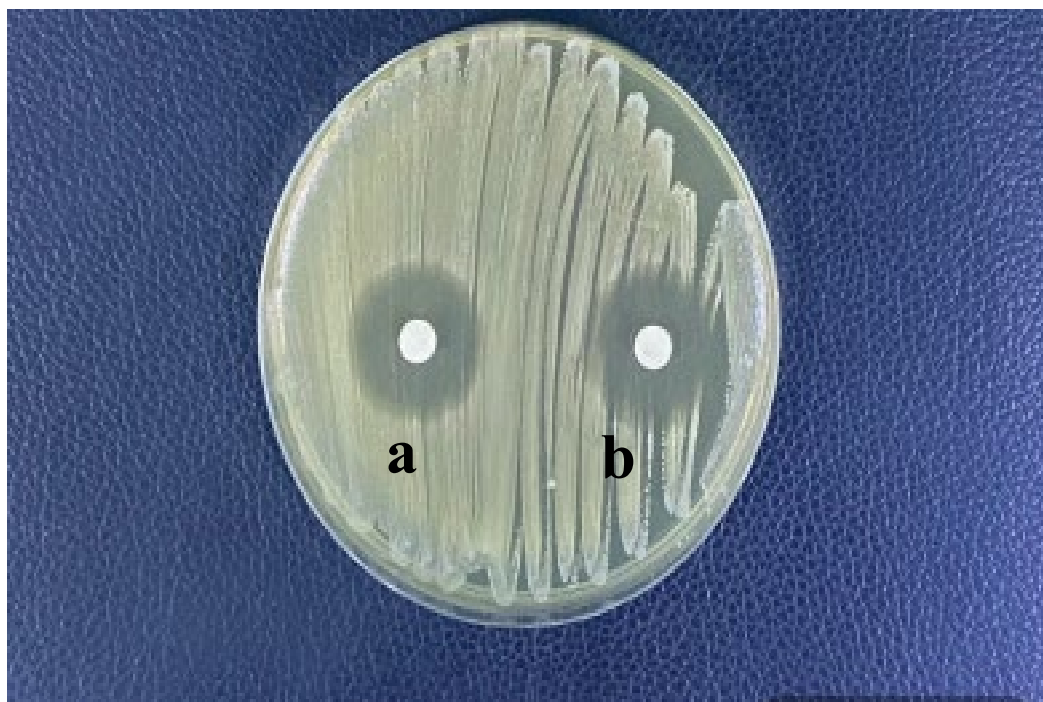


Fig (3.50) Inhibition zone of NPs on *E.coli* a) AuNPs b) AgNPs

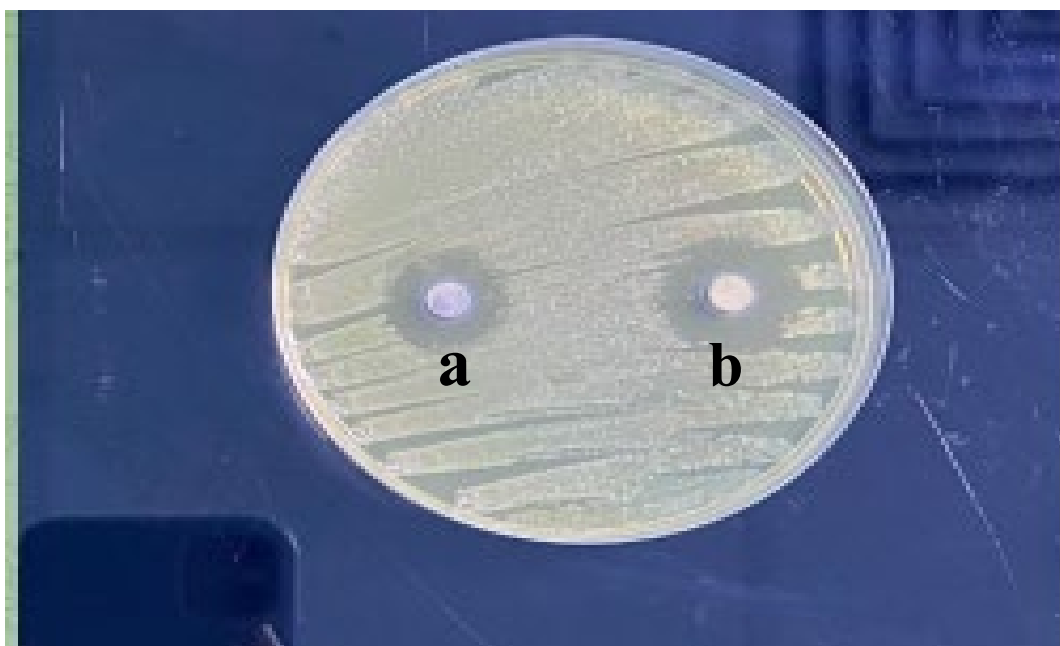


Fig (3.51) Inhibition zone of NPs on *E.coli* a) Ag₂O₃NPs b) SeNPs

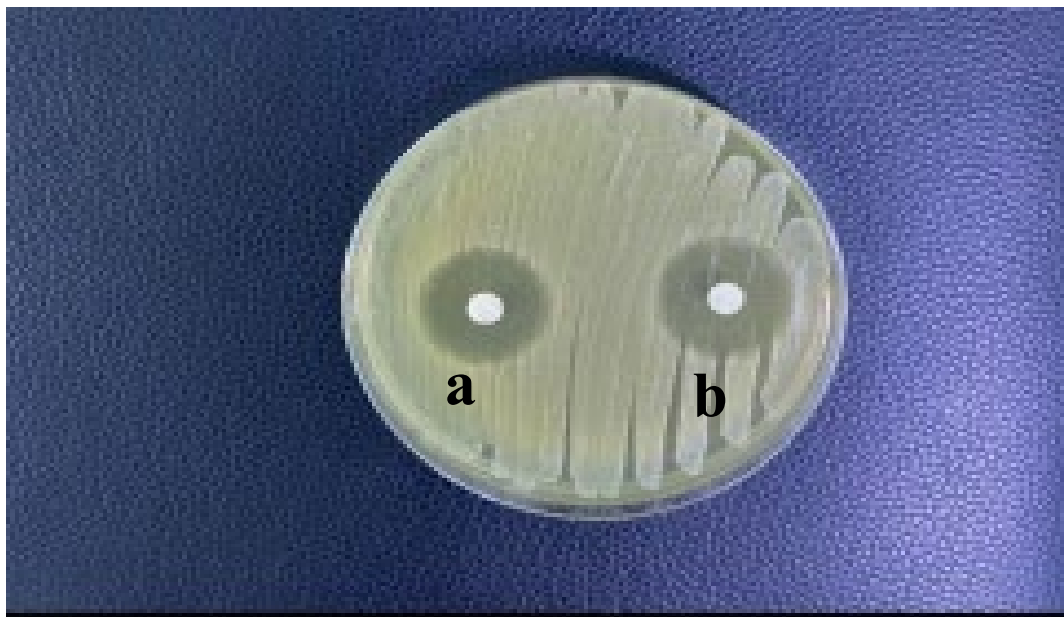


Fig (3.52) Inhibition zone of NPs on *S. aureus* a) AuNPs b) AgNPs

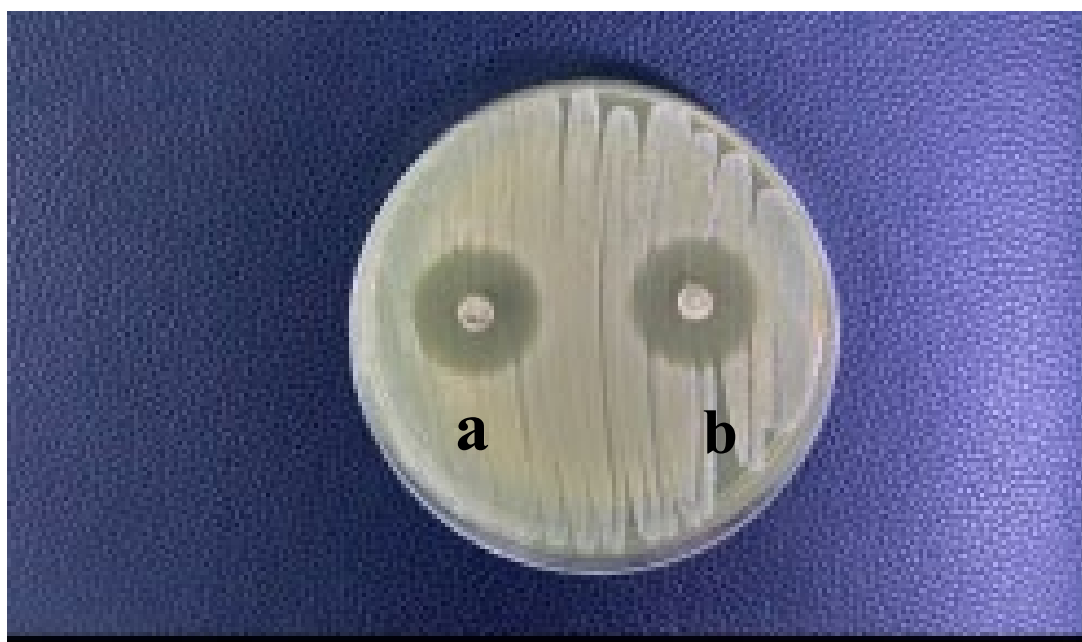


Fig (3.53) Inhibition zone of NPs on *S. aureus* a) Ag₂O₃NPs b) SeNPs

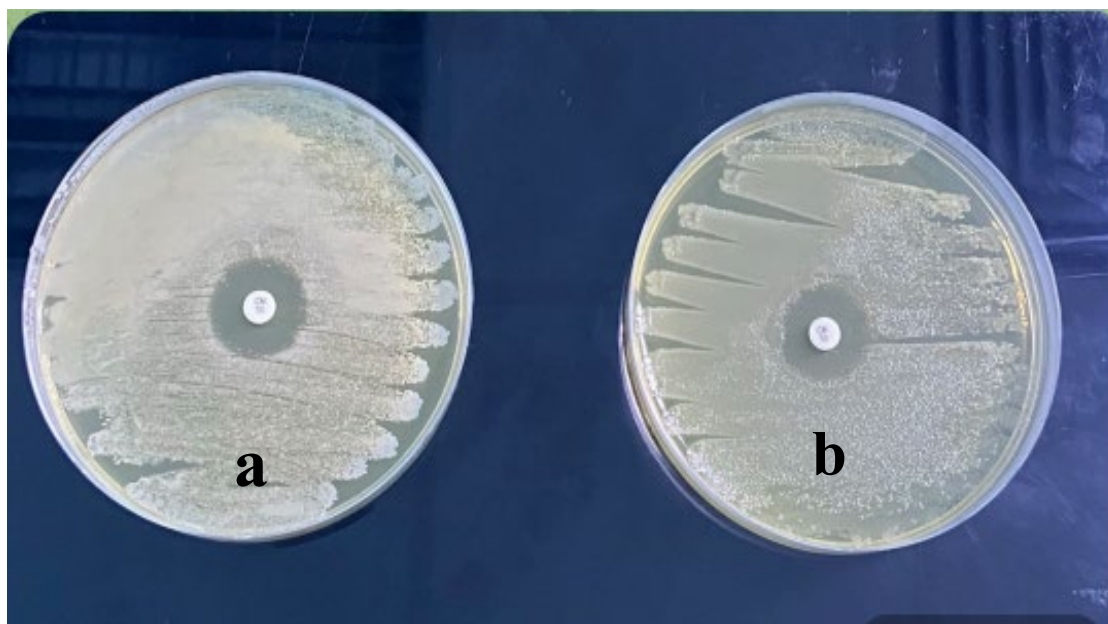


Fig (3.54) Inhibition zone of Gentamycin on a) *S. aureus* b) *E.coli*.

The results indicate that the biosynthesized NPs were more effective (more sensitive) on *S. aureus* bacteria compared to *E. coli* bacteria and this antibiotic is because the nanoparticles can adhere to the bacterial cell wall of *S. aureus* and then penetrate its wall, which leads to cell death (Mohanlall&Biyela,2022). The size of NPs has a significant impact on their antibacterial action; smaller particles have demonstrated stronger antibacterial activity because of their increased capacity to penetrate bacteria (Yousaf *et al.*,2020). According to the reports of (Abdel-Kareem & Zohri, 2018), (El-Bendary *et al.*,2020) and (Ghaderi *et al.*,2021) metal NPs can exhibit high anti-bacterial properties against pathogenic bacteria. High concentrations of reactive oxygen species (ROS), including hydroxyl radicals, hydrogen peroxide, hypochlorous acid, and superoxide anion, are produced as part of another antibacterial mechanism. The overproduction of these ROS in the cell inhibits both respiration and cell growth (Mohanlall&Biyela,2022)

3.4.2.2 Anticancer Activity

According to the results of the study, Table (3.13) shows that the cytotoxicity obtained in the laboratory for the biosynthesized AuNPs from the filtrate of

A.baumannii increases with an increasing concentration towards cancer cells when exposed to different concentrations of AuNPs, as the inhibition ratio started at concentrations (10, 20, 40, 80, 160 µg/ml) towards HT-29 cells and was (7.10, 16.24, 39.78, 61.93, 92.60) respectively, while the inhibition ratios were (1.01, 4.11, 29.21, 36.22, 69.84) respectively towards HepG2 cells at the same concentrations. On the other hand, AuNPs did not show cytotoxicity towards normal cells, as the inhibition ratio was very low (2.21, 2.31, 2.91, 4.30, 8.41) at the same concentrations. Moreover, the most obvious effect after treating cells with biosynthetic AuNPs is the change in cell shape or cell morphology, which is consistent with (El Domany *et al.*, 2018), since the findings demonstrated that, in comparison to conventional AuNPs, biosynthetic AuNPs exhibit greater anticancer activity against HepG2 and HCT-116 cells. The aforementioned findings showed that various AuNP concentrations are more harmful to colon cancer cells than to liver cancer cells and normal cells. This is because AuNPs' anticancer effects are heavily influenced by a variety of physical characteristics, including size, shape, and surface coverage. Regarding size, it has been claimed that tiny AuNPs can destroy tumour cells. (Chang *et al.*, 2021). In a previous study (Hassan *et al.*, 2024), AuNPs showed inhibitory activity against liver and breast cancer cells. Human gliomas, colon cancer, lung epithelial cancer, Lewis lung carcinoma, breast cancer, uterine cancer, and human lung cancer are among the cancers that have been treated using AuNPs due to their potential (Chang *et al.*, 2021). The results showed that the cytotoxicity of AuNPs towards HT-29 cells Fig (3.55) was higher compared to HepG2 cells Fig (3.56) and MEF cells Fig (3.57), where the IC₅₀ value for (HT-29, HepG2, MEF) cells was (111, 73, 1100) respectively Fig (3.58). The statistical analysis's findings verified that there were notable variations in the concentrations.

Table (3.13) the results of the statistical analysis of AuNPs concentrations on HT-29, HepG2 and MEF cell line

Con.µg/ml	HT-29 cell line	HepG2 cell line	MEF cell line
10	7.10 ± 1 e	1.01 ± 1 c	2.21 ± 1 b
20	16.24 ± 1.1 d	4.11 ± 1 c	2.31 ± 1 b
40	39.78 ± 1.2 c	29.21 ± 1 b	2.91 ± 1 b
80	61.93 ± 1.3 b	36.22 ± 1.1 b	4.30 ± 1.2 a
160	92.60 ± 1.3 a	69.84 ± 1.1 a	8.41 ± 1.2 a

The different letters in the same column indicate that there are statistical differences at the level of $(0.05 \geq P)$. Mean ± SD. n=3

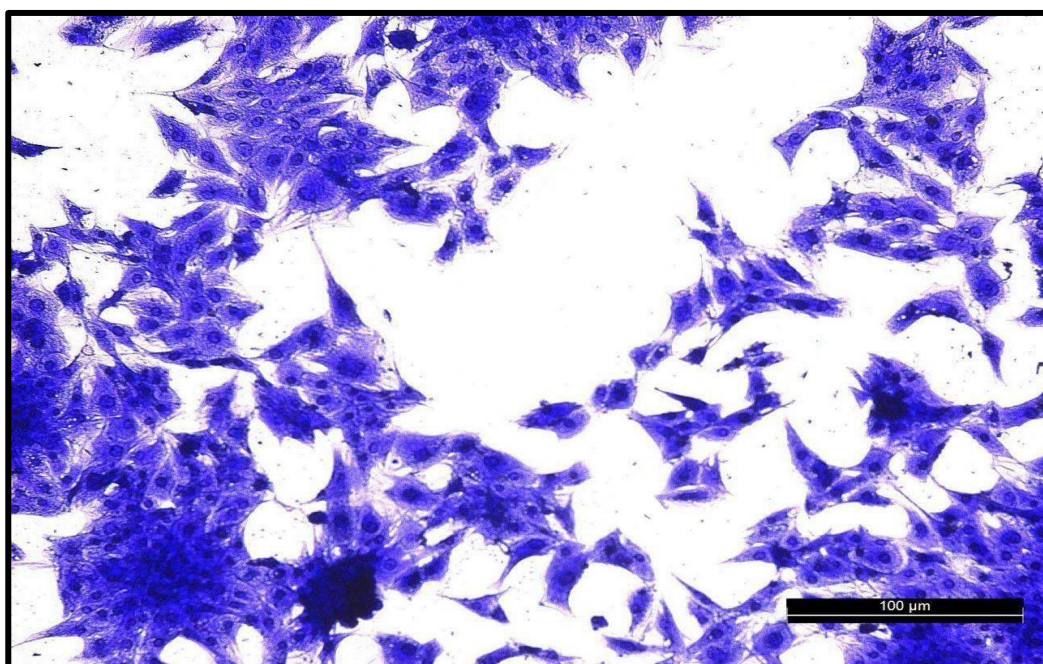


Fig (3.55) HT -29 cell line treated with a concentration of 160 µg/ml of AuNPs produced by *A.baumannii* with crystal violet dye

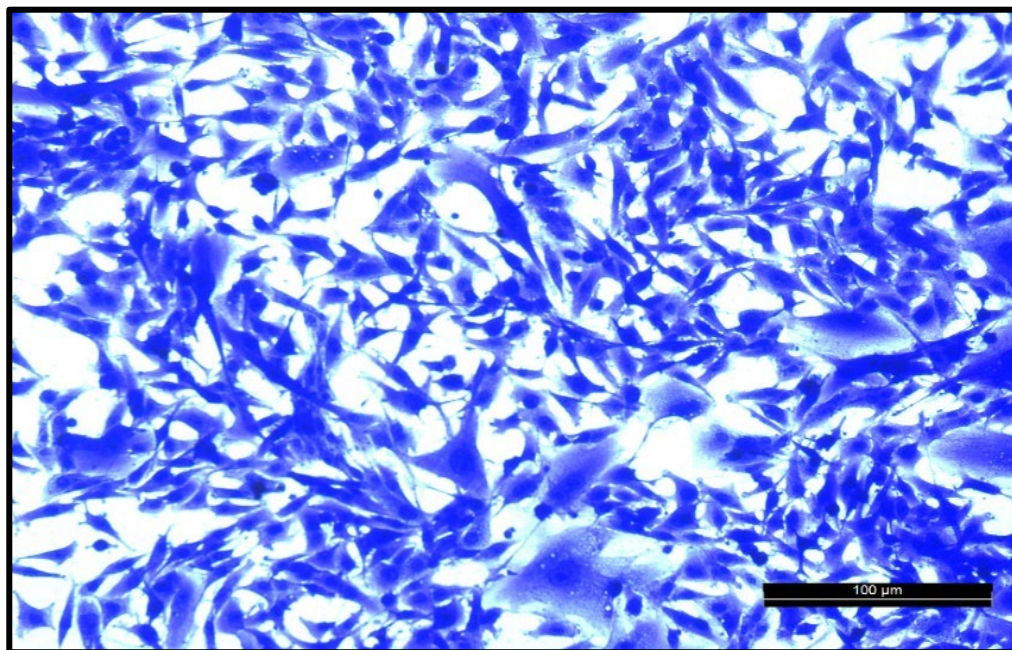


Fig (3.56) HepG2 cell line treated with a concentration of 160 μg/ml of AuNPs produced by *A.baumannii* with crystal violet dye

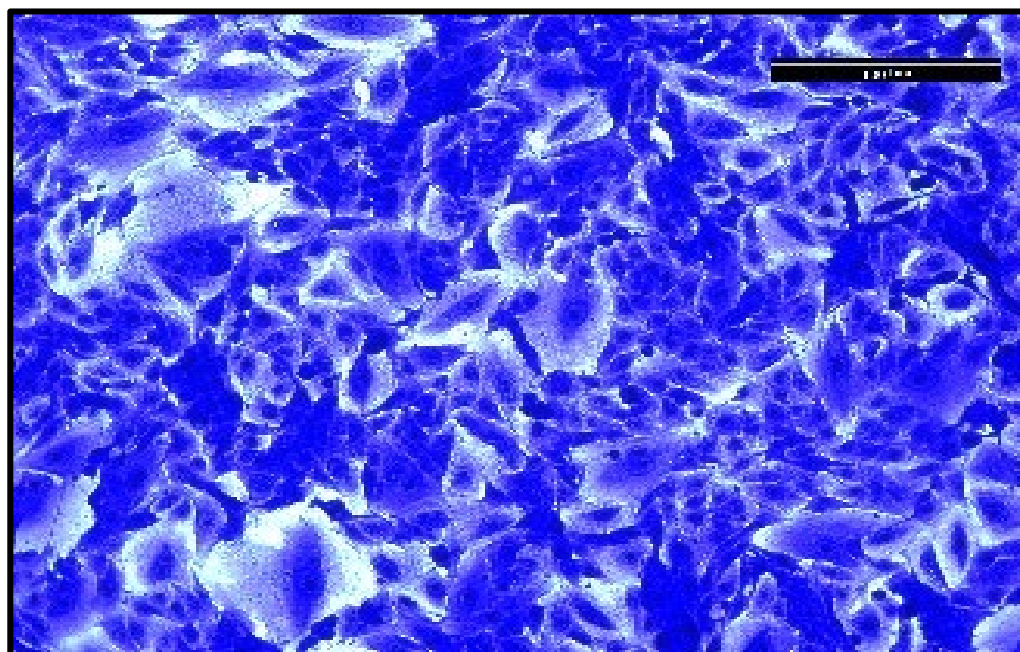


Fig (3.57) MEF cell line treated with a concentration of 160 μg/ml of AuNPs produced by *A.baumannii* with crystal violet dye

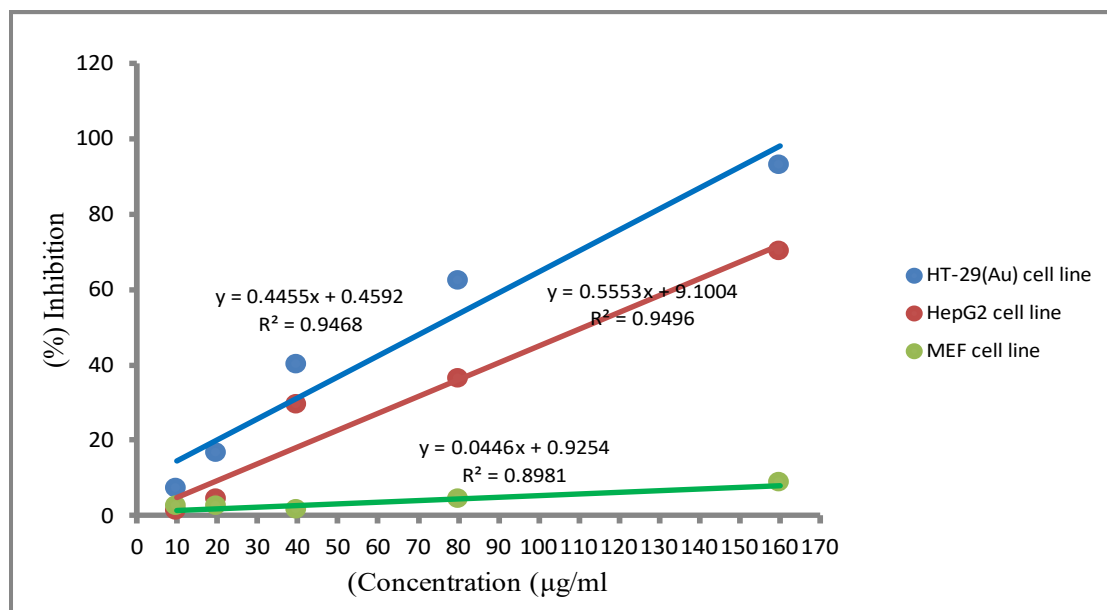


Fig (3.58) Curves IC_{50} of AuNPs for HT-29 , HepG2 and MEF cells

AgNPs can play a major role in tumour inhibition through their toxic effects on targeted cancer cells. The results shown in Table (3.14) indicate that the cytotoxicity of biosynthesized AgNPs from *P. aeruginosa* filtrate increased consistently with increasing concentration. The inhibition ratio at concentrations (10, 20, 40, 80, 160) towards HT-29 cells was (20.45, 22.46, 49.90, 65.12, and 89.87) respectively, while the inhibition ratio towards HepG2 cells was (3.73, 18.88, 25.67, 42.10, 73.38) respectively at the same concentrations. Compared to MEF when exposed to the same concentrations of the nanomaterial, the cytotoxicity ratio was very weak, as the inhibition ratio reached 14.84% at the highest concentration of 160. showed that the concentration of bio-synthesized AgNPs affects cell viability, indicating the cancer cell line's antagonistic action (Ansar *et al.*,2020)

In a previous study bio-synthesized AgNPs by *Microbacterium* were used as anticancer agents and the results revealed inhibitory activity against breast cancer cells (Dewan & Hateet,2022). As reported (BalaKumaran *et al.*,2022) when

comparing AgNPs and AuNPs in terms of the cellular effect towards cancer cells, the results confirmed that AgNPs have a high effectiveness towards breast cancer cells, much better than AuNPs towards liver cancer cells. In a similar study, the toxicity of biosynthetic AgNPs increased with increasing concentration, but no toxic effect was shown towards breast cancer cells at low concentrations (Sonker *et al.*,2017). The inclusion of substances like sulforaphane and indole-3-carbinal, which encourage DNA repair and seem to stop the proliferation of cancer cells, may be the cause of AgNPs' anti-cancer properties as shown by cytotoxic assay (Ansar *et al.*,2020) . The results show that HT-29 cells Fig (3.59) were more affected during their test at different concentrations of AgNPs compared to HepG2 cells Fig (3.60) and MEF cells fig (3.61) where the IC₅₀ value for (HT-29, HepG2, MEF) cells was (102,62,489) respectively Fig (3.62). The statistical analysis's findings verified that there were notable variations in the concentrations.

Table (3.14) the results of the statistical analysis of AgNPs concentrations on HT-29, HepG2 and MEF cell line

Con.µg/ml	HT-29 cell line	HepG2 cell line	MEF cell line
10	20.45 ± 1 d	3.37 ± 1.1 e	0 ± 0 c
20	22.46 ± 1 d	18.88 ± 1.1 d	0 ± 0 c
40	49.90 ± 1.1 c	25.67 ± 1.1 c	4.22 ± 1.1 b
80	65.12 ± 1.2 b	42.10 ± 1.2 b	9.87 ± 1.2 a
160	89.87 ± 1.3 a	73.38 ± 1.2 a	14.84 ± 1.3 a

The different letters in the same column indicate that there are statistical differences at the level of (0.05≥P). Mean ± SD. n=3

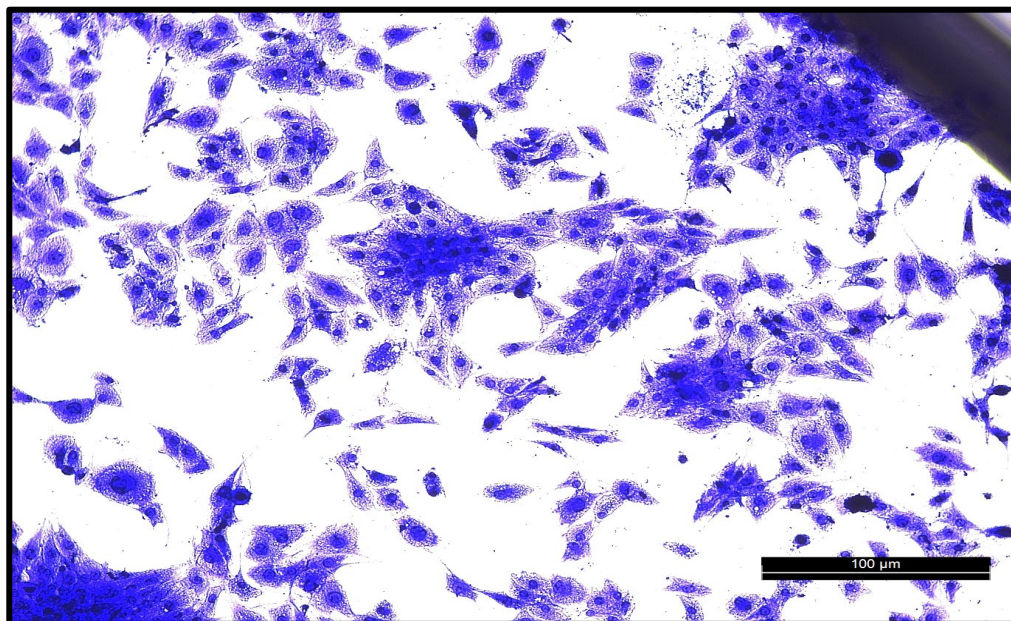


Fig (3.59) HT -29 cell line treated with a concentration of 160 μg/ml of AgNPs produced by *P. aeruginosa* with crystal violet dye

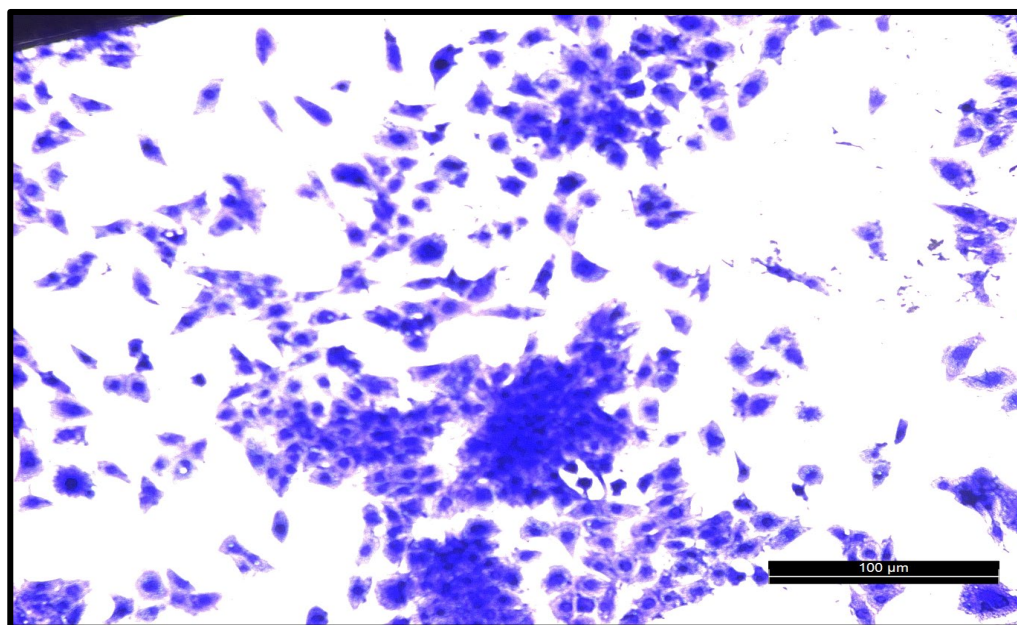


Fig (3.60) HepG2 cell line treated with a concentration of 160 μg/ml of AgNPs produced by *P. aeruginosa* with crystal violet dye

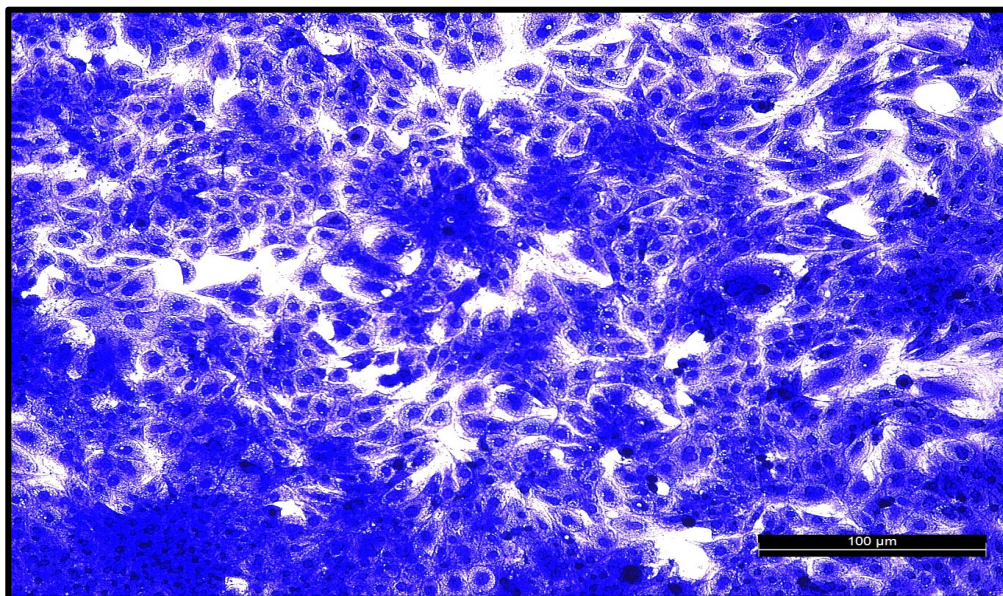


Fig (3.61) MEF cell line treated with a concentration of 160 $\mu\text{g/ml}$ of AgNPs produced by *P. aeruginosa* with crystal violet dye

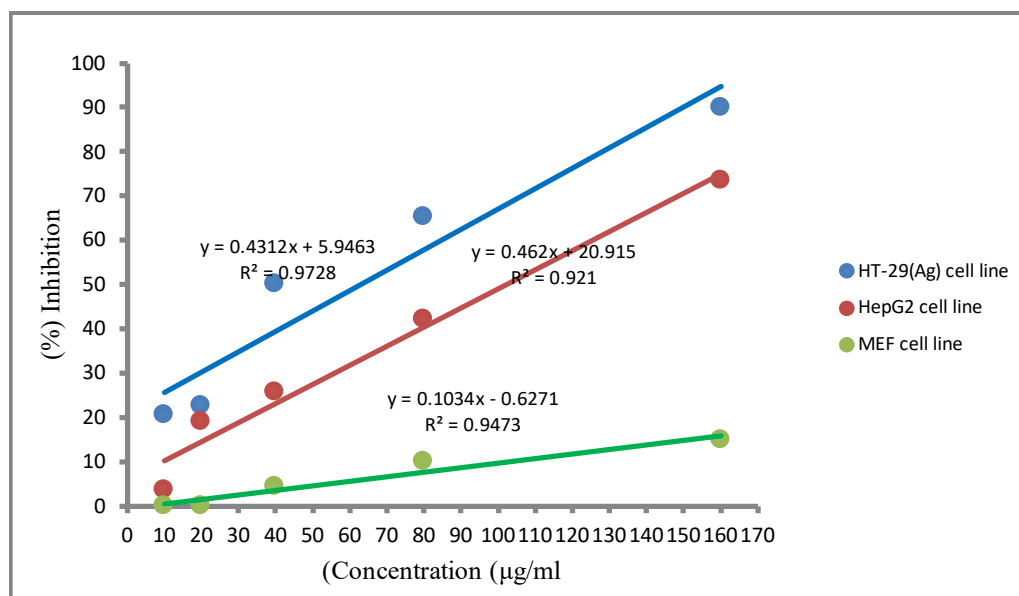


Fig (3.62) Curves IC_{50} of AgNPs for HT-29 , HepG2 and MEF cells

From the anticancer activity report, Table (3.15) shows that bio-synthesized $\text{Ag}_2\text{O}_3\text{NPs}$ from *P. aeruginosa* filtrate have inhibitory activity against HT-29 cells and HepG2 cells without affecting normal cells MEF, as the inhibition ratio of the particles at concentrations (10, 20, 40, 80, 160) towards HT-29 cells was (5.34,

9.98, 19.22, 41.60, 86.11) respectively, while towards HepG2 cells it was (2.01, 8.31, 15.97, 32.16, 63.84) respectively at the same concentrations, while MEF was not affected when exposed to the same concentrations, as the inhibition ratio reached 19.64% at the highest concentration of 160. According to the study (Sujatha et al., 2023) (184), increased DNA damage in HCC liver cancer cells frequently results in a drop in MMP, which ultimately causes cell death. Since mitochondria are engaged in the development of cytotoxicity, MMP is a fundamental analysis of mitochondrial function that can be utilized as a sign of normal cells. Important events in mitochondria occur in cases of cytotoxicity. As reported by (Pradheesh *et al.*, 2020) biosynthesized silver oxide nanoparticles showed good anticancer behaviour at different concentrations. The current findings are consistent with earlier research that found that exposure to nanoparticles caused cell death through apoptosis and that DNA damage, which in turn causes apoptosis or necrosis, is connected to oxidative stress and excessive reactive oxygen species generation (Sufyani *et al.*, 2019). In a related comprehensive investigation, MCF-7 and PVA1 cancer cell lines demonstrated low to moderate cytotoxicity and inhibitory effects from AgONPs, while the Caco-2 cancer cell line showed no inhibitory impact at all (Khatoon *et al.*, 2024) The results indicate that silver oxide nanoparticles have higher cytotoxicity towards HT-29 cells Fig (3.63) compared HepG2 cells Fig (3.64) and normal cells Fig (3.65) where the IC_{50} value of the particles for (HT-29, HepG2, MEF) cells was (125, 94, 671) respectively Fig (3.66). The statistical analysis's findings verified that there were notable variations in the concentrations

Table (3.15) results of statistical analysis of Ag₂O₃NPs concentrations on HT-29, HepG2 and MEF cell line

Con.µg/ml	HT-29 cell line	HepG2 cell line	MEF cell line
10	5.34 ± 1 d	2.01± 1.1 d	0 ± 0 c
20	9.98 ± 1 d	8.31 ± 1.1 d	0 ± 0 c
40	19.22 ± 1.1 c	15.97 ± 1.1 c	2.91 ± 1 b
80	41.60 ± 1.1 b	32.16 ± 1.2 b	6.85 ± 1.1 a
160	86.11 ± 1.2 a	63.84 ± 1.2 a	19.64 ± 1.2 a

The different letters in the same column indicate that there are statistical differences at the level of (0.05≥P).

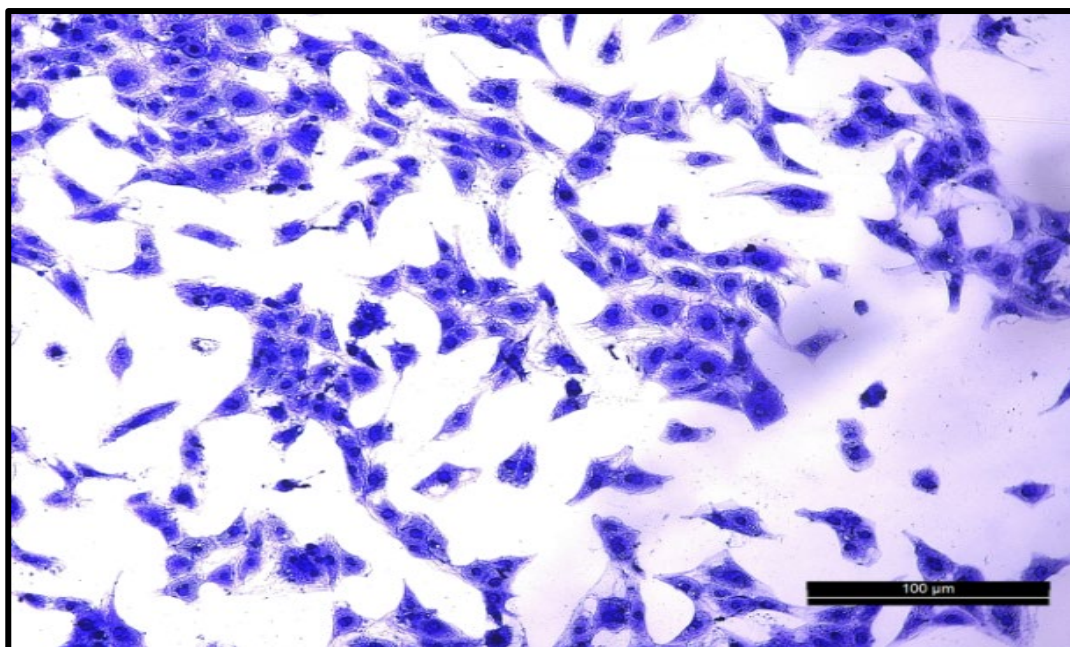


Fig (3.63) HT-29 cell line treated with a concentration of 160 µg/ml of Ag₂ONPs produced by *P. aeruginosa* with crystal violet dye

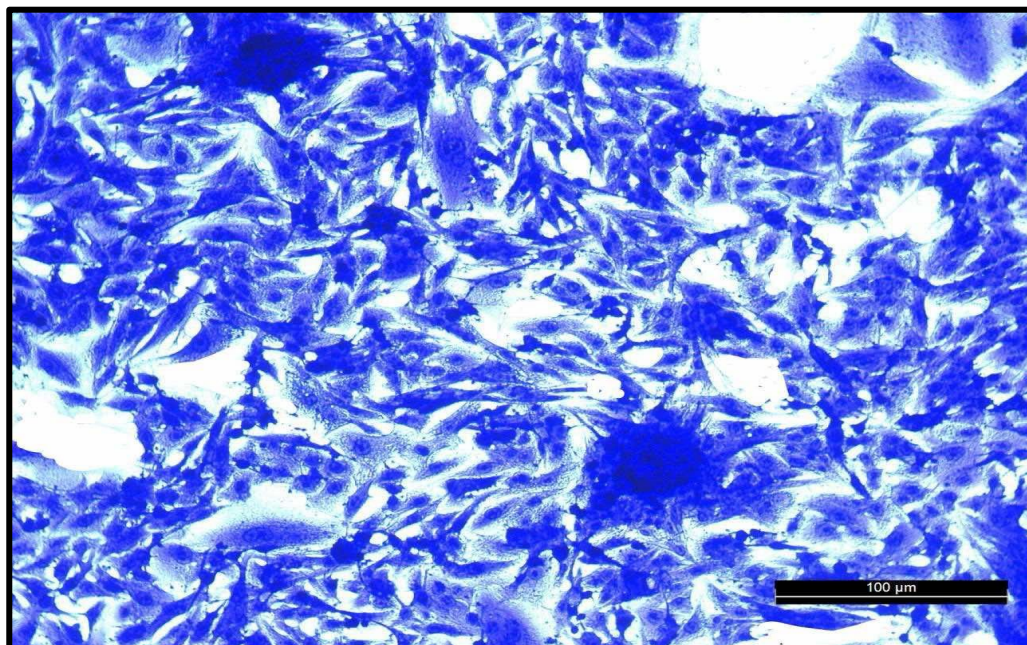


Fig (3.64) HepG2 cell line treated with a concentration of 160 μg/ml of Ag₂ONPs produced by *P. aeruginosa* with crystal violet dye

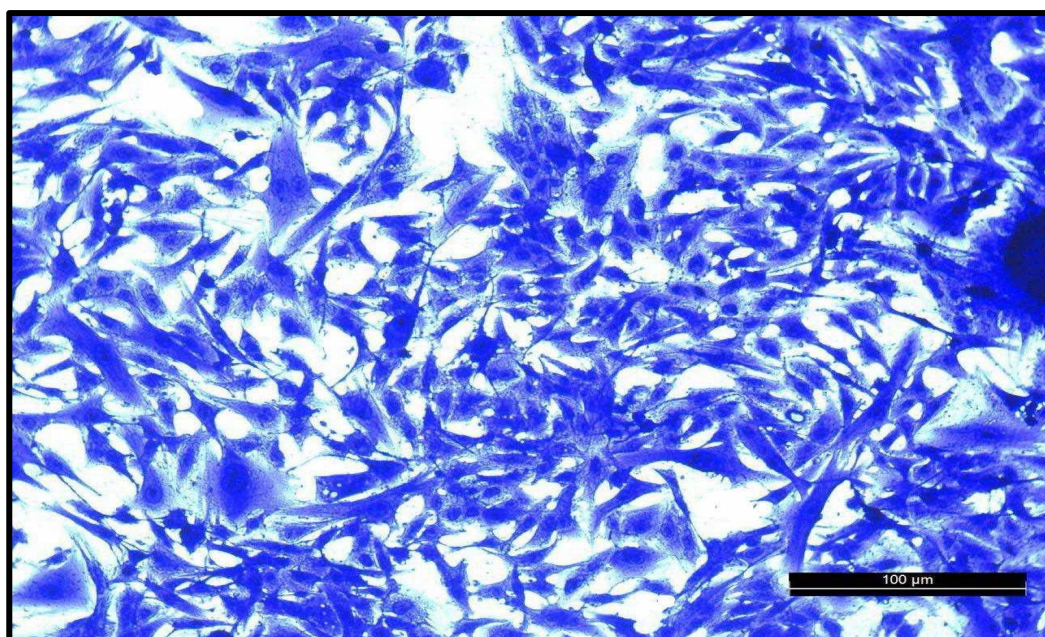


Fig (3.65) MEF cell line treated with a concentration of 160 μg/ml of Ag₂ONPs produced by *P. aeruginosa* with crystal violet dye

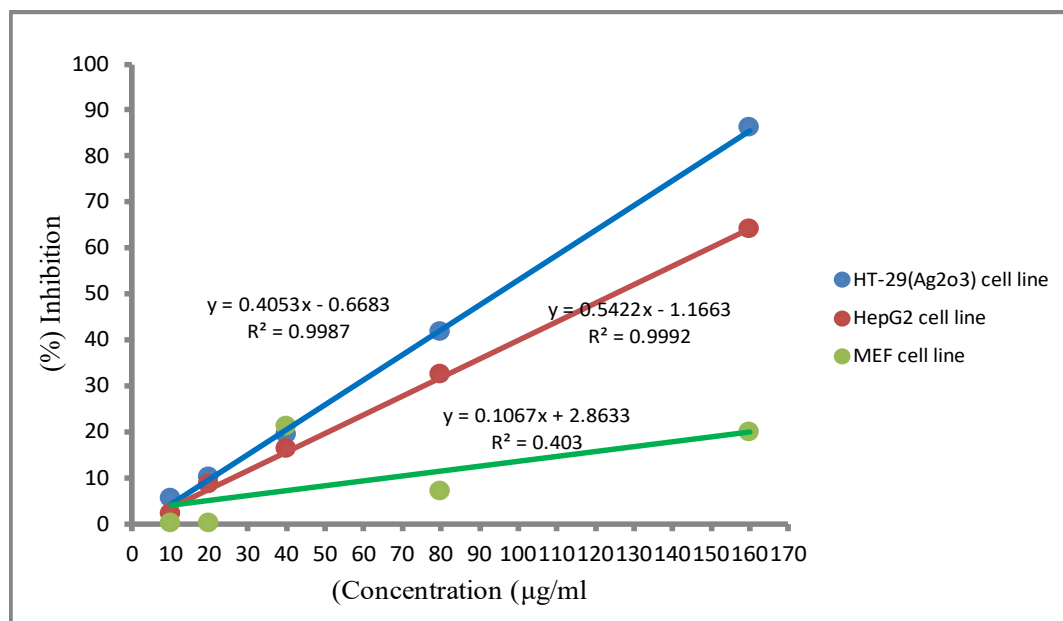


Fig (3.66) Curves IC₅₀ of Ag₂ONPs for HT-29 , HepG2 and MEF cells

To confirm the anti-cancer potential of SeNPs, toxicity testing experiments were conducted on HT-29 and HepG2 cells compared to normal cells MEF, where the biosynthesized SeNPs from *S. marcescens* filtrate showed inhibitory capacity towards cancer cells in a concentration-dependent manner. Table (3.16) where the inhibition rate of the particles at concentrations (10, 20, 40, 80, 160) towards cells HT-29 was (10.19, 21.23, 41.48, 69.19, 78.16) respectively, while towards cells HepG2 was (15.51, 38.33, 50.02, 62.16, 89.12) respectively at the same concentrations. As for the cytotoxicity towards MEF, it was very low compared to cancer cells, as the inhibition rate reached 10.64% at the highest concentration of 160. Therefore, SeNPs are low toxicity to normal cells and selective anti-cancer drugs. By targeting cancer cells and avoiding normal cells, SeNPs may lessen the harm caused by chemotherapy (Abbas & Abou, 2020). In a study by (Liao *et al.*, 2020), the anticancer impact of SeNPs on prostate cancer cell lines (LNCaP) was demonstrated by testing different concentrations of SeNPs (25, 50, and 100 µg/ml). The results showed that when 50 µg/ml of SeNPs were given, the low expression of cyclin D1 and the high expression of p21 protein caused cell cycle

arrest. However (Cui *et al.*, 2018) synthesized SeNPs and evaluated their cytotoxic effect on HepG2 cells. SeNP treatment resulted in increased ROS expression, decreased MMP, elevated caspase-9, and decreased Bcl-2, suggesting the mechanism of cell death. However, (Ranjitha *et al.* 2019) described a technique for creating SeNPs with a suspension of *Streptomyces griseoruber*, and the HT-29 cell line was then used to assess their anticancer potential. Comparing the conjugated SeNPs to the unconjugated SeNPs, the results demonstrated an enhanced anticancer impact. The HT-29 cell line exhibited increased apoptosis in response to conjugated SeNPs. The results show that the toxicity of SeNPs towards HT-29 cells Fig (3.67) was higher compared to HepG2 cells Fig (3.68) and normal cells Fig (3.69), where the IC₅₀ value for (HT-29, HepG2, MEF) cells was (75, 59, 683) respectively Fig (3.70). The statistical analysis's findings verified that there were notable variations in the concentrations.

Table (3.16) the results of the statistical analysis of SeNPs concentrations on HT-29, HepG2 and MEF cell line

Con.µg/ml	HT-29 cell line	HepG2 cell line	MEF cell line
10	10.19 ± 1	15.51 ± 1 e	0 ± 0 c
20	21.23 ± 1 d	38.33 ± 1 d	0 ± 0 c
40	41.48 ± 1 c	50.02 ± 1.1 c	3.11 ± 1.1 b
80	69.19 ± 1.1 b	62.16 ± 1.1 b	6.90 ± 1.2 a
160	78.16 ± 1.2 a	89.12 ± 1.3 a	10.64 ± 1.3 a

The different letters in the same column indicate that there are statistical differences at the level of (0.05≥P).

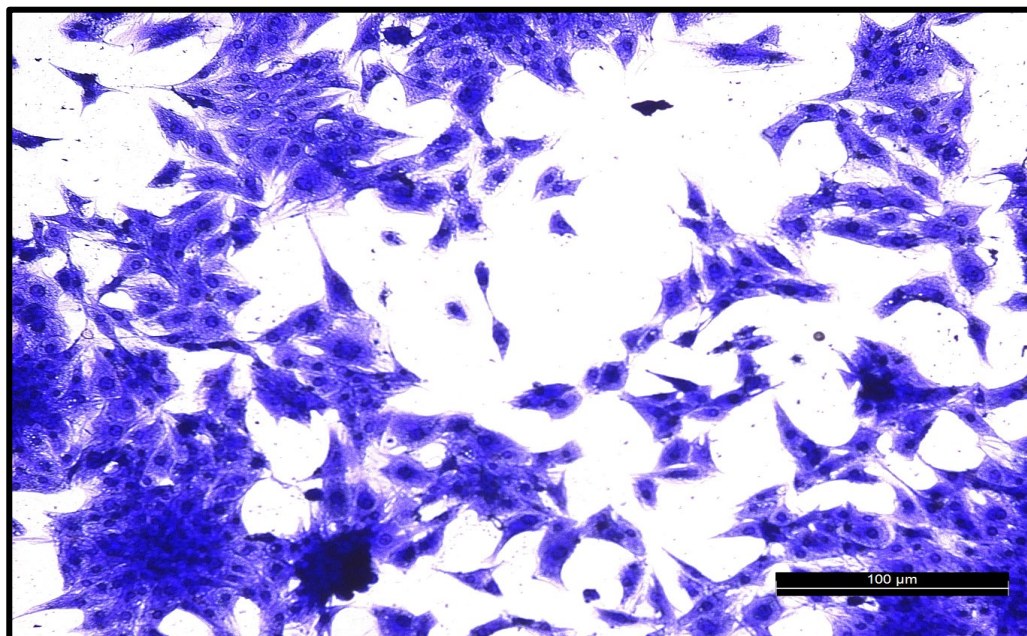


Fig (3.67) HT-29 cell line treated with a concentration of 160 μg/ml of SeNPs produced by *S. marcescens* with crystal violet dye

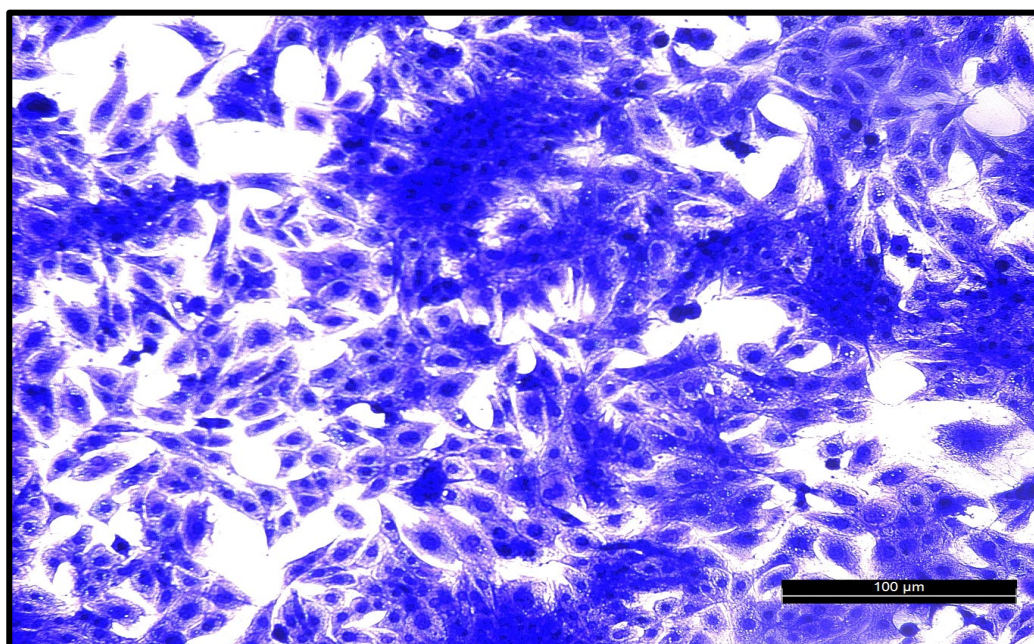


Fig (3.68) HepG2 cell line treated with a concentration of 160 μg/ml of SeNPs produced by *S. marcescens* with crystal violet dye

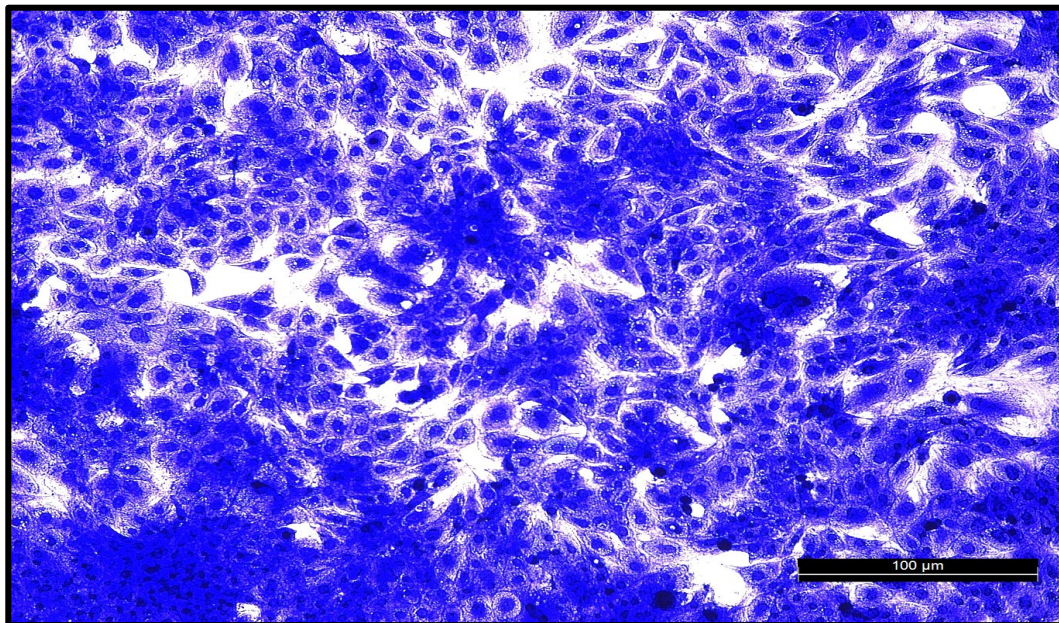


Fig (3.69) MEF cell line treated with a concentration of 160 µg/ml of SeNPs produced by *S. marcescens* with crystal violet dye

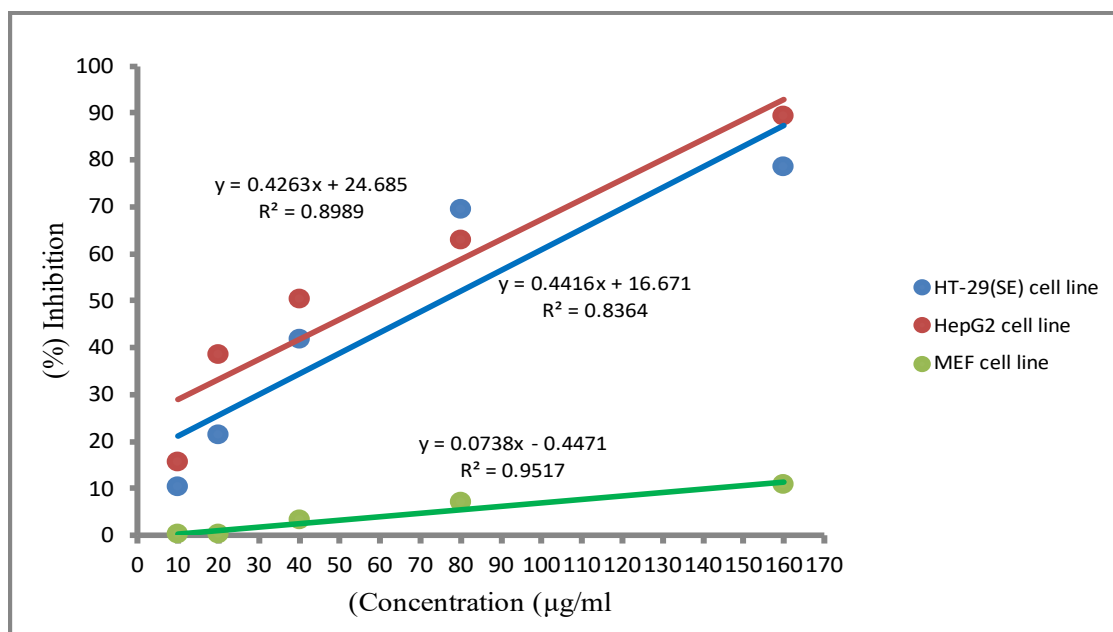
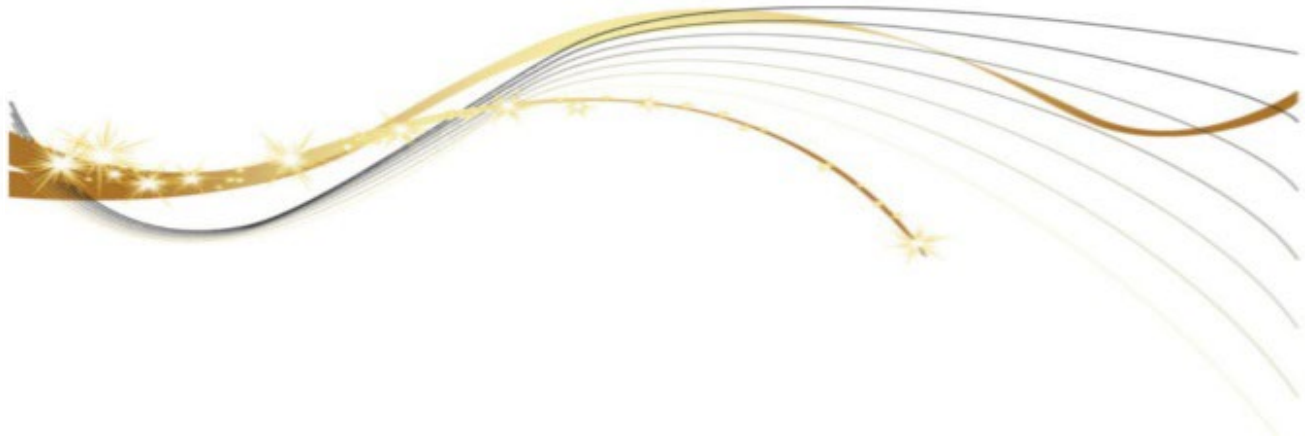


Fig (3.70) Curves IC₅₀ of SeNPs for HT-29 , HepG2 and MEF



Conclusions
and
Recommendation



Conclusions and Recommendation

Conclusions

1-The ability of pathogenic bacteria isolated in the current study to synthesize types of NPs such as Au, Ag, Ag₂O and Se particles.

2-The bio-synthesized NPs in the current study have inhibitory activity against some types of pathogenic bacteria.

3-The bio-synthesized NPs have cytotoxicity against colon cancer cells (HT-29) and liver cancer cells (HepG2) compared to normal cells (MEF) depending on the concentration difference.

4-The possibility of isolating new species of pathogenic bacteria, identifying them molecularly and registering them in the Gene bank.

Conclusions and Recommendation

Recommendations

- 1-Isolation of some species of bacteria and fungi causing diseases from other sources and their use in the bio-synthesis of types of NPs.
- 2-Bio-synthesis of other NPs from pathogenic bacterial species under study.
- 3-Testing conditions for biosynthesis are different from the current conditions.
- 4-Evaluation of the biological activity of bio-Synthesis NPs in the study as an anti-microbial activity such as anti-fungal and anti-virals.
- 5-Study the toxicity of bio-synthesis NPs in the study of cancer cell lines such as prostate cancer and oesophageal cancer compared to the normal cell line.
- 6- Test the activities of NPs on animal's model.
- 7- Test the microbial activities on resistance strains.



References

Abbas, H. A., & Hegazy, W. A.(2017). Targeting the virulence factors of *Serratia marcescens* by ambroxol. *Room. Arch. Microbiol. Immunol* , 76 , 27-32.

Abdel Kareem, M. M., & Zohri, A. A. (2018). Extracellular mycosynthesis of gold nanoparticles using *Trichoderma hamatum*: optimization, characterization and antimicrobial activity. *Letters in applied microbiology* , 67 (5), 465-475.

Abdulateef, S. A., Owaif, H. A. A., & Hussein, M. H. (2023). Importance of virulence factors in bacterial pathogenicity: a review. *International Journal of Medical Science and Clinical Research Studies*, 3(4), 765-769.

Abdulhassan,A.J.(2016). Effect of Silver and Titanium Nanoparticles Synthesized by *Lactobacillus* as Antimicrobial ,Antioxidant and Some Physiological Parameters.Master Thesis.University of Kufa , Faculty of Science – Iraq. pp 86-93

Aguilar-Garay, R., Lara-Ortiz, L.F., Campos-López, M., Gonzalez-Rodriguez, D.E., Gamboa-Lugo, M.M., Mendoza-Pérez, J.A., ... & Nicolás-Álvarez, D.E. (2024) . A comprehensive review of silver and gold nanoparticles as effective antibacterial agents. *Pharmaceuticals*, 17 (9), 1134

Akintola, AO, Kehinde, BD, Ayoola, PB, Adewoyin, AG, Adedosu, OT, Ajayi, JF, & Ogunsona, SB (2020, March). Antioxidant properties of silver nanoparticles biosynthesized from methanolic leaf extract of *Blighia sapida*. In *IOP conference series: Materials Science and Engineering* (Vol. 805, No. 1, p. 012004). IOP Publishing.

Al Sufyani, N.M., Hussien, N.A., & Hawsawi, Y.M. (2019). Characterization and anticancer potential of silver nanoparticles

biosynthesized from *Olea chrysoyfolia* and *Lavandula dentata* leaf extracts on HCT116 colon cancer cells. *Journal of Nanomaterials*, 2019 (1), 7361695

Alagesan, V., & Venugopal, S. (2019). Green synthesis of selenium nanoparticle using leaves extract of *Withania somnifera* and its biological applications and photocatalytic activities. *Bionanoscience*, 9, 105-116.

Alfryyan, N., Kordy, M. G. M., Gabbar, M. A., Soliman, H. A., and Shaban, M. (2022). Characterization of the biosynthesized intracellular and extracellular plasmonic silver nanoparticles using *Bacillus cereus* and their catalytic reduction of methylene blue. *Scientific Reports*, 12(1), 12495.

Alsohaimi IH, Nassar AM, Seaf Elnasr TA, Cheba B amar (2020). A novel composite silver nanoparticles loaded calcium oxide stemming from egg shell recycling: A potent photocatalytic and antibacterial activities. *J Clean Prod.* 2020;248(9);2031-2040.

Amendola, V., Pilot, R., Frasconi, M., Maragò, O. M., & Iatì, M. A. (2017). Surface plasmon resonance in gold nanoparticles: a review. *Journal of Physics: Condensed matter*, 29 (20), 203002.

Ansar, S., Tabassum, H., Aladwan, N. S., Naiman Ali, M., Almaarik, B., AlMahrouqi, S., ... & Alsubki, R. (2020). Eco-friendly silver nanoparticles synthesis by *Brassica oleracea* and its antibacterial, anticancer and antioxidant properties. *Scientific Reports*, 10(1), 18564.

Anwanwan, D., Singh, S. K., Singh, S., Saikam, V., & Singh, R. (2020). Challenges in liver cancer and possible treatment approaches. *Biochimica et Biophysica Acta (BBA)-Reviews on Cancer*, 1873(1), 188314.

Bai, K., Hong, B., He, J., Hong, Z., & Tan, R. (2017). Preparation and antioxidant properties of selenium nanoparticles-loaded chitosan microspheres. *International journal of nanomedicine*, 4527-4539.

BalaKumaran, M.D., Ramachandran, R., Balashanmugam, P., Jagadeeswari, S., & Kalaichelvan, P.T. (2022). Comparative analysis of antifungal, antioxidant and cytotoxic activities of mycosynthesized silver nanoparticles and gold nanoparticles. *Materials Technology*, 37 (6), 411-421

Bharadwaj, K. K., Rabha, B., Pati, S., Sarkar, T., Choudhury, B. K., Barman, A., ... & Mohd Noor, N. H. (2021). Green synthesis of gold nanoparticles using plant extracts as the beneficial prospect for cancer theranostics. *Molecules*, 26 (21), 6389

Bhosale, R. R.;Kulkarni, A.S.; Gilda, S.S.; Aloorkar, N.H.; Osmani R.A. and Harka B.R. (2014). Innovative Eco-friendly Approaches for Green Synthesis of Silver Nanoparticles. *Int J Pharm Sci Nanotech*, 7(1): 2328–2337

Biondo,C.(2022). New insights into bacterial pathogenesis. *Pathogens*, 12(1), 38. Botteon CEA, Silva LB, Ccana-Ccapatinta G, Silva TS. (2021). Biosynthesis and characterization of gold nanoparticles using Brazilian red propolis and evaluation of its antimicrobial and anticancer activities. *Sci Rep* 11:1–16

Brandelli, A., & Veras, F. F. (2023). Biosynthesis of Gold Nanoparticles by Fungi. *Mycosynthesis of Nanomaterials: Perspectives and Challenges*, 146.

Bray F, Ferlay J, Soerjomataram I, et al. (2018). Global cancer statistics 2018: GLOBOCAN estimates of incidence and mortality worldwide for 36 cancers in 185 countries. *CA Cancer J Clin* 68:394–424.

Burlec, A. F., Corciova, A., Boev, M., Batir-Marin, D., Mircea, C., Cioanca, O., ... & Hancianu, M. (2023). Current overview of metal nanoparticles' synthesis, characterization, and biomedical applications, with a focus on silver and gold nanoparticles. *Pharmaceuticals*, 16(10), 1410.

Cao, W., Chen, H. D., Yu, Y. W., Li, N., & Chen, W. Q. (2021). Changing profiles of cancer burden worldwide and in China: a secondary analysis of the global cancer statistics 2020. *Chinese Medical Journal*, 134(07), 783-791.

Capes-Davis, A., & Freshney, R. I. (2021). *Freshney's culture of animal cells: A manual of basic technique and specialized applications*. John Wiley & Sons.

Chang, Y., Zheng, C., Chinnathambi, A., Alahmadi, T. A., & Alharbi, S. A. (2021). Cytotoxicity, anti-acute leukaemia, and antioxidant properties of green-synthesized gold nanoparticles using Cannabis sativa L leaf aqueous extract. *Arabian Journal of Chemistry*, 14 (4), 103060

Chaturvedi, V. K., Singh, A., Singh, V. K., & Singh, M. P. (2019). Cancer nanotechnology: a new revolution for cancer diagnosis and therapy. *Current drug metabolism*, 20 (6), 416-429.

Clarance, P., Luvankar, B., Sales, J., Khusro, A., Agastian, P., Tack, J. C., ... & Kim, H. J. (2020). Green synthesis and characterization of gold nanoparticles using endophytic fungi *Fusarium solani* and its in-vitro anticancer and biomedical applications. *Saudi Journal of Biological Sciences*, 27(2), 706-712.

Conrado, R., Gomes, T. C., Roque, G. S. C., & De Souza, A. O. (2022). Overview of bioactive fungal secondary metabolites: cytotoxic and antimicrobial compounds. *Antibiotics*, 11 (11), 1604

Cooper, D.; Denneulin, T.; Bernier, N.; Béch , A. and Rouvi re, J. L. (2016). Strain mapping of semiconductor specimens with nm-scale resolution in a transmission electron microscope. *Micron*, 80: 145– 165

Cucchetti, A., Cescon, M., Erroi, V., & Pinna, A. D. (2013). Cost-effectiveness of liver cancer screening. *Best Practice & Research Clinical Gastroenterology*, 27(6), 961-972.

Cui, D., Liang, T., Sun, L., Meng, L., Yang, C., Wang, L., ... & Li, Q. (2018). Green synthesis of selenium nanoparticles with extract of hawthorn fruit induced HepG2 cells apoptosis. *Pharmaceutical biology*, 56 (1), 528-534.

Dakal, T. C., Kumar, A., Majumdar, R. S., and Yadav, V. (2016). Mechanistic basis of antimicrobial actions of silver nanoparticles. *Frontiers in Microbiology*, 7, 1831

Dash, C., and Payyappilli, R. (2016). KOH string and vancomycin susceptibility test as an alternative method to Gram staining. *Journal of International Medicine and Dentistry*, 3(2), 88–90.

Dehbanipour, R., & Ghalavand, Z. (2022). Acinetobacter baumannii: Pathogenesis, virulence factors, novel therapeutic options and mechanisms of resistance to antimicrobial agents with emphasis on tigecycline. *Journal of Clinical Pharmacy and Therapeutics*, 47 (11), 1875-1884.

Deng, Y., Xu, H., Su, Y., Liu, S., Xu, L., Guo, Z., ... & Feng, J. (2019). Horizontal gene transfer contributes to virulence and antibiotic resistance of *Vibrio harveyi* 345 based on complete genome sequence analysis. *BMC genomics* , 20, 1-19.

Dewan, T. M., & Hateet, R. R. (2022). Detect the Antibacterial and Antitumor of synthesized Silver Nanoparticles Using Microbacterium sp.

Dewan, T. M., & Hateet, R. R. (2023). Biosynthesis of Silver Nanoparticles from Microbacterium sp. for Determination of Antibacterial and Antitumor. *Iraqi Journal of Industrial Research*, 10 (2), 105-116.

Dharmaraj, D., Krishnamoorthy, M., Rajendran, K., Karuppiah, K., Annamalai, J., Durairaj, K. R., ... & Ethiraj, K. (2021). Antibacterial and cytotoxicity activities of biosynthesized silver oxide (Ag₂O) nanoparticles

using *Bacillus paramycooides*. *Journal of Drug Delivery Science and Technology*, 61, 102111.

Diksha, D., Gupta, S. K., Gupta, P., Banerjee, U. C., & Kalita, D. (2023). Antibacterial potential of gold nanoparticles synthesized from leaf extract of *Syzygium cumini* against multidrug-resistant urinary tract pathogens. *Cureus*, 15 (2).

Duman, H., Eker, F., Akdaşçi, E., Witkowska, A. M., Bechelany, M., & Karav, S. (2024). Silver nanoparticles: A comprehensive review of synthesis methods and chemical and physical properties. *Nanomaterials*, 14(18), 1527.

Durán, N., Marcato, P. D., Durán, M., Yadav, A., Gade, A., & Rai, M. (2011). Mechanistic aspects in the biogenic synthesis of extracellular metal nanoparticles by peptides, bacteria, fungi, and plants. *Applied microbiology and biotechnology*, 90, 1609-1624.

Ealia, S. A. M., & Saravanakumar, M. P. (2017, November). A review on the classification, characterisation, synthesis of nanoparticles and their application. In *IOP conference series: materials science and engineering* (Vol. 263, No. 3, p. 032019). IOP Publishing.

El Domany, E. B., Essam, T. M., Ahmed, A. E., & Farghali, A. A. (2018). Biosynthesis physicochemical optimization of gold nanoparticles as an anti-cancer and synergetic antimicrobial activity using *Pleurotus ostreatus* fungus. *Journal of Applied Pharmaceutical Science*, 8(5), 119-128.

El-Bendary, MA, Afifi, SS, Moharam, ME, Abo El-Ola, SM, Salama, A., Omara, EA, ... & Gawdat, NA (2021). Biosynthesis of silver nanoparticles using isolated *Bacillus subtilis*: characterization, antimicrobial activity, cytotoxicity, and their performance as antimicrobial agent for textile materials. *Preparative Biochemistry & Biotechnology*, 51 (1), 54-68.

El-Saadony, M. T., El-Wafai, N. A., El-Fattah, H. I. A., & Mahgoub, S. A. (2019). Biosynthesis, optimization and characterization of silver nanoparticles using a soil isolate of *Bacillus pseudomycooides* MT32 and their antifungal activity against some pathogenic fungi. *Adv. Anim. Vet. Sci* , 7 (4), 238-249.

El-Sapagh, S. H., El-Zawawy, N. A., Elshobary, M. E., Alquraishi, M., Zabed, H. M., & Nouh, H. S. (2024). Harnessing the power of *Neobacillus niacini* AUMC-B524 for silver oxide nanoparticle synthesis: Optimization, characterization, and bioactivity exploration. *Microbial Cell Factories*, 23(1), 220.

Elzoghby, A. O. (2019). Pharmaceutical Nanotechnology in Egypt: diverse applications and promising outcomes. *Nanomedicine* , 14 (6), 649-653.

Fahmy, H. M., Mohamed, F. M., Marzouq, M. H., Mustafa, A. B. E. D., Alsoudi, A. M., Ali, O. A., ... & Mahmoud, F. A. (2018). Review of green methods of iron nanoparticle synthesis and applications. *BioNanoScience*, 8, 491-503.

Fernando, S.S.N., Gunasekara, T.D.C.P., & Holton, J. (2018). Antimicrobial nanoparticles: applications and mechanisms of action.

Ferraa S, Barebita H, Moutataouia M.(2021) Effect of barium oxide on structural features and thermal properties of vanadium phosphate glasses. *Chem Phys Lett.* 2021;765(10):138304.

Forough, M. & Farhadi, K. (2010). Biological and green synthesis of silver nanoparticles. *Turkish J. Eng. Env. Sci.* 34 (2010), 281 – 287.

Ghaderi, R.S., Adibian, F., Sabouri, Z., Davoodi, J., Kazemi, M., Amel Jamehdar, S., ... & Daroudi, M. (2022). Green synthesis of selenium nanoparticle by *Abelmoschus esculentus* extraction and assessment of its antibacterial activity. *Materials Technology* , 37 (10), 1289-1297.

Gharieb, M. M., Soliman, A. M., & Omara, M. S. (2023). Biosynthesis of selenium nanoparticles by potential endophytic fungi *Penicillium citrinum* and *Rhizopus arrhizus*: characterization and optimization. *Biomass Conversion and Biorefinery*, 1-10.

Granados-Romero, J. J., Valderrama-Treviño, A. I., Contreras-Flores, E. H., Barrera-Mera, B., Herrera Enríquez, M., Uriarte-Ruíz, K., ... & Arauz-Peña, G. (2017). Colorectal cancer: a review. *Int J Res Med Sci*, 5(11), 4667.

Gungure, A. S., Jule, L. T., Nagaprasad, N., & Ramaswamy, K. (2024). Studying the properties of green synthesized silver oxide nanoparticles in the application of organic dye degradation under visible light. *Scientific Reports*, 14 (1), 26967

Haddadian, A., Robattorki, F. F., Dibah, H., Soheili, A., Ghanbarzadeh, E., Sartipnia, N., ... & Mirzaie, A. (2022). Niosomes-loaded selenium nanoparticles as a new approach for enhanced antibacterial, anti-biofilm, and anticancer activities. *Scientific Reports* , 12 (1), 21938

Hassan, A. F., Hateet, R. R., & Al-Shakban, M. A. (2024). Anti-tumor Activity of Gold Oxide Nanoparticles Synthesized Using *Nocardia Asteroids*. *Journal of Nanostructures* , 14 (1), 73-82.

Ibrahim, N. B. & Hateet, R. R., (2021). Biosynthesis of silver nanoparticles from *Staphylococcus lentus* isolated from *Ocimum basilicum* and their antibacterial activity. *Comunicata Scientiae*, 12, e3545-e3545.

Hatipoğlu, A. (2021). Rapid green synthesis of gold nanoparticles: Synthesis, characterization, and antimicrobial activities. *Prog. Nutr* , 23 , e2021242.

Holban, A. M., Gestal, M. C., & Grumezescu, A. M. (2016). Control of biofilm-associated infections by signalling molecules and nanoparticles. *International Journal of Pharmaceutics*, 510 (2), 409-418.

Horikoshi, S., & Serpone, N. (Eds.). (2013). *Microwaves in nanoparticle synthesis: fundamentals and applications*. John Wiley & Sons.

Hosseini, M., Mashreghi, M., & Eshghi, H. (2016). Biosynthesis and antibacterial activity of gold nanoparticles coated with reductase enzymes. *Micro & Nano Letters*, *11* (9), 484-489.

Ijaz, I., Gilani, E., Nazir, A., & Bukhari, A. (2020). Detail review on chemical, physical and green synthesis, classification, characterizations and applications of nanoparticles. *Green chemistry letters and reviews*, *13* (3), 223-245.

Jadoun, S., Arif, R., Jangid, N. K., & Meena, R. K. (2021). Green synthesis of nanoparticles using plant extracts: A review. *Environmental Chemistry Letters*, *19* (1), 355-374.

Jha, A. K., & Prasad, K. (2010). Green synthesis of silver nanoparticles using *Cycas* leaf. *International Journal of Green Nanotechnology: Physics and Chemistry*, *1*(2), P110-P117.

Jin, Y., He, Y., Liu, L., Tao, W., Wang, G., Sun, W., ... & Wang, M. (2021). Effects of super nutritional selenium nanoparticles on immune and antioxidant capacity in Sprague-Dawley rats. *Biological Trace Element Research*, 1-9.

Kang, M. G., Khan, F., Tabassum, N., Cho, K. J., Jo, D. M., & Kim, Y. M. (2023). Inhibition of biofilm and virulence properties of pathogenic bacteria by silver and gold nanoparticles synthesized from *Lactiplantibacillus* sp. strain C1. *ACS omega*, *8*(11), 9873-9888.

Karnwal, A., Kumar Sachan, R. S., Devgon, I., Devgon, J., Pant, G., Panchpuri, M., ... & Kumar, G. (2024). Gold nanoparticles in nanobiotechnology: from synthesis to biosensing applications. *ACS omega*, *9*(28), 29966-29982.

Khalid, K., Tan, X., Mohd Zaid, H. F., Tao, Y., Lye Chew, C., Chu, D. T., ... & Chin Wei, L. (2020). Advanced in developmental organic and inorganic nanomaterial: a review. *Bioengineered*, 11(1), 328-355.

Khan, I., Saeed, K., & Khan, I. (2019). Nanoparticles: Properties, applications and toxicities. *Arabian journal of chemistry*, 12(7), 908-931.

Khan, N., Ali, S., Latif, S., & Mehmood, A. (2022). Biological synthesis of nanoparticles and their applications in sustainable agricultural production. *Natural Science*, 14 (06), 226-234

Khatoon, U. T., & Velidandi, A. (2024). Silver oxide nanoparticles: Synthesis via chemical reduction, characterization, antimicrobial, and cytotoxicity studies. *Inorganic Chemistry Communications*, 159, 111690.

Kotakadi, V. S., Gaddam, S. A., Venkata, S. K., Sarma, P. V. G. K., and Sai Gopal, D. V. R. (2016). Biofabrication and spectral characterization of silver nanoparticles and their cytotoxic studies on human CD34 +ve stem cells. *3 Biotech*, 6(2), 1–11.

Kuipers, E. J., Grady, W. M., Lieberman, D., Seufferlein, T., Sung, J. J., Boelens, P. G., ... & Watanabe, T. (2015). Colorectal cancer. *Nature reviews. Disease primers*, 1, 15065.

Lewczuk, B., & Szyryńska, N. (2021). Field-emission scanning electron microscope as a tool for large-area and large-volume ultrastructural studies. *Animals*, 11(12), 3390.

Liao, C., Huang, X., Wang, Q., Yao, D., & Lu, W. (2022). Virulence factors of *Pseudomonas aeruginosa* and antivirulence strategies to combat its drug resistance. *Frontiers in cellular and infection microbiology*, 12, 926758.

Liao, G., Tang, J., Wang, D., Zuo, H., Zhang, Q., Liu, Y., & Xiong, H. (2020). Selenium nanoparticles (SeNPs) have potent antitumor activity

against prostate cancer cells through the upregulation of miR-16. *World Journal of Surgical Oncology*, 18, 1-11.

Lim, Z. Z. J., Li, J. E. J., Ng, C. T., Yung, L. Y. L., & Bay, B. H. (2011). Gold nanoparticles in cancer therapy. *Acta Pharmacologica Sinica*, 32(8), 983-990.

Lin, W., Zhang, J., Xu, J. F., & Pi, J. (2021). The advancement of selenium nanoparticles against infectious diseases. *Frontiers in pharmacology*, 12, 682284

Logothetidis, S. (Ed.). (2012). Nanomedicine and nanobiotechnology. Springer Science & Business Media.

Lunardi, C. N., Gomes, A. J., Rocha, F. S., De Tommaso, J., & Patience, G. S. (2021). Experimental methods in chemical engineering: Zeta potential. *The Canadian Journal of Chemical Engineering*, 99(3), 627-639.

Madkour, L. H. (2017). Ecofriendly green biosynthesized of metallic nanoparticles: bio-reduction mechanism, characterization and pharmaceutical applications in the biotechnology industry. *Drugs Ther*, 3, 1-11.

Martínez-Esquivias, F., Gutiérrez-Angulo, M., Pérez-Larios, A., Sánchez-Burgos, J. A., Becerra-Ruiz, J. S., & Guzmán-Flores, J. M. (2022). Anticancer activity of selenium nanoparticles in vitro studies. *Anti-Cancer Agents in Medicinal Chemistry (Formerly Current Medicinal Chemistry-Anti-Cancer Agents)*, 22 (9), 1658-1673.

Mattiuzzi, C., & Lippi, G. (2019). Current cancer epidemiology. *Journal of epidemiology and global health*, 9(4), 217-222.

Melanin, (2023) nanoparticles obtained from preformed recombinant melanin by bottom-up and top-down approaches. *Polymers*, 15 (10), 2381

Menon, S., Agarwal, H., Rajeshkumar, S., Jacqueline Rosy, P., & Shanmugam, V. K. (2020). Investigating the antimicrobial activities of the biosynthesized selenium nanoparticles and its statistical analysis. *Bionanoscience* , 10 (1), 122-135.

Merck. (2020). IR spectrum table and chart. URL: [https://www. Sigma-Aldrich. com/technicaldocuments/articles/biology/ir-spectrum-table. html](https://www.Sigma-Aldrich.com/technicaldocuments/articles/biology/ir-spectrum-table.html).

Minelli, C. (2016). talk on 'Measuring nanoparticle properties: are we high and dry or all at sea?' at 'Nanoparticle Characterisation–Challenges for the Community'event–IOP.

Minhas, L. A., Kaleem, M., Jabeen, A., Ullah, N., Farooqi, H. M. U., Kamal, A., ... & Mumtaz, A. S. (2023). Synthesis of silver oxide nanoparticles: A novel approach for antimicrobial properties and biomedical performance, featuring *Nodularia haraviana* from the Cholistan desert. *Microorganisms*, 11(10), 2544.

Mohanlall V & Biyela B,(2022) Biocatalytic and biological activities of *Kigelia africana* mediated silver monometallic and copper-silver bimetallic nanoparticles. *Indian J Biochem Biophys*, 59 (2022) 94.

Mora, C., McKenzie, T., Gaw, I. M., Dean, J. M., von Hammerstein, H., Knudson, T. A., ... & Franklin, E. C. (2022). Over half of known human pathogenic diseases can be aggravated by climate change. *Nature Climate Change* , 12 (9), 869-875.

Mourdikoudis, S., Pallares, R.M., & Thanh, N.T. (2018). Characterization techniques for nanoparticles: comparison and complementarity upon studying nanoparticle properties. *Nanoscale* , 10 (27), 12871-12934.

Muhammad N, Zhao H, Song W, et al. (2021). Silver nanoparticles functionalized paclitaxel nanocrystals enhance the overall anti-cancer effect on human cancer cells. *Nanotechnology* 32:85105.

Muhammad, S., Ali, A., Zahoor, S., Xinghua, X., Shah, J., Hamza, M., ... & Iqbal, A. (2023). Synthesis of Silver oxide nanoparticles and its antimicrobial, anticancer, anti-inflammatory, wound healing, and immunomodulatory activities-A review. *Acta Scientific Applied Physics Volume*, 3(7).

Nassar, A. R. A., Eid, A. M., Atta, H. M., El Naghy, W. S., & Fouda, A. (2023). Exploring the antimicrobial, antioxidant, anticancer, biocompatibility, and larvicidal activities of selenium nanoparticles fabricated by endophytic fungal strain *Penicillium verhagenii*. *Scientific reports*, 13(1), 9054.

Neamah, S. A., Albukhaty, S., Falih, I. Q., Dewir, Y. H., & Mahood, H. B. (2023). Biosynthesis of zinc oxide nanoparticles using *Capparis spinosa* L. fruit extract: Characterization, biocompatibility, and antioxidant activity. *Applied Sciences*, 13 (11), 6604

Nguyen, N. P. U., Dang, N. T., Doan, L., & Nguyen, T. T. H. (2023). Synthesis of silver nanoparticles: from conventional to ‘modern’ methods—a review. *Processes*, 11(9), 2617.

Ogarev, V. A., Rudoi, V. M., & Dement’Eva, O. V. (2018). Gold nanoparticles: synthesis, optical properties, and application. *Inorganic Materials: Applied Research*, 9(1), 134-140.

Pallavi, S. S., Rudayni, H. A., Bepari, A., Niazi, S. K., and Nayaka, S. (2022). Green synthesis of silver nanoparticles using *Streptomyces hirsutus* strain SNPGA-8 and their characterization, antimicrobial activity, and anticancer activity against human lung carcinoma cell line A549. *Saudi Journal of Biological Sciences*, 29(1), 228–238.

Pantidos, N., & Horsfall, L. E. (2014). Biological synthesis of metallic nanoparticles by bacteria, fungi and plants. *Journal of Nanomedicine & Nanotechnology*, 5(5), 1.

Patel, H. & Joshi, J.(2023) Green and chemical approach for synthesis of Ag₂O nanoparticles and their antimicrobial activity. *J. Sol-Gel Sci. Technol.* **105**(3), 814–826 (2023).

Pavelić, K., Pavelić, S. K., Bulog, A., Agaj, A., Rojnić, B., Čolić, M., & Trivanović, D. (2023). Nanoparticles in medicine: current status in cancer treatment. *International Journal of Molecular Sciences*, *24* (16), 12827

Pechyen, C., Tangnorawich, B., Toommee, S., Marks, R., & Parcharoen, Y. (2024). Green synthesis of metal nanoparticles, characterization, and biosensing applications. *Sensors International*, 100287

Pradheesh, G., Suresh, S., Suresh, J., & Alexramani, V. (2020). Antimicrobial and Anticancer Activity Studies on Green Synthesized Silver Oxide Nanoparticles from the Medicinal Plant *Cyathea nilgiriensis* Holttum. *International Journal of Pharmaceutical Investigation*, *10* (2).

Prema, P., Iniya, P. A., & Immanuel, G. (2016). Microbial mediated synthesis, characterization, antibacterial and synergistic effect of gold nanoparticles using *Klebsiella pneumoniae* (MTCC-4030). *RSC Advances*, *6* (6), 4601-4607.

Purohit, J., Chattopadhyay, A., & Singh, N. K. (2019). Green synthesis of microbial nanoparticles: approaches to application. *Microbial Nanobionics: Volume 2, Basic Research and Applications*, 35-60.

Pyrzynska, K., & Sentkowska, A. (2021). Biosynthesis of selenium nanoparticles using plant extracts. *Journal of Nanostructure in Chemistry*, 1-14.

Qamar, S. R. U., & Ahmad, J. N. (2021). Nanoparticles: Mechanism of biosynthesis using plant extracts, bacteria, fungi, and their applications. *Journal of Molecular Liquids*, *334*, 116040

Rajan, A., Rajan, A. R., & Philip, D. (2017). Elettaria cardamomum seed mediates the rapid synthesis of gold nanoparticles and its biological activities. *OpenNano*, 2, 1-8.

Ranjitha, V. R., Muddegowda, U., & Ravishankar Rai, V. (2019). Potent activity of bioconjugated peptide and selenium nanoparticles against colorectal adenocarcinoma cells. *Drug Development and Industrial Pharmacy*, 45 (9), 1496-1505.

Rutherford, G., Xiao, B., Carvajal, C., Farrell, M., Santiago, K., Cashwell, I., & Pradhan, A. (2015). Photochemical growth of highly densely packed gold nanoparticle films for biomedical diagnostics. *ECS Journal of Solid State Science and Technology*, 4(10), S3071

Sadiq, Z., Safiabadi Tali, S. H., Hajimiri., Al-Kassawneh, M., & Jahanshahi-Anbuhi, S. (2024). Gold nanoparticles-based colourimetric assays for environmental monitoring and food safety evaluation. *Critical Reviews in Analytical Chemistry*, 54 (7), 2209-2244.

Sahoo, S.K., Ma, W. and Labhasetwar, V. (2004) 'Efficacy of transferrin-conjugated paclitaxel-loaded nanoparticles in a murine model of prostate cancer', *Int'l. J. Cancer*, Vol. 112, No. 2, pp.335–340

Sajid, M., & Plotka-Wasyłka, J. (2020). Nanoparticles: Synthesis, characteristics, and applications in analytical and other sciences. *Microchemical Journal*, 154, 104623.

Saleh, M. N., and Khoman Alwan, S. (2020). Biosynthesis of silver nanoparticles from bacteria *Klebsiella pneumonia*: Their characterization and antibacterial studies. *Journal of Physics: Conference Series*, 1664(1), 012115.

Salman, Y. M. & Abd Atae, F. G. (2021). Antibacterial and immunological effects of biosynthesized magnesium oxide (MgO) nanoparticles produced by

bacteria. M.Sc. thesis. College of Science, Department of Biology, Babylon. University Babylon.Iraq.

Salyer, S. J., Silver, R., Simone, K., & Behraves, C. B. (2017). Prioritizing zoonoses for global health capacity building themes from One Health zoonotic disease workshops in 7 countries, 2014–2016. *Emerging infectious diseases*, 23(Suppl 1), S55.

Samuel, M. S., Ravikumar, M., John J, A., Selvarajan, E., Patel, H., Chander, P. S., ... & Chandrasekar, N. (2022). A review on green synthesis of nanoparticles and their diverse biomedical and environmental applications. *Catalysts*, 12(5), 459.

Sans-Serramitjana, E., Obreque, M., Muñoz, F., Zaror, C., Mora, MDLL, Viñas, M., & Betancourt, P. (2023). Antimicrobial activity of selenium nanoparticles (SeNPs) against potentially pathogenic oral microorganisms: A scoping review. *Pharmaceutics*, 15 (9), 2253

Suleiman, R. Z. (2024). A comparative approach to understanding bacterial pathogenicity: The role of enzymatic and hemolytic virulence factors. *Journal of Medical Genetics and Clinical Biology*, 1(6), 150-161

Shah, S. S., Shaikh, M. N., Khan, M. Y., Alfasane, M. A., Rahman, M. M., & Aziz, M. A. (2021). Present status and future prospects of jute in nanotechnology: A review. *The Chemical Record*, 21(7), 1631-1665.

Shahriari, M., Hemmati, S., Zangeneh, A., & Zangeneh, M. M. (2019). Biosynthesis of gold nanoparticles using *Allium noeanum* Reut. Ex Regel leaves aqueous extract; Characterization and analysis of their cytotoxicity, antioxidant, and antibacterial properties. *Applied organometallic chemistry*, 33 (11), e5189.

Shankar, A., & Sharma, K. K. (2022). Fungal secondary metabolites in food and pharmaceuticals in the era of multi-omics. *Applied Microbiology and Biotechnology*, 106 (9), 3465-3488.

Sharma, R.; Bisen, D. P.; Shukla, U. and Sharma, B. G. (2012). X-ray diffraction: a powerful method of characterizing nanomaterials. *Recent Research in Science and Technology*, 4(8), 77–79.

Shoeibi, S., & Mashreghi, M. (2017). Biosynthesis of selenium nanoparticles using *Enterococcus faecalis* and evaluation of their antibacterial activities. *Journal of Trace Elements in Medicine and Biology*, 39, 135-139.

Sidhu, P. K., and Nehra, K. (2020). Bacteriocin-capped silver nanoparticles for enhanced antimicrobial efficacy against food pathogens. *IET Nanobiotechnology*, 14(3), 245–252.

Singh, G., Babele, P.K., Shahi, S.K., Sinha, R.P., Tyagi, M.B., & Kumar, A. (2014). Green synthesis of silver nanoparticles using cell extracts of *Anabaena doliolum* and screening of its antibacterial and antitumor activity. *Journal of Microbiology and Biotechnology*, 24 (10), 1354-1367.

Singh, P., Kim, Y. J., Singh, H., Wang, C., Hwang, K. H., Farh, M. E. A., and Yang, D. C. (2015). Biosynthesis, characterization, and antimicrobial applications of silver nanoparticles. *International Journal of Nanomedicine*, 10, 2567–2577.

Sirisha, T., Aleem Bash, P., and Kavitha, B. (2017). Isolation and characterization of pathogenic bacteria from Kundu river water of Nandyal, Kurnool, Andhra Pradesh, India. *Journal of Applied Sciences*, 17(9), 475–481

Smuleac, V.; Xiao, L. and Bhattacharyya, D.(2013). Greener and Other Approaches To Synthesize Fe and Pd Nanoparticles in Functionalized Membranes and Hydrogel, ACS Symposium Series, Vol. 1124, Chapter 3, pp 41–58.

Sonker, A. S., Pathak, J., Kannaujiya, V. K., & Sinha, R. P. (2017). Characterization and in vitro antitumor, antibacterial and antifungal activities of green synthesized silver nanoparticles using cell extract of Nostoc sp. strain HKAR-2. *Canadian Journal of Biotechnology*, 1(1), 26.

Sowndarya, P., Ramkumar, G., & Shivakumar, M. S. (2017). Green synthesis of selenium nanoparticles conjugated Clausena dentata plant leaf extract and their insecticidal potential against mosquito vectors. *Artificial cells, nanomedicine, and biotechnology*, 45 (8), 1490-1495.

Spagnoletti, F. N., Spedalieri, C., Kronberg, F., & Giacometti, R. (2019). Extracellular biosynthesis of bactericidal Ag/AgCl nanoparticles for crop protection using the fungus *Macrophomina phaseolina*. *Journal of Environmental Management*, 231, 457-466.

Srinath, B. S., & Rai, R. V. (2015). Biosynthesis of gold nanoparticles using extracellular molecules produced by *Enterobacter aerogenes* and their catalytic study. *Journal of Cluster Science*, 26, 1483-1494.

Stabnikova, O., Khonkiv, M., Kovshar, I., & Stabnikov, V. (2023). Biosynthesis of selenium nanoparticles by lactic acid bacteria and areas of their possible applications. *World Journal of Microbiology and Biotechnology*, 39 (9), 230

Sujatha, V., Kaviyasri, G., Venkatesan, A., Thirunavukkarasu, C., Acharya, S., Dayel, S. B., ... & Ramesh, T. (2023). Biomimetic formation of silver oxide nanoparticles through *Diospyros montana* bark extract: Its application in dye degradation, antibacterial and anticancer effect in human hepatocellular carcinoma cells. *Journal of King Saud University-Science*, 35 (3), 102563

Sukhanova, A., Bozrova, S., Sokolov, P., Berestovoy, M., Karaulov, A., & Nabiev, I. (2018). Dependence of nanoparticle toxicity on their physical and chemical properties. *Nanoscale research letters*, 13, 1-21.

Sunderam, V., Thiyagarajan, D., Lawrence, A. V., Mohammed, S. S., & Selvaraj, A. (2019). In-vitro antimicrobial and anticancer properties of green synthesized gold nanoparticles using *Anacardium occidentale* leaves extract. *Saudi Journal of Biological Sciences*, 26 (3), 455-459.

Sung, H., Ferlay, J., Siegel, R. L., Laversanne, M., Soerjomataram, I., Jemal, A., & Bray, F. (2021). Global cancer statistics 2020: GLOBOCAN estimates of incidence and mortality worldwide for 36 cancers in 185 countries. *CA: a cancer journal for clinicians*, 71(3), 209-249.

Sung, H., Ferlay, J., Siegel, R. L., Laversanne, M., Soerjomataram, I., Jemal, A., & Bray, F. (2021). Global cancer statistics 2020: GLOBOCAN estimates of incidence and mortality worldwide for 36 cancers in 185 countries. *CA: a cancer journal for clinicians*, 71(3), 209-249.

Sunita, P., Sivaraj, R., Venkatesh, R., Vanathi, P., Vanathi, P., & Rajiv, P. (2015). Anticancer potential of green synthesized silver nanoparticles: a review. *Int J Curr Res Rev*, 7 (10), 21539-21544.

Susanti, D., Haris, M. S., Taher, M., and Khotib, J. (2022). Natural products-based metallic nanoparticles as antimicrobial agents. *Frontiers in Pharmacology*, 13, 1900.

Syed, B., Nagendra Prasad, M. N., and Satish, S. (2016). Synthesis and characterization of silver nanobactericides produced by *Aneurinibacillus migulanus* 141, a novel endophyte inhabiting *Mimosa pudica* L. *Arabian Journal of Chemistry*, 12(8), 3743–3752.

Szczyglewska, P., Feliczak-Guzik, A., & Nowak, I. (2023). Nanotechnology—general aspects: A chemical reduction approach to the synthesis of nanoparticles. *Molecules*, 28 (13), 4932

Tabassum, N., Khan, F., Jeong, G. J., Jo, D. M., & Kim, Y. M. (2024). Silver nanoparticles synthesized from *Pseudomonas aeruginosa* pyoverdine: Aitibiofilm and antivirulence agents. *Biofilm*, 7, 100192

Thakur, N., Thakur, N., Bhullar, V., Sharma, S., Mahajan, A., Kumar, K., ... & Pathak, D. (2021). TiO₂ nanofibers fabricated by electrospinning technique and degradation of MO dye under UV light. *Zeitschrift für Kristallographie-Crystalline Materials*, 236 (8-10), 239-250.

Thirumurugan, D., Cholarajan, A., Raja, S. S., & Vijayakumar, R. (2018). An introductory chapter: secondary metabolites. *Secondary metabolites-sources and applications*, 1, 13

Truong, L. B., Medina-Cruz, D., Mostafavi, E., & Rabiee, N. (2021). Selenium nanomaterials to combat antimicrobial resistance. *Molecules*, 26 (12), 3611

Vahabi, K., Mansoori, G. A., & Karimi, S. (2011). Biosynthesis of silver nanoparticles by fungus *Trichoderma reesei* (a route for large-scale production of AgNPs). *Insciences J.*, 1(1), 65-79.

Varlamova, E. G., Goltyaev, M. V., Mal'tseva, V. N., Turovsky, E. A., Sarimov, R. M., Simakin, A. V., & Gudkov, S. V. (2021). Mechanisms of the cytotoxic effect of selenium nanoparticles in different human cancer cell lines. *International Journal of Molecular Sciences*, 22 (15), 7798

Vijayaram, S., Razafindralambo, H., Sun, Y. Z., Vasantharaj, S., Ghafarifarsani, H., Hoseinifar, S. H., & Raeeszadeh, M. (2024). Applications of green synthesized metal nanoparticles—a review. *Biological Trace Element Research*, 202(1), 360-386.

Wang, L., Xu, J., Yan, Y., Liu, H., Karunakaran, T., & Li, F. (2019). Green synthesis of gold nanoparticles from *Scutellaria barbata* and its anticancer activity in pancreatic cancer cells (PANC-1). *Artificial cells, nanomedicine, and biotechnology*, 47 (1), 1617-1627.

Wilson, J. W., Schurr, M. J., LeBlanc, C. L., Ramamurthy, R., Buchanan, K. L., & Nickerson, C. A. (2002). Mechanisms of bacterial pathogenicity. *Postgraduate medical journal*, 78 (918), 216-224.

Wu, M., & Li, X. (2015). *Klebsiella pneumoniae* and *Pseudomonas aeruginosa*. In *Molecular medical microbiology* (pp. 1547-1564). Academic Press.

Wypij, M., Jędrzejewski, T., Trzcińska-Wencel, J., Ostrowski, M., Rai, M., & Golińska, P. (2021). Green synthesized silver nanoparticles: antibacterial and anticancer activities, biocompatibility, and analyses of surface-attached proteins. *Frontiers in microbiology*, 12, 632505.

Xu, F., Li, Y., Zhao, X., Liu, G., Pang, B., Liao, N., ... & Shi, J. (2024). Diversity of fungus-mediated synthesis of gold nanoparticles: properties, mechanisms, challenges, and solving methods. *Critical Reviews in Biotechnology*, 44(5), 924-940.

Yadav, R. K., Jangeer, S., Parashar, R., Sharma, G., Meena, P., Meena, M. K., & Patel, D. D. (2023)A Critical Review on Nanoparticles Synthesis: Physical, Chemical and Biological Perspectives. *IJCRTII* .

Yao, Y., Zhou, Y., Liu, L., Xu, Y., Chen, Q., Wang, Y., ... & Shao, A. (2020). Nanoparticle-based drug delivery in cancer therapy and its role in overcoming drug resistance. *Frontiers in molecular biosciences*, 7, 193

Yousaf, H., Mehmood, A., Ahmad, K. S., & Raffi, M. (2020). Green synthesis of silver nanoparticles and their applications as an alternative

antibacterial and antioxidant agent. *Materials Science and Engineering: C*, 112, 110901.

Zaib, S., & Iqbal, J. (2019). Nanotechnology: Applications, techniques, approaches, & the advancement in toxicology and environmental impact of engineered nanomaterials. *Importance & Applications of Nanotechnology*, 8.

Zhang, H., Zhou, H., Bai, J., Li, Y., Yang, J., Ma, Q., & Qu, Y. (2019). Biosynthesis of selenium nanoparticles mediated by Fungus *Mariannaea* sp. HJ and their characterization. *Colloids and Surfaces A: Physicochemical and Engineering Aspects*, 571, 9-16.

Zonaro, E., Lampis, S., Turner, R. J., Qazi, S. J. S., & Vallini, G. (2015). Biogenic selenium and tellurium nanoparticles synthesized by environmental microbial isolates effectively inhibit bacterial planktonic cultures and biofilms. *Frontiers in microbiology*, 6, 584

Appendix1: Identification of bacteria using the 16S rDNA gene
Acinetobacter baumannii

TAGCGATGAAATGCGTATAGATCGGGAGGAATACCGATGGCGAAGGCATCCATCT
GGCATAATACTGACGCTGAGGTAAGAAAGCATGGGGAGCAAACAGGATTAGATAC
CCTGGTAGTCCATGCCGTAAACGATGTCTACTAGCCGTTGCCGCCTTTGAGGCTTTA
GTGGCGCAGCTAACGCGATAAGTAGACCGCCTGGGGAGTACGGTCGCAAGACTAA
AACTCAAATGAATTGACGGGGGCCCCGCACAAGCGGTGGAGCATGTGGTTTAATTCG
ATGCAACGCGAAGAACCTTACCTGGCCTTGACATACTAGAACTTTCCAGAGATGG
ATTGGTGCCTTCGGGAATCTAGATACAGGTGCTGCATGGCTGTCGTCAGCTCGTGT
CGTGAGATGTTGGGTAAAGTCCCGCAACGAGCGCAACCCTTTTCCTTACTTGCCAG
CATTTCCGGATGGGAACTTTAAGGATACTGCCAGTGACAACTGGAGGAAGGCGGG
GACGACGTCAAGTCATCATGGCCCTTACGGCCAGGGCTACACACGTGCTACAATGG
TCGGTACAAAGGGTTGCTACACAGCGATGTGATGCTAATCTCAAAAAGCCGATCGT
AGTCCGGATTGGAGTCTGCAACTCGACTCCATGAAGTCGGAATCGCTAGTAATCGC
GGATCAGAATGCCGCGGTGAATACGTTCCCGGGCCTTGACACACCGCCC

Appendix2: *Pseudomonas aeruginosa*

TCCTGGATTTCAGCGGCGGACGGGTGAGTAATGCCTAGGAATCTGCCTGGTAGTGGG
GGATAACGTCCGGAAACGGGCGCTAATACCGCATAACGTCCTGAGGGAGAAAGTGG
GGGATCTTCGGACCTCACGCTATCAGATGAGCCTAGGTTCGGATTAGCTAGTTGGTG
GGGTAAAGGCCTACCAAGGCGACGATCCGTAACCTGGTCTGAGAGGATGATCAGTC
ACACTGGAAGTGGAGACACGGCCAGACTCCTACGGGAGGCAGCAGTGGGGAATATT
GGACAATGGGCGAAAGCCTGATCCAGCCATGCCGCGTGTGTGAAGAAGGTCTTCG
GATTGTAAAGCACTTTAAGTTGGGAGGAAGGGCAGTAAGTTAATACCTTGCTGTTT
TGACGTTACCAACAGAATAAGCACCGGCTAACTTCGTGCCAGCAGCCGCGGTAATA
CGAAGGGTGCAAGCGTTAATCGGAATTACTGGGCGTAAAGCGCGCGTAGGTGGTT
CAGCAAGTTGGATGTGAAATCCCCGGGCTCAACCTGGGAACTGCATCCAAAACACTAC
TGAGCTAGAGTACGGTAGAGGGTGGTGGAAATTCCTGTGTAGCGGTGAAATGCGTA
GATATAGGAAGGAACACCAGTGGCGAAGGCGACCACCTGGACTGATACTGACACT
GAGGTGCGAAAGCGTGGGGAGCAAACAGGATTAGATACCCTGGTAGTCCACGCCG
TAAACGATGTCGACTAGCCGTTGCGATCCTTGAGATCTTAGTGGCGCAGCTAACGC
GATAAGTCGACCGCCTGGGGAGTACGGCCGC

Appendix3: *Pseudomonas aeruginosa*

TCCTGGATTTCAGCGGCGGACGGGTGAGTAATGCCTAGGAATCTGCCTGGTAGTGGG
GGATAACGTCCGGAAACGGGCGCTAATACCGCATAACGTCCTGAGGGAGAAAGTGG
GGGATCTTCGGACCTCACGCTATCAGATGAGCCTAGGTTCGGATTAGCTAGTTGGTG
GGGTAAAGGCCTACCAAGGCGACGATCCGTAACCTGGTCTGAGAGGATGATCAGTC
ACACTGGAAGTGGAGACACGGTCCAGACTCCTACGGGAGGCAGCAGTGGGGAATAT
TGGACAATGGGCGAAAGCCTGATCCAGCCATGCCGCGTGTGTGAAGAAGGTCTTCG
GATTGTAAAGCACTTTAAGTTGGGAGGAAGGGCAGTAAGTTAATACCTTGCTGTTT
TGACGTTACCAACAGAATAAGCACCGGCTAACTTCGTGCCAGCAGCCGCGGTAATA
CGAAGGGTGCAAGCGTTAATCGGAATTACTGGGCGTAAAGCGCGCGTAGGTGGTT
CAGCAAGTTGGATGTGAAATCCCCGGGCTCAACCTGGGAACTGCATCCAAAACCTAC
TGAGCTAGAGTACGGTAGAGGGTGGTGGAAATTCCTGTGTAGCGGTGAAATGCGTA
GATATAGGAAGGAACACCAGTGGCGAAGGCGACCACCTGGACTGATACTGACACT
GAGGTGCGAAAGCGTGGGGAGCAAACAGGATTAGATACCCTGGTAGTCCACGCCG
TAAACGATGTCGACTAGCCGTTGCGATCCTTGAGATCTTAGTGGCGCAGCTAACGC
GATAAGTCGACCGCCTGGGGAGTACGGCCGC

Appendix4: *Serratia marcescens*

CGAGCGGTAGCACAGGGGAGCTTGCTCCCTGGGTGACGAGCGGCGGACGGGTGAG
TAATGTCTGGGAAACTGCCTGATGGAGGGGGATAACTACTGGAAACGGTAGCTAA
TACCGCATAACGTTCGCAAGACCAAAGAGGGGGACCTTCGGGCCTCTTGCCATCAGA
TGTGCCCAGATGGGATTAGCTAGTAGGTGGGGTAATGGCTCACCTAGGCGACGATC
CCTAGCTGGTCTGAGAGGATGACCAGCCACACTGGAAGTGGAGACACGGTCCAGAC
TCCTACGGGAGGCAGCAGTGGGGAATATTGCACAATGGGCGCAAGCCTGATGCAG
CCATGCCGCGTGTGTGAAGAAGGCCTTCGGGTTGTAAAGCACTTTCAGCGAGGAGG
AAGGTGGTGAAGTAAATACGTTCAATGACGTTACTCGCAGAAGAAGCACCGG
CTAACTCCGTGCCAGCAGCCGCGGTAATACGGAGGGTGCAAGCGTTAATCGGAATT
ACTGGGCGTAAAGCGCACGCAGGCGGTTTGTAAAGTCAGATGTGAAATCCCCGGGC
TCAACCTGGGAACTGCATTTGAAACTGGCAAGCTAGAGTCTCGTAGAGGGGGGGT
AGAATTCCAGGTGTAGCGGTGAAATGCGTAGAGATCTGGAGGAATACCGGTGGCG
AAGGCGGCCCCCTGGACGAAGACTGACGCTCAGGTGCGAAAGCGTGGGGAGCAA
CAGGATTAGATACCCTGGTAGTCCACGCTGTAACGATGTCGATTTGGAGGTTGTG
CCCTTGAGGCGTGGCTTCCGGAGCTAACGCGTTAAATCGACCGCCTGGGGAGTACG
GCCGCAAGGTTAGAACTCAAATGAATTGACGGGGGCCCGCACAAGCGGTGGAGCA
TGTGGTTTAATTCGATGCAACGCGAAGAACCTTACCTACTCTTGACATCCAGAGAA
CTTATCAGAGATGCTTTGGTGCCTTCGGGAACTCTGAGACAGGTGCTGCATGGCTG
TCGTCAGCTCGTGTGTGAAATGTTGGGTTAAGTCCCGCAACGAGCGCAACCCTTA
TCCTTTGTTGCC

الخلاصة

اجريت الدراسة في مختبر التقنيات الحيوية في كلية العلوم / جامعة ميسان اضافة الى بعض المؤسسات الصحية (مستشفى الصدر، مستشفى الزهراوي، مستشفى الطفل والولادة) خلال فترة زمنية امتدت من شهر كانون الثاني الى شهر نيسان. اذ هدفت الدراسة الحالية الى تخليق بعض الجسيمات النانوية بواسطة بعض البكتيريا المسببة للأمراض المعزولة من مصادر مختلفة، تم جمع عشرة أنواع من العزلات البكتيرية المعزولة من (الدم، الجروح، الحروق، الادرار) وتم التشخيص الجزيئي لاربعة انواع منها بواسطة تفاعل البلمرة المتسلسل (PCR) Polymerase chain reaction اضافة الى تشخيصها بواسطة جهاز Vitek-2 حيث اظهرت نتائج التشخيص ان العزلة البكتيرية التي تم عزلها من الدم كانت *Acinetobacter baumannii* بينما العزلة البكتيرية التي تم عزلها من الجروح هي *Pseudomonas aeruginosa* و العزلة البكتيرية التي عزلت من الحروق ايضا كانت *Pseudomonas aeruginosa* اضافة الى العزلة البكتيرية التي عزلت من الادرار فكانت *Serratia marcescens* وتم تسجيل ثلاثة منها في بنك الجينات بعدها اجريت عمليات التخليق الحيوي للحصول على الجسيمات النانوية قيد الدراسة

فعند معاملة الرواشح البكتيرية بملح رابع كلوريد الذهب ($AuCl_4$) اظهرت النتائج تغير لوني لراشح العزلة *A. baumannii* من اللون الاصفر الشفاف الى الاحمر الداكن بعد الحضان لمدة 24 ساعة كموشر على قدرتها لتخليق جسيمات الذهب النانوية (AuNPs) بينما لم يحدث تغير لوني لرواشح العزلات الاخرى عند معاملتهم بالملح نفسه. من جهة اخرى تم العمل على التخليق الحيوي لجسيمات الفضة واوكسيد الفضة النانوية حيث تمت معاملة الرواشح البكتيرية بملح نترات الفضة ($AgNO_3$) وبعد الحضان لمدة 72 ساعة نجح التخليق الحيوي بالتغير اللوني لراشحي العزلتين *P. aeruginos* *P. aeruginos* من اللون الاصفر الشفاف الى البني الداكن كموشر لتخليق كل من جسيمات الفضة واوكسيد الفضة النانوية (Ag_2ONPs , $AgNPs$) على التوالي في حين لم يظهر تغير لوني لرواشح العزلات الاخرى عند المعاملة بالملح نفسه. وقد اختبرت العزلات البكتيرية عند الخطوات نفسها من اجل تخليق جسيمات السيلينيوم النانوية حيث اظهرت النتائج تغير لوني فقط لراشح العزلة *S. marcescens* من اللون الاصفر الشفاف الى البرتقالي الفاتح عند معاملة الرواشح البكتيرية بملح سيلنيت الصوديوم (Na_2SeO_3) ولمدة حضان 48 ساعة كدليل اولي لحدوث التخليق الحيوي لجسيمات السيلينيوم النانوية (SeNPs) في حين لم تظهر رواشح العزلات الاخرى تغير لوني عند المعاملة بالملح نفسه. من اجل تأكيد التخليق الحيوي للجسيمات النانوية المصنعة تم اجراء بعض الفحوصات الفيزيوكيميائية المتقدمة حيث اظهرت النتائج ان رنين البلازمون السطحي (SPR) للجسيمات المصنعة حيويًا من (*A.baumannii*, *P.aeruginosa*, *P.aeruginosa*, *S.marcescens*) تم تحديده عند طول موجي (560,426,430,298 نانومتر) على التوالي. كما اظهر تحليل الاشعة تحت الحمراء (FTIR) ان الجسيمات النانوية محاطة بمجموعات وظيفية ترتبط بينها في حين اظهر تحليل جهد زينا (Zeta Potential) استقرار الجسيمات حيث كانت جسيمات السيلينيوم النانوية اكثر استقرارا عند (-19.8) مقارنة مع الجسيمات الاخرى اما طبيعة البنية البلورية للجسيمات النانوية فكانت جسيمات بلورية مكعبة بالنسبة لجسيمات الذهب والفضة النانوية وسداسية بالنسبة لجسيمات السيلينيوم النانوية عند الفحص ب تحليل حيود الاشعة السينية (XRD) اما بالنسبة لشكل وحجم وتوزيع الجسيمات فقد تم فحصها بواسطة مجهر الالكترونات الماسح عالي الدقة (FESEM) والمجهر الالكتروني النافذ (TEM) فكانت الجسيمات بعضها كروية الشكل ومنتظمة وبعضها قريب من الشكل الكروي غير منتظمة وموزعة بشكل متجانس وتمتلك احجام ضمن النطاق النانوي فكان معدل حجم الجسيمات (الذهب، الفضة، اوكسيد الفضة، السيلينيوم) (68، 45، 88، 92) نانومتر على التوالي عند فحصها ب FESEM ومعدل حجم الجسيمات (22، 29، 17، 51) نانومتر على التوالي عند

فحصها ب TEM بينما تم تأكيد وجود عناصر (الذهب , الفضة , اوكسيد الفضة , السيلينيوم) في الرواشح البكتيرية المدروسة بواسطة فحص (EDX) .

وقد اجريت بعض التطبيقات الحيوية بما فيها اختبار الفاعلية المضادة للبكتيريا للجسيمات النانوية المصنعة ضد نوعين من البكتيريا المسببة للأمراض هما ، *Echerichia.coli* و *Staphylococcus.aureus* ، باستخدام طريقة انتشار القرص. أظهرت النتائج أن الجسيمات النانوية المصنعة تمتلك فعالية جيدة ضد كلا النوعين من العزلات البكتيرية المختبرة و اكدت نتائج التحليل الاحصائي وجود فروق ذات دلالة احصائية عند مستوى 0.05 بين القيم مقارنة مع المضاد الحيوي الجنتاميسين. كما تم اختبار السمية الخلوية للجسيمات النانوية المصنعة ضد خلايا سرطان القولون البشري (HT-29) وخلايا سرطان الكبد البشري (Hep-G2) مقارنة مع الخلايا الطبيعية لجنين الفأر (MEF) باستخدام تراكيز مختلفة (10، 20، 40، 80، 160 ميكروغرام / مول). وكشفت النتائج امتلاك الجسيمات النانوية المصنعة قدرة تثبيطية ضد الخلايا السرطانية المذكورة بطريقة تعتمد على التركيز، حيث بلغ التركيز المثبط لنصف الخلايا IC50 لجسيمات النانو الذهبية المصنعة بواسطة *A. baumannii* ضد خطوط الخلايا (MEF,HepG2,HT-29) هي (1100,73,111) ميكروجرام/مول على التوالي. بينما بلغ IC50 لجسيمات الفضة النانوية المصنعة بواسطة *P. aeruginosa* هي (489,62,102) ميكروجرام/مول على التوالي. بينما كان IC50 لجسيمات اوكسيد الفضة النانوية المصنعة بواسطة *P. aeruginosa* هي (671,94,125) ميكروجرام/مول على التوالي، في حين بلغ IC50 لجسيمات السيلينيوم النانوية المصنعة بواسطة *S. marcescens* هي (683,59,75) ميكروجرام/مول على التوالي. وأكدت نتائج التحليل الإحصائي باستخدام برنامج Graph Pad Prism وجود فروق معنوية بين التركيزات المثبطة لخلايا السرطان عند مستوى دلالة 0.05



جمهورية العراق

وزارة التعليم العالي والبحث العلمي

جامعة ميسان

كلية العلوم

قسم علوم الحياة

التخليق الحيوي لبعض الجسيمات النانوية من البكتيريا المرضية

وتقييم فعاليتها ضد بكتيرية والحد سرطانة

رسالة مقدمة الى

كلية العلوم / جامعة ميسان جزء من متطلبات نيل

شهادة الماجستير في علوم الحياة

من الطالبة

حوراء خلف عبود

بكالوريوس علوم الحياة / جامعة ميسان (2019)

بإشراف

الاستاذ المساعد الدكتور رشيد رحيم حنيت